Self-heating in normal metals and superconductors

A. Vl. Gurevich and R. G. Mints

Institute for High Temperatures, USSR Academy of Sciences, Moscow 127412, Union of Soviet Socialist Republics

This review is devoted to the physics of current-carrying superconductors and normal metals having two or more stable states sustained by Joule self-heating. The creation, propagation, and localization of electrothermal domains and switching waves leading to the transition from one stable state to another in uniform and nonuniform samples are treated in detail. The connection between thermal bistability and hysteresis, dropping and stepped current-voltage characteristics, self-induced oscillations of current and voltage, self-replication of electrothermal domains, and the formation of periodic and stochastic resistive structures are considered.

CONTENTS

LIST OF SYMBOLS

A	area of the cross section of a sample
$D(I)$	length of an electrothermal or resistive domains
$F(T,j)$	effective power of heat release on a nonuniformity
G	latent specific heat of a phase transition
I	transport current
I_0	external current from a dc unit
L	thermal length
L_c	total length of a conductor
L_q	characteristic length of an external perturbation
$\mathscr{L}$	inductance of a circuit
P	perimeter of the cross section of a sample
Q	power of Joule heat release
Q_c	minimum energy of a perturbation initiating the thermal destruction of superconductivity
Q_d	enthalpy of resistive domain
Q_p	total energy of external perturbation
$\dot{Q}_p(x,t)$	specific power of external perturbation
Q_0	thermal unit of perturbation energy
$R(I)$	static differential resistance of the domain containing conductor
$S(T)$	function defined by Eq. (3.5)
T	temperature of a conductor
T_0	temperature of a coolant
$T_{1,3}$	stable-state temperatures of a current-carrying conductor
T_c	critical temperature
T_k	boiling crisis transition temperature
T_m	maximum temperature within a thermal domain
$T_r(j)$	temperature of the resistive transition of a superconductor
$U(j)$	static voltage on a domain containing conductor
$W(T)$	specific power of heat transfer to a coolant
$Z(\omega)$	impedance of a domain containing conductor
$d=A/P$	
$f=W(T)-Q(T,j)$	
$h(T)$	heat-transfer coefficient
$i=j/j_c$	dimensionless current
j	current density

j_c	critical current density
j_m	minimum normal-zone existence current density
j_p	minimum normal-zone propagating current density
j_r	recovery current density
j_2	N-S boundary delocalization current density
l	characteristic length of a nonuniformity
$q(T)$	steady-state heat flux from the conductor into the coolant
r	resistance of external circuit
t_h	characteristic thermal time
t_q	characteristic time of a perturbation
$v(j)$	velocity of switching wave
v_h	characteristic thermal velocity
$x_{n,s}$	volume fractions of normal metal (n) and superconductor (s)
α	Stekly parameter
γ_n	increment of thermal perturbations
$\theta(x,t)$	dimensionless temperature
κ	thermal conductivity
ν	specific heat
$\xi(I)$	dimensionless parameter in stepwise heat production model [see Eq. (6.5)]
ρ	resistivity

I. INTRODUCTION

The present review paper is devoted to nonlinear phenomena in normal metals and superconductors in the cases of bistability under strong Joule self-heating. This means that a specimen can be in one of two stable homogeneous states forming at sufficiently high density of transport current, $j > j_m$, and having distinct temperatures $T = T_1$ and T_3.

The thermal bistability of a current-carrying conductor was first discussed by Busch in 1921 [still earlier relevant papers are cited in a review of Büttiker and Landauer (1982)]. Nevertheless, this effect was not studied in solids until the 1950s, although fairly detailed data were already accumulated in other fields of physics, such as gas discharge. The situation changed at the end of the 1950s and the beginning of the 1960s, owing to markedly increased attention to the properties of semiconductors in strong electric fields and to the properties of superconductors with high critical current density ($j_c \sim 10^5$–10^6 A/cm^2). Hard superconductors such as niobium-titanium alloys and niobium stannide were discovered in this period, and superconducting composites based on these materials were developed; they were characterized by $j_c \sim 10^4$–10^5 A/cm^2 in magnetic fields with induction $B = 5$–10 T [see, for example, the review of Hulm and Matthias (1981)]. Much effort was also spent on detailed studies of thin superconducting films with j_c reaching 10^6–10^8 A/cm^2. It was found that in many cases the superconducting state is destroyed in these materials by Joule self-heating and may occur at currents much lower than the critical current I_c (Newhouse, 1964; Altov *et al.*, 1977). The reason for this is the transition of the superconductor to a self-sustained mode in which the Joule heat release becomes sufficient to raise the temperature above T_c, i.e., the transition to the thermal bistability.

Joule self-heating can result in thermal bistability not only in superconductors, but also in other materials. Indeed, it will appear if the heat balance condition $\rho(T)j^2 = W(T)$ holds for several values of T. This situation occurs either if the resistivity $\rho(T)$ depends on T quite sharply in a narrow interval [Fig. 1(a)] or if the specific heat transfer power $W(T)$ from the specimen to the coolant is N shaped [Fig. 1(b)].

While the presence of three intersection points of the heat-release $Q(T) = \rho(T)j^2$ and heat-transfer $W(T)$ curves is mostly caused by a stepwise increase in $\rho(T)$ at $T \simeq T_c$ [Fig. 1(a)], the transition from one stable state, $T = T_1$, to the other, $T = T_3$, in the fixed-current regime is accompanied by a significant increase in the electric field within the specimen. This situation is found in all phase transitions of metals from high-conductivity to low-conductivity states, for instance, in superconducting, structural, and magnetic transitions, in melting, evaporation, ordering of solid solutions, etc. A similar dependence $\rho(T)$ is also typical for any pure metal in the low-temperature range where $\rho(T)$ grows sharply owing to the "switching in" of the phonon mechanism of electron scattering.

A conductor kept at a fixed voltage may contain, in all cases outlined above, domains of the "hot" phase with $T = T_3$, which at the same time are the domains of electric field [Fig. 2 (b)]. Such domains appear in various systems. We can cite the "hot spot" in superconducting point contacts and microbridges (Iwanyshin and Smith, 1972; Skocpol, Beasley, and Tinkham, 1974a), resistive domains in superconducting thin films and composite superconductors (Volkov and Kogan, 1974; Gurevich and Mints, 1980), electrothermal domains in normal metals due to melting (Abramov *et al.*, 1983), evaporation (Atrazhev and Yakubov, 1980), structural (Barelko *et al.*, 1981) and magnetic transitions (Landauer, 1977; Ross and Lister, 1977; Ausloos, 1981), a sharp $\rho(T)$ dependence at low temperatures (Kadigrobov and Slutskin, 1978;

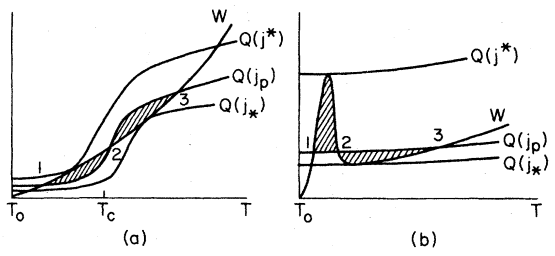

FIG. 1. A graphic solution of the heat balance equation at different j ($j_* < j < j^*$) in the case of (a) "stepwise" function $\rho(T)$ and (b) N-shaped function $W(T)$.

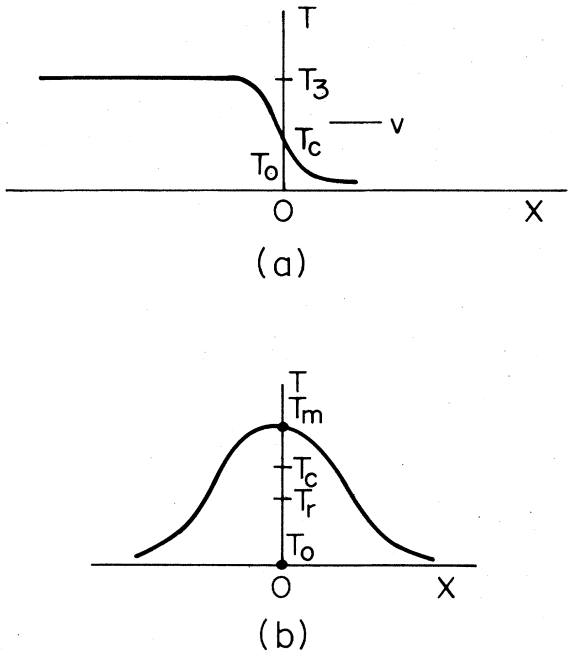

FIG. 2. Temperature distribution in (a) domain wall and (b) electrothermal domain.

Abramov *et al.*, 1983, 1985; Boiko *et al.*, 1984; Kadigrobov *et al.*, 1984), magnetic breakdown (Kadigrobov and Slutskin, 1978), etc. Despite the diversity in labels and in the conditions under which such domains appear, the essential physical phenomenon is common to all of them, namely, the thermal bistability of a current-carrying conductor as a result of sufficiently intensive Joule self-heating.

The N-shaped dependence of heat transfer $W(T)$ [Fig. 1(b)] occurs in semimetals when the energy exchange between electrons and the lattice is hampered by a "narrow phonon bottleneck" (Vakser and Gurevich, 1982). A similar situation appears when a current-carrying conductor is cooled by a liquid coolant whose properties may change abruptly under high heat flux from the specimen. A typical example is the so-called boiling crisis of a coolant, i.e., the transition from the nucleate to film boiling regime (Kutateladze, 1979). As a result, the bistability of a current-carrying conductor cooled by a boiling coolant may be caused by a vapor film formed on its surface. The corresponding thermal domains were observed at helium (Altov *et al.*, 1977), nitrogen (Ivanchenko *et al.*, 1983), and room temperatures (Zhukov *et al.*, 1979, 1983).

The bistability mechanisms described above can arise simultaneously. This occurs, for example, in composite superconductors with high-conductivity normal matrices. The thermal bistability of the matrix and the transition to film boiling in helium may lead to complications in the current-induced destruction of superconductivity in such materials. The heat balance condition can be met here at five or more values of T (the case of multistability).

The transition from one stable state $T=T_1$ to another, $T=T_3$, in the fixed-current mode is initiated by an external perturbation, which results in local heating of the specimen and in the formation of a domain of a phase with $T\simeq T_3$. If the Joule heat release is sufficiently intensive ($I>I_p$), this domain begins to expand and grows to occupy the whole specimen. The dynamics of this transition essentially depends on the velocity of propagation of the boundaries of the "hot" domain, which may be regarded as switching waves transforming the system from the state with $T=T_1$ to that with $T=T_3$ [Fig. 2(a)]. For example, the thermal breakdown of superconductivity is possible if $I>I_p$, where I_p is the so-called minimum normal-zone propagating current (Maddock *et al.*, 1969). The current I_p is a function of the parameters of the superconductor and the coolant; I_p may be much lower than the critical current I_c.

Thermal bistability can thus appear under very different conditions. Bistable (and multistable) systems are capable of the most diverse behavior, e.g., they manifest hysteresis, dropping and stepped current-voltage (I-V) characteristics, periodic or stochastic dissipative structures, various dynamic effects, such as uniform transitions between stable states, propagation of switching waves [Fig. 2(a)] or of electrothermal domains [Fig. 2(b)], their localization in inhomogeneous media, self-induced oscillations or periodic division of such domains, etc. The objective of the present review is to analyze these phenomena in homogeneous and inhomogeneous bistable systems from a unified standpoint, using normal metals and superconductors as a typical example. We have not attempted an exhaustive survey of all possible experimental situations, but have treated only the qualitative features inherent in each specific mechanism of thermal bistability. For this reason, the review cites mostly pioneer publications and some more recent papers.

The organization of the review is as follows. Section II treats uniform Joule self-heating, including the conditions for the existence of thermal bistability in normal metals and in both hard and composite superconductors. Particular attention is paid to the possible homogeneous states of such systems as well as to the transitions between these states due to external perturbations.

Section III analyzes the interface between the "hot" ($T=T_3$) and "cold" ($T=T_1$) phases [Fig. 2(a)] and its propagation, which transforms the system from one stable state to another. It discusses how the velocity of this wave depends on current and on the parameters of the specimen and the coolant, and analyzes the specifics of switching-wave propagation in normal metals and superconductors.

Section IV discusses thermal domains in homogeneous conductors, the conditions for their existence, current-voltage characteristics, and domain stability depending on the parameters of the external electric circuit. Resistive domains in composite superconductors, the "hot spot" in superconducting microbridges, and electrothermal domains in normal metals due to a "stepped" $\rho(T)$ curve [Fig. 1(a)] are used as examples.

Section V is devoted to inhomogeneous systems. The

main emphasis is on the localization of domains and switching waves on inhomogeneities and the localization-induced steps on I-V characteristics, as well as various hysteresis effects.

Section VI deals with the breakdown of a metastable homogeneous state of $T=T_1$ caused by a strong local perturbation, for a current-carrying superconductor chosen as an example. We shall be mostly interested in the dynamics of normal-zone nucleation and in the minimal energy required for breakdown of the superconducting state.

Section VII deals with a number of dynamic effects in bistable systems, such as the motion of electrothermal domains, the dynamics of localization of domains and switching waves on inhomogeneities, and the self-induced domain oscillations in a specimen connected to an electric circuit.

Section VIII treats the peculiarities of normal phase propagation in superconducting composites with high thermal and electric resistance between the normal metal and the superconductor. Stable resistive domains and the dynamic regime of domain division, resulting in the formation of a periodic resistive structure in such systems, are discussed.

In the Conclusion we briefly discuss other physical systems in which the phenomena considered here are also possible.

II. HOMOGENEOUS STATES OF CURRENT-CARRYING CONDUCTORS. BISTABILITY THRESHOLD

We begin with some general information on systems with thermal bistability. Throughout this paper we consider current-carrying conditions whose transverse dimensions are sufficiently small (wires and films). In this case the condition of steady-state heat balance for homogeneous states is

$$Q(T)=W(T)\ , \tag{2.1}$$

$$W(T)=\frac{h(T)}{d}(T-T_0)\ , \tag{2.2}$$

where $Q(T)=jE(T)$ is the power of the Joule heat release, $E(T)$ is the electric field strength at a given temperature T of the specimen, j is the current density averaged over the conductor section, $dW(T)$ is the heat flux per unit surface area from the conductor into the coolant kept at a temperature T_0, $h(T)$ is the heat-transfer coefficient, $d=A/P$, A is the area, and P is the perimeter of the cross section of the specimen. Equation (2.1) holds if temperature T varies slowly across the cross section, i.e.,

$$d \ll d_c \sim \frac{\kappa}{h}\ , \tag{2.3}$$

where κ is the thermal conductivity of the conductor. Let us estimate d_c at low temperatures. At $T_0=4.2$ K, κ in, say, commercial copper is about 1 W/cm K. In the free convection or nuclear boiling regimes of liquid helium, $h\simeq 1$ W/cm^{2}K (Grigor'iev *et al.*, 1977; Kirichenko and Rusanov, 1983). Hence $d_c\sim 1$ cm. In the film boiling regime of liquid helium $h\simeq 0.025$ W/cm^{2}K (Maddock *et al.*, 1969), so that $d_c\simeq 40$ cm. Likewise we can estimate d_c of thin superconducting films in which h is determined mainly by the Kapitza resistance at the interface with the substrate. Thus, in a tin microbridge 0.1 μm thick, 3 μm wide, and 42 μm long, $h\simeq 2.2$–3 W/cm^{2}K at $T_0\gtrsim T_\lambda$ and $h\simeq 7.3$ W/cm^{2}K at $T_0\lesssim T_\lambda$, where T_λ is the lambda point in helium (Skocpol, 1981). This gives $d_c\sim 10^{-2}$ cm for $\kappa\simeq 0.05$ W/cm K.

Thermal bistability arises in the interval $j_*<j<j^*$, where curves $Q(T)$ and $W(T)$ in Fig. 1 have three intersection points. Outside of this interval a specimen can be in only one homogeneous state ($T=T_1$ at $j<j_*$ and $T=T_3$ at $j>j^*$). The critical current densities j_* and j^* are found from the condition of contact of the curves $Q(T)$ and $W(T)$, i.e., they are the smaller and larger roots of the system of equations

$$Q(T,j)=W(T)\ , \tag{2.4}$$

$$\frac{\partial Q(T,j)}{\partial T}=\frac{\partial W(T)}{\partial T}\ . \tag{2.5}$$

The stability of the homogeneous states corresponding to the points 1, 2, and 3 in Fig. 1 can be investigated by using the dynamic equation

$$\nu\frac{\partial T}{\partial t}=Q(T,j)-W(T)\ , \tag{2.6}$$

where $\nu(T)$ is the specific heat of the specimen. Linearizing Eq. (2.6) with respect to small perturbations $\delta T\propto\exp(\lambda t)$, we find the required stability criterion

$$\frac{\partial W}{\partial T}>\frac{\partial Q}{\partial T}\ . \tag{2.7}$$

We see that the states corresponding to the temperatures T_1 and T_3 in Fig. 1 are stable, and those corresponding to T_2 are unstable. This results in a hysteresis in the interval $j_*<j<j^*$. Indeed, as j increases, the specimen is in the "cold" state $T=T_1$ up to $j=j^*$, after which the temperature jumps from $T=T_1$ to $T=T_3$. If the current is then diminished, the reverse transition from $T=T_3$ to $T=T_1$ occurs only at $j=j_*<j^*$. This hysteresis is clearly seen on the N-shaped current-voltage characteristics (Fig. 3).

As T increases, resistivity $\rho(T)$ of systems with N-shaped I-V characteristics increases (see Fig. 1). The external parameter for these systems is the current density j, and the electric field $E(T)$ is determined by the specimen temperature (see, for example, Volkov and Kogan, 1968; Bonch-Bruevich *et al.*, 1972). In this review we consider precisely this case. Situations are also possible in which $\rho(T)$ decreases with increasing T [the metal-insulator transition (Kalafati *et al.*, 1979), the ferromagnetic-superconductor transition (Dharmadurai, 1981), etc.]. The Joule self-heating in these systems results in S-shaped I-V curves. The external parameter here is the electric field E, and the current density is determined by the specimen temperature T. In this case the phases get separated transversely to the direction of

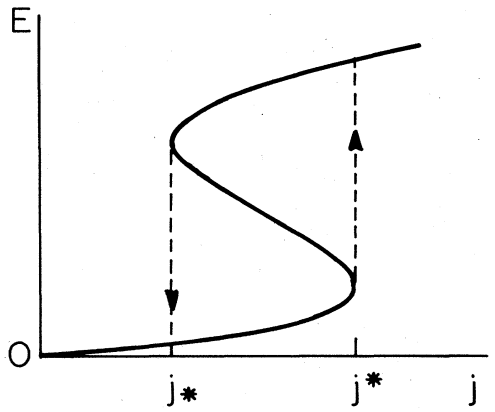

FIG. 3. The I-V characteristic of a bistable conductor.

current, so that current channels are formed (see Volkov and Kogan, 1968; Bonch-Bruevich *et al.*, 1972).

A. Hard superconductors and thin superconducting films. Stekly parameter

Consider the heat balance condition (2.1) for a thin wire made of a hard superconductor, or a thin superconducting film. The transport current I is uniformly distributed over the specimen cross section.

The Joule heat release in the superconductor, $Q=jE(T)$, is zero at $j<j_c(T)$, where j_c is the critical current density.[1] This condition can be rewritten in the form $T<T_r(j)$, where T_r is found from the equation $j=j_c(T_r)$. In the temperature range $T_r<T<T_c$ the superconductor is in the resistive state, and at $T>T_c$ in the normal state (T_c is the critical temperature at $j=0$). The resistive state in hard superconductors is known to be caused by the viscous flow of the vortex structure, while in thin films and whiskers it is caused by the motion of magnetic flux tubes or by the appearance of phase-slip centers (see, for example, Campbell and Evetts, 1972; Skocpol, Beasley, and Tinkham, 1974b; Huebener, 1979). Thus the I-V characteristic of a hard superconductor in the resistive state is linear:

$$j=j_c(T,B)+\frac{1}{\rho_f}E\ , \tag{2.8}$$

where $\rho_f\sim\rho_s B/B_{c2}$ is the resistivity in the viscous flow mode of magnetic flux, ρ_s is the resistivity in the normal state, B is the magnetic induction, $B_{c2}=\mu_0 H_{c2}$, and H_{c2} is the upper critical magnetic field. Consequently, in hard superconductors,

$$Q(T)=0,\quad T<T_r(j)\ , \tag{2.9}$$

$$Q(T)=j[j-j_c(T)]\rho_f,\quad T>T_r(j)\ . \tag{2.10}$$

[1]In the present review we deal with phenomena for which the creep of magnetic flux at $j<j_c$ is negligible.

The dependence $Q=Q(T)$ has the typical "stepped" shape [Fig. 1(a)] due to the N-S transition in the relatively narrow temperature interval $T_r<T<T_c$. Let us consider the heat balance condition in a hard superconductor in the simplest case of $j_c(T)$ decreasing linearly with increasing T, $B\approx B_{c2}$, and ρ_f and h varying only slightly in the temperature range $T_r\lesssim T\lesssim T_c$ (Stekly, 1965; Altov *et al.*, 1977). It will be convenient to rewrite Eq. (2.1) in a dimensionless form, converting to the dimensionless temperature $\theta=(T-T_0)/(T_c-T_0)$ and dimensionless current $i=j/j_c$, where $j_c\equiv j_c(T_0)$. If $i>1$ ($j>j_c$), the curves $Q(\theta)$ and $W(\theta)$ have a single intersection point corresponding to the resistive ($\theta=\theta_2$) or normal ($\theta=\theta_3$) state [Fig. 4(a)]:

$$\theta_2(i)=\frac{\alpha i(i-1)}{1-\alpha i},\quad 1<i<\alpha^{-1/2},\quad \alpha<1\ , \tag{2.11}$$

$$\theta_3(i)=\alpha i^2,\quad i>\alpha^{-1/2},\quad \alpha<1\ . \tag{2.12}$$

The dimensionless quantity α is called the Stekly parameter; it is the ratio of the characteristic heat generation in the normal state, $\rho_s j_c^2$, to the heat transfer, $(T_c-T_0)h/d$ (see, for example, Altov *et al.*, 1977; Wilson, 1983):

$$\alpha=\frac{\rho_s j_c^2 d}{h(T_c-T_0)}\ . \tag{2.13}$$

The quantity α characterizes the relative role of Joule self-heating in superconductors: self-heating is important if $\alpha>1$ and negligible if $\alpha\ll 1$. Self-heating results in nonlinearity of I-V characteristics of superconductors of the second kind because $j_c(T)$ in Eq. (2.8) is a function of specimen temperature $T(E)$, which in turn is found from the heat balance equation. Thus, at $\alpha<1$, the I-V characteristic can be found by substituting Eq. (2.11) into (2.8):

$$j=\frac{j_c+\rho_s^{-1}E}{1+\dfrac{\alpha E}{\rho_s j_c}},\quad E<E_c=\frac{\rho_s j_c}{\sqrt{\alpha}},\quad B\simeq B_{c2}\ . \tag{2.14}$$

Self-heating thus decreases the differential conductivity $\sigma(E)=\partial j/\partial E$, and at $E>E_c$ the specimen transforms to the normal state ($\theta_2>1$). A drop in $\sigma(E)$ in a strong electric field was observed in superconductors with low j_c

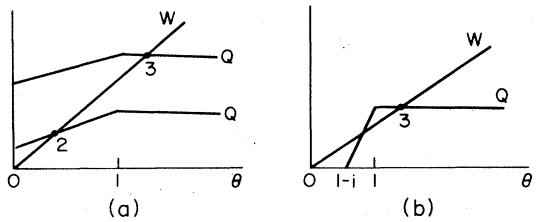

FIG. 4. Graphic solutions of the heat balance equation in a type-II superconductor for constant thermal and electrical parameters and linear temperature dependence of j_c: (a) $\alpha<1$; (b) $\alpha>1$.

(Vinnikov *et al.*, 1976; Goncharov *et al.*, 1980). Typical I-V characteristics then have the form shown in Fig. 5. In contrast, in hard superconductors $j_c \gg E\rho_s^{-1}$ so that their I-V characteristics remain almost linear in a wide interval E, even with Joule self-heating taken into account. Furthermore,

$$\sigma(E)=(1-\alpha)\rho_s^{-1} . \tag{2.15}$$

If $\alpha>1$, the differential conductivity becomes negative, pointing to a thermal instability of the resistive state. At $\alpha>1$ it can occur only if $j<j_c$, when the $Q(T)$ and $W(T)$ curves have three intersection points [Fig. 4(b)]. This thermal bistability appears in the interval $j_m<j<j_c$ where j_m is the minimal current density required for heating the specimen to $T>T_c$. In the case under discussion, the temperature of the superconductor at $j=j_m$ is T_c [Fig. 4(b)], so that $\rho_s(T_c)j_m^2=(T_c-T_0)h(T_c)/d$ and

$$j_m=\left[\frac{h(T_c)T_c}{\rho_s(T_c)d}\right]^{1/2}\left[1-\frac{T_0}{T_c}\right]^{1/2} . \tag{2.16}$$

The quantity $I_m=j_mA$ is often referred to as the minimum normal-zone existence current (Altov *et al.*, 1977). This current depends on the superconductor characteristics and on the coolant parameters, and can be substantially lower than the critical current I_c, which is determined by vortex pinning, surface barrier, etc. In this case superconductivity can be destroyed by self-heating even at $j<j_c$.

Using the Stekly parameter (2.13), one finds that $j_m=j_c\alpha^{-1/2}$, so that the condition of $Q(T)$ and $W(T)$ intersecting at three points within $j_m<j<j_c$ can be written in the form

$$j_c\alpha^{-1/2}<j<j_c . \tag{2.17}$$

Thermal bistability in a current-carrying superconductor thus occurs only if $\alpha>1$. It is clear from Eq. (2.17) that the Stekly parameter α determines the width of the current interval in which superconductivity can be destroyed by Joule self-heating. As follows from Eq. (2.13), $\alpha>1$ in materials with high critical current density and low conductivity in the normal state. This is typical of thin superconducting films and hard superconductors in which self-heating is an important factor.

The quantity $\alpha(T_0)$ decreases with increasing T_0, vanishing at $T_0=T_c$. There exists, therefore, a temperature interval $T_c-\Delta T<T_0<T_c$ in the vicinity of T_c where definitely $\alpha(T_0)<1$ and self-heating is negligibly small. The width of this interval, ΔT, follows from the dependence of j_c on T_0. For example, if $j_c(T_0)=(1-T_0/T_c)j_0$, then $\alpha(T_0)=(1-T_0/T_c)\alpha_0$, where α_0 is the value assumed by $\alpha(T_0)$ at $T_0=0$. As a result,

$$\frac{\Delta T}{T_c}=\frac{hT_c}{\rho_s d j_0^2}=\alpha_0^{-1} . \tag{2.18}$$

For thin films we can choose for j_c, for example, the pair-breaking current density $j_c\simeq(1-T_0/T_c)^{3/2}j_0$ (Ginzburg, 1958). Then

$$\frac{\Delta T}{T_c}=\frac{1}{j_0}\left[\frac{hT_c}{\rho_s d}\right]^{1/2}=\alpha_0^{-1/2} . \tag{2.19}$$

As an illustration, we shall estimate the characteristic value of the Stekly parameter α for a niobium-titanium alloy wire at $T_0=4.2$ K and $B=3$ T. Assuming $j_c=3\times10^5$ A/cm^2, $\rho_s=3\times10^{-5}$ Ω cm, $d=10$ μm, $h\simeq1$ W/cm^{2}K (for nucleate boiling of liquid helium), one finds $\alpha=450$, $j_m=0.05j_c$. Likewise, we can evaluate α for a thin film. For example, for a lead film on a sapphire substrate ($j_0=2\times10^8$ A/cm^2, $h=2.5$ W/cm^{2}K, $T_c=7.2$ K, $\rho_s\simeq10^{-7}$ Ω cm) we obtain, for $d=220$ Å, $\alpha_0\simeq440$, $j_m\simeq0.05j_c$.

We thus find that in both cases $\alpha\gg1$. This situation is typical for hard superconductors and thin superconducting films. Superconductivity in these materials can therefore be destroyed by Joule self-heating at $I\sim I_c\alpha^{-1/2}$, i.e., at currents well below the critical value I_c.

We conclude this section with several remarks concerning the applicability of the heat balance equation (2.1) to superconductors. The resistive state of superconductors is essentially inhomogeneous. In type-II superconductors this is caused by the formation of the vortex lattice, and in thin films and whiskers by the formation of magnetic flux tubes or of phase-slip centers (see, for example, Huebener, 1979; Tinkham, 1981). The macroscopic equation (2.1) is valid if the specimen temperature changes slowly whatever the microscopic scale. In other words, it is necessary that the London penetration depth λ_L and the penetration depth of the longitudinal electric field, l_E, be much less than the characteristic thermal length $L=(d\kappa/h)^{1/2}$, where κ is the thermal conductivity. It is also necessary that the electron and phonon distribution functions in quasiequilibrium (see, for example, Aronov *et al.*, 1981; Elesin and Kopaev, 1981). These conditions are normally met in hard and composite superconductors

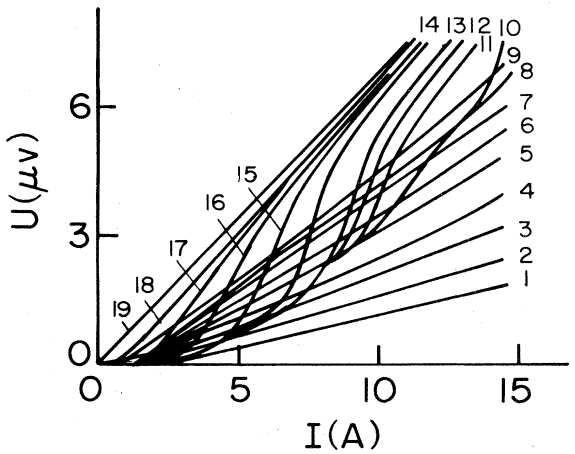

FIG. 5. I-V characteristic of deformed niobium in different magnetic fields H/H_{c2} (Vinnikov, Grigoriev, and Zharikov, 1976): (1) 0.28; (2) 0.36; (3) 0.44; (4) 0.52; (5) 0.60; (6) 0.67; (7) 0.71; (8) 0.78; (9) 0.83; (10) 0.915; (11) 0.92; (12) 0.93; (13) 0.95; (14) 0.96; (15) 0.97; (16) 0.98; (17) 0.99; (18) 0.995; (19) 1.3.

whose transverse dimensions are, as a rule, macroscopic, and in not excessively thin and pure superconducting films, with the exception of a narrow temperature range close to T_c.

Strictly speaking, it is necessary to take into account, in addition to the heat balance equation, the superconductor electrodynamics, i.e., we need to analyze the appropriate Maxwell equations. This may prove to be important for the stability of the critical state in hard and composite superconductors, yielding magnetic flux jumps (Wilson *et al.*, 1970; Mints and Rakhmanov, 1981, 1984). Throughout this review we assume the corresponding stability criteria to be satisfied, so that the analysis can be restricted to thermal processes only.

B. Normal metals

Thermal bistability of normal metals occurs in the interval $j_* < j < j^*$ where the $Q(T)$ and $W(T)$ curves have three intersection points (Fig. 1). Outside of this interval the conductor has a single, stable homogeneous state ($T=T_1$ for $j<j_*$ and $T=T_3$ for $j>j^*$). As an example, consider the case of bistability caused by a sharp growth of $\rho(T)$ in pure metals at low temperatures [Fig. 1(a)]. We shall find an expression for j^* based on the temperature dependences $\rho(T)$ and $W(T)$ at $T \ll T_D$, where T_D is the Debye temperature. We set $\rho(T)=KT^s$, $W(T)=(T^p-T_0^p)Y/d$, where K, Y, s, and p are positive constants independent of T and T_0 (for the sake of simplification, we neglect the residual resistivity). This form of $W(T)$ describes, for instance, the Kapitza resistance at the metal film-substrate interface ($p \simeq 4$) (Anderson, 1981; Wyatt, 1981; Kashani and Van Sciver, 1985), heat transfer to the liquid far from the boiling crisis ($p \simeq 1$), and heat transfer to gas coolant in the free convection mode ($p \simeq 1$) (Kutateladze, 1979; Kirichenko and Rusanov, 1983). Substituting the above-given formulas for $\rho(T)$ and $W(T)$ into Eqs. (2.4) and (2.5), one finds

$$j^* = \left[1-\frac{p}{s}\right]^{(s/p-1)/2} \left[\frac{pY}{sdKT_0^{s-p}}\right]^{1/2}, \tag{2.20}$$

$$T^* = \frac{T_0}{\left[1-\frac{p}{s}\right]^{1/p}}, \tag{2.21}$$

where T^* is the specimen temperature at $j=j^*$. An increase in current above the critical current density j^* results in a stepwise rise in T from $T=T^*$ to $T=T_3$ (see Fig. 1). This thermal instability of the low-temperature state (at $T=T_1$) occurs for $s>p$. This inequality holds, for example, for a metal film on a substrate when the electric resistance is described by the Bloch formula $\rho \propto T^5$ ($s=5, p=4$). Then $T^*=1.5T_0$, and the quantity $j^*=0.73(Y/dKT_0)^{1/2}$ increases as T_0 and d decrease.

Now we consider a situation of specimen bistability due to the boiling crisis of the coolant [Fig. 1(b)]. If the temperature dependence $\rho(T)$ is negligible, then

$$j^* = \left[\frac{q_{\max}}{d\rho}\right]^{1/2}, \quad j_* = \left[\frac{q_{\min}}{d\rho}\right]^{1/2}, \tag{2.22}$$

where $q(T)$ is the heat flux into the coolant per unit surface area of the specimen, $q_{\max}$ is the maximum value of $q(T)$ in the nucleate boiling mode, and $q_{\min}$ is its minimum value in the film boiling mode.

Figure 6 shows a typical $q=q(T)$ curve for liquid helium. In this case $q_{\max} \approx 0.7$ W/cm^{2}K, $q_{\min} \approx 0.15$ W/cm^{2}K, whence $j^*/j_* = (q_{\max}/q_{\min})^{1/2} = 2.16$. For commercial copper wire 1 mm in diameter ($\rho = 3\times10^{-8}$ Ωcm at $T_0=4.2$ K), Eqs. (2.22) give $j^*=3.06\times10^4$ A/cm^2 and $j_*=1.41\times10^4$ A/cm^2.

Likewise, we can consider thermal bistability due to the phase transition, resulting in a jump in $\rho(T)$ at $T=T_c$ (Fig. 7). An example of this transition is the melting of a metal as a result of Joule self-heating. In this case

$$j^* = \left[\frac{q(T_c)}{d\rho_-}\right]^{1/2}, \quad j_* = \left[\frac{q(T_c)}{d\rho_+}\right]^{1/2}, \tag{2.23}$$

where ρ_- and ρ_+ are the electric resistivities in the solid and liquid states, respectively, at $T=T_c$. Thus, in aluminum $\rho_+/\rho_- = 2.3$ (Zinoviev, 1984), so that $j^*/j_* = (\rho_+/\rho_-)^{1/2} = 1.52$.

If a conductor is immersed horizontally in a gas coolant, then in the free convection mode $q(T) \propto d^{-3(1+k)}(T-T_0)^{1+k}$, $k=0.125$–0.133 (Kutateladze, 1979). Substituting the expression for $q(T)$ into Eq. (2.23), we find (Abramov *et al.*, 1983)

$$I^* = j^* A \propto d^{1+1.5k}(T_c-T_0)^{(1+k)/2}. \tag{2.24}$$

Figure 8 plots I^* as a function of d in aluminum at liquid-nitrogen and room temperatures. Typically, j^* here is about 4×10^3–6×10^4 A/cm^2.

Note that in some metals, such as gallium, manganese, and bismuth, $\rho(T)$ decreases upon melting (Zinoviev, 1984). In contrast to the metals discussed in the present review, these conductors have S-shaped, not N-shaped, current-voltage characteristics, and bistability is produced

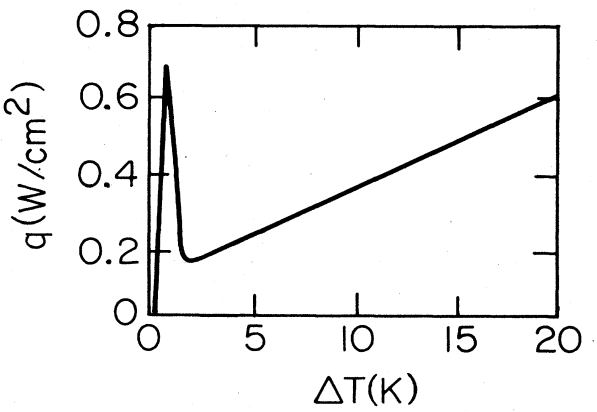

FIG. 6. Temperature dependence of the rate of heat flux $q(T)$ through liquid helium at $T_0=4.2$ K, $p=1$ atm (Maddock, James, and Norris, 1969).

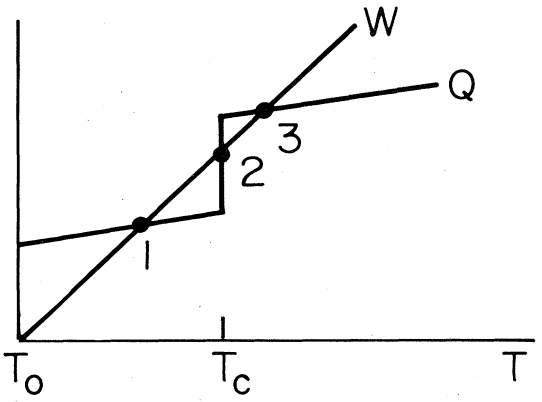

FIG. 7. Graphic solution of heat balance equation in the case of a first-order phase transition in a normal metal.

by varying E, not j.

It must be mentioned in conclusion that the heat balance equation (2.1) is written for the case of equal electron and lattice temperatures, $T_e = T$. This condition is violated if the rate of energy transfer between electrons and the lattice is much less than the power of heat transfer to the coolant, $(T_e - T)\nu_e/\tau_\varepsilon \ll (T - T_0)h/d$; i.e.,

$$d \ll d_h \sim \frac{h\tau_\varepsilon}{\nu_e} ,$$

where τ_ε is the inelastic collision time in electron-phonon collisions, and $\nu_e = \gamma T_e$ is the electron specific heat. The difference between T_e and T arises in thin films and whiskers at low temperatures, when

$$\tau_\varepsilon \sim \frac{\hbar}{k_B T_D}(T_D/T)^3$$

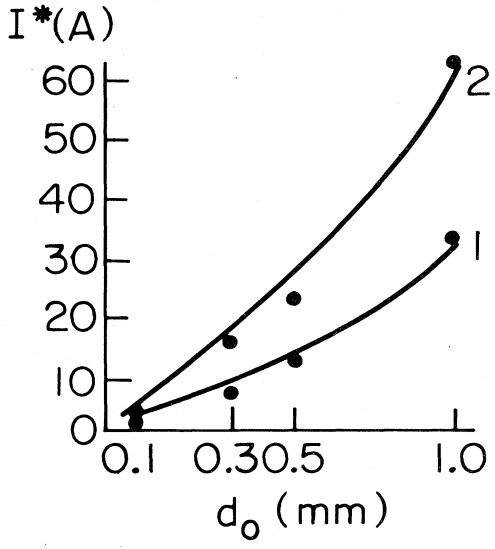

FIG. 8. The curves $I^* = I^*(d_0)$ for aluminum in the case of free convection of the coolant gas: curve 1, air, $T_0 = 300$ K; curve 2, helium vapor, $T_0 = 78$ K (Abramov *et al.*, 1983); $d_0 = d/4$.

and $d_h \propto T^{-4}$, where k_B is the Boltzmann constant and T_D is the Debye temperature. Thus at $T = T_c$ in tin film $\tau_\varepsilon = 2\times10^{-10}$ s, $h = 3$ W/cm^2 K, $\nu_e \simeq 3.6\times10^{-4}$ J/cm^3 K, whence $d_h \sim 100$ Å. The heat balance condition in the form (2.1) holds, therefore, for $d_h \ll d \ll d_c$. This is the case treated throughout this review. The effects of electron overheating on the S-N transition in thin films were discussed by Shklovsky (1975).

C. Composite superconductors

The practical applications of hard superconductors are mostly based on the use of composite materials, in which superconducting filaments are embedded in a normal high-conductivity metal matrix (see, for example, Brechna, 1973; Wilson, 1983). This technique greatly reduces the thermal, electrodynamical, and mechanical instabilities characterizing hard superconductors (Wilson *et al.*, 1970; Mints and Rakhmanov, 1981, 1984).

Unfortunately, at sufficiently high transport current densities the contact of the superconducting and normal metals is not sufficiently effective to prevent thermal bistability. As a result, superconductivity in composite materials can also be destroyed by Joule self-heating at currents $I > I_m$ much lower than the maximum possible superconducting current I_c. We have mentioned already that this behavior may be caused by the N-S phase transition in the superconducting filaments, by steep temperature dependence of resistivity $\rho_n(T)$ of the normal matrix, and by the boiling crisis in the coolant. A composite superconductor is thus an example of a system in which various mechanisms of thermal bistability, each typical of a hard superconductor, normal metal, or coolant, can manifest themselves simultaneously. Consequently, thermal multistability may develop, creating a much more complicated situation. For this reason, we rely in this section on a lucid graphic analysis of the heat balance equation (Stekly, 1965; Maddock, James, and Norris, 1969).

Figure 9 gives an example of the graphical solution of Eq. (2.1) for different values of j. The heat release $Q(T)$ in a composite superconductor is described by the formula

$$Q(T) = \begin{cases} 0, & T < T_r(j) , \\ [j - j_c(T)]j\rho, & T > T_r(j) , \end{cases} \tag{2.25}$$

$$\rho = \frac{\rho_n \rho_f}{x_n \rho_f + x_s \rho_n} , \tag{2.26}$$

where $j = I/A$ and $j_c = I_c/A$ are the cross-section-averaged densities of the transport and critical currents, x_n and x_s are the volume fractions of the normal metal (n) and the superconductor (s), and ρ_n and ρ_f are their respective resistivities; $x_n + x_s = 1$.

If current is sufficiently high, the curves $Q(T)$ and $W(T)$ in Fig. 9 intersect at several points. The points 0, 1, and 3 correspond to the stable values of the specimen temperature $T = T(j)$, namely, to the superconductor,

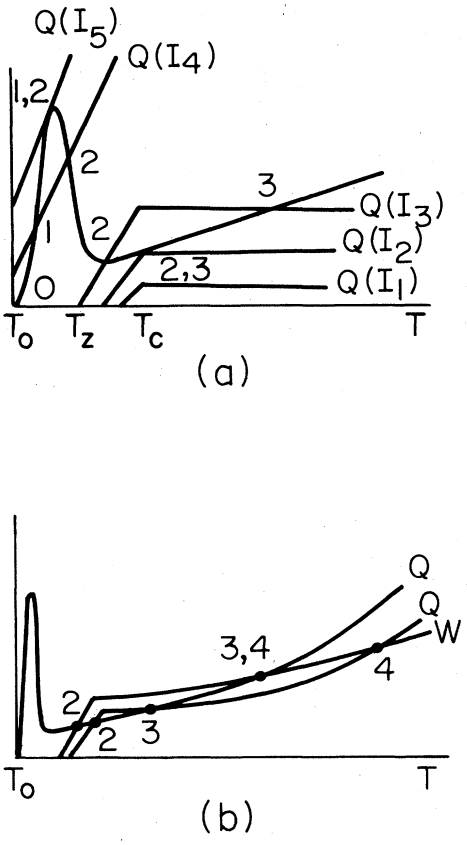

FIG. 9. Example of a graphic solution of the heat balance equation for a composite superconductor: (a) $\alpha(T_0)<1$; (b) $\alpha(T_0)>1$; $I_{\rm I}<I_{\rm II}<I_{\rm III}<I_{\rm IV}<I_{\rm V}$.

resistive, and normal states, respectively. The normal state can exist only under sufficiently intensive self-heating when j exceeds the critical value j_m which corresponds to the merger of points 2 and 3 in Fig. 9. The quantity j_m defined in this manner is the minimum current density for the existence of the normal phase.

The quantity j_m depends on how the curves $Q(T)$ and $W(T)$ come in contact for the first time (as j increases). Two cases are possible here. In the first of them $Q(T)$ and $W(T)$ touch at $T=T_c$ because of the knee on the function $Q(T)$ (see Fig. 9). Then j_m is given by Eq. (2.16) with $\rho_s \to \rho \ll \rho_s$ and the thermal bistability condition $j_m < j_c$ is equivalent to the inequality $\alpha > 1$, where

$$\alpha = \frac{I_c^2 \rho(T_c)}{AP(T_c - T_0)h(T_c)} \tag{2.27}$$

is the Stekly parameter of the composite superconductor (Stekly, 1964; Altov *et al.*, 1977; Wilson, 1983). The currents j_m and j_c are related by a simple formula,

$$j_m = j_c \alpha^{-1/2} . \tag{2.28}$$

A situation is also possible in which the curves $Q(T)$ and $W(T)$ come in contact not at $T=T_c$. In this case j_m is found from the system of Eqs. (2.4) and (2.5), and is dependent on the specific form of the functions $Q(T)$ and $W(T)$.

Let us analyze the thermal destruction of superconductivity in a current-carrying composite superconductor, choosing some simple examples. Figure 9(a) illustrates the situation in which $\rho(T)$ is weakly dependent on T and $\alpha(T_0)<1$, where $\alpha(T_0)$ is the value of the Stekly parameter for $\rho=\rho(T_0)$ and $h \equiv h(T_0)$. In this case the superconducting state at $j<j_m$ is absolutely stable. Metastability sets in the range $j_m<j<j_c$ because a strong perturbation may destroy superconductivity and transform the specimen to the stable normal state at $T=T_3$. At $j>j_c$ the composite transforms to the resistive metastable state represented by point 1 in Fig. 9(a). This state exists at $j_c<j<j_q$, where j_q corresponds to the merger of points 1 and 2. An increase in current density above j_q results in a jumpwise transition to the stable normal state $T=T_3$ (provided it exists at $j>j_q$), or in runaway heating of the specimen. This effect arises because at $j>j_q$ the Joule self-heating becomes so intensive that the generated heat cannot be completely transferred to the coolant.

An elementary estimate of j_q can be obtained by approximating $W(T)$ by broken lines (Fig. 9) and assuming $\rho(T)=\text{const}$ and $j_c(\theta)=(1-\theta)j_0$. Then

$$j_q = \left[\tfrac{1}{2}(1-\delta_W) + \left[\tfrac{1}{4}(1-\delta_W)^2 + \frac{\delta_W}{\alpha} \right]^{1/2} \right] j_c , \tag{2.29}$$

where $\delta_W = \Delta T_k/(T_c - T_0)$, and $\Delta T_k = T_k - T_0$ is the maximum possible temperature difference between the specimen and the coolant in the nucleate boiling regime (Fig. 6). In superconductor composites based on niobium stannide or niobium-titanium alloys the quantity $\delta_W \ll 1$ ($T_0=4.2$ K), so that Eq. (2.19) is simplified:

$$j_q = \left[\left(\frac{1}{\alpha} - 1 \right) \frac{\Delta T_k}{T_c - T_0} + 1 \right] j_c . \tag{2.30}$$

Hence a decrease in the Stekly parameter widens the interval $j_c<j<j_q$ in which the resistive state is stable. Assuming $\alpha=0.5$, $\Delta T_k=1$ K, $T_c=10$ K, $T_0=4.2$ K, one finds $j_q=1.17 j_c$.

If $\alpha(T_0)>1$ or $\partial W/\partial T \mid_{T_0} < \partial Q/\partial T \mid_{T_0, j_c}$, the resistive state is unstable. This case is illustrated in Fig. 9(b), where the temperature dependence $\rho(T)$ is also taken into account. As a result of this dependence, the stable normal state $T=T_3$ exists in a finite interval $j_m<j<j_b$, where the quantity j_b corresponds to the merger of points 3 and 4 in Fig. 9(b). An increase in current density above j_b results in the runaway heating of the specimen, similar to what takes place in normal metals at $j>j^*$. The two quantities j_b and j_q are distinct roots of the system of equations (2.4) and (2.5).

Figure 10 plots more complicated situations corresponding to multistability of current-carrying composite superconductors. In Fig. 10(a) this complication is caused by a S-N transition and the transition to film boiling of the coolant. Such a situation is realized in composite superconductors clad in thermal insulation. As a result, the

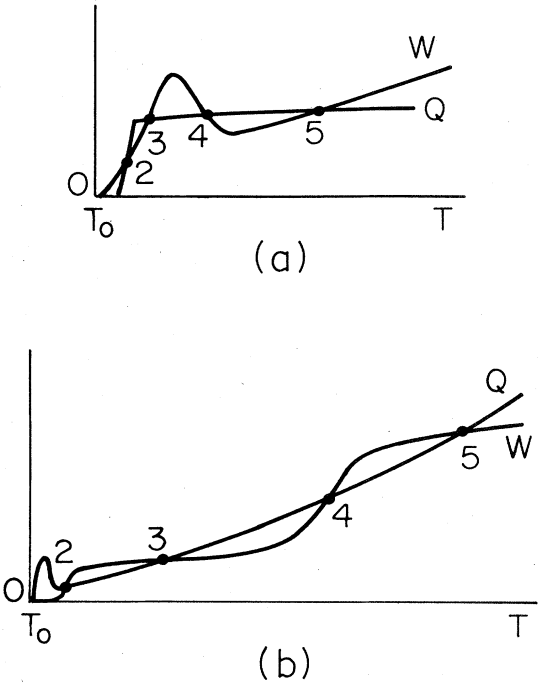

FIG. 10. Graphic solution of heat balance equation in the case of multistability of composite superconductors due to (a) thermal insulation and (b) steep temperature dependence $\rho_n(T)$ of the normal matrix.

temperature range of stable nucleate boiling, ΔT_k, is widened and five intersection points appear on the curves $Q(T)$ and $W(T)$ (see, for example, Maddock *et al.*, 1969; Dresner, 1976; Altov *et al.*, 1977).

The transition to the film boiling regime is not significant in the case shown in Fig. 10(b). Here the multistability of the composite superconductor is caused by the S-N transition and by the temperature dependence $\rho(T)$ typical of a normal matrix fabricated of a sufficiently pure metal.

The fact that the curves $Q(T)$ and $W(T)$ have several intersection points results in N-shaped current-voltage characteristics of composite superconductors, just like those found in normal metals. Each branch of the I-V characteristic corresponds to one possible homogeneous state $T=T(j)$ of the composite: the dropping branches correspond to unstable, and the rising branches to stable states $T=T(j)$. The N-shaped form of the current-voltage characteristics results in various hysteresis effects in the destruction and recovery of superconductivity in current-carrying conductors (Altov *et al.*, 1977). The factors that play an important role here are the prehistory of the specimen and the types of external perturbations. Such perturbations can lead to jumpwise transitions between stable states, e.g., a transition from $T=T_0$ to $T=T_3$ or from $T=T_0$ to $T=T_5$ in Fig. 10(b).

The dynamics of these transitions is described by Eq. (2.6). Assume that the specimen temperature jumps at $t=0$ to a value $T=T(0)$. Further evolution of $T(t)$ will be governed by the sign of the difference $f(T)=W(T)-Q(T)$: temperature will decrease if $f[T(0)]>0$, and it will increase if $f[T(0)]<0$. This statement is illustrated in Fig. 11, where the arrows indicate the direction of relaxation of the initial perturbation. Thus it is sufficient to heat a specimen to a temperature $T>T_2$ in order to achieve the transition from the superconducting ($T=T_0$) to the normal state ($T=T_3$). Note that such a transition can also be fluctuation induced, e.g., induced by external thermal noise (Pasmanter, Bedeaux, and Mazur, 1978; Chechetkin, Levchenko, and Sigov, 1985).

III. PROPAGATION OF SWITCHING WAVES IN BISTABLE CONDUCTORS

Homogeneous transitions between the stable states $T=T_1$ and $T=T_3$, discussed in the preceding section, are realized either in sufficiently short specimens or in the presence of uniform perturbations. But in most cases the transitions between these states (these phases) are initiated by local perturbations, which result in the nucleation of a new phase, which then propagates to cover the whole specimen. In this section we treat the steady-state propagation of the boundaries of such a domain (of domain walls), separating two phases with $T=T_1$ and $T=T_3$ [Fig. 2(a)].

The distribution of temperature along a homogeneous current-carrying conductor is described by the nonlinear heat conduction equation

$$[\nu(T)+G\delta(T-T_c)]\frac{\partial T}{\partial t}=\frac{\partial}{\partial x}\kappa(T)\frac{\partial T}{\partial x}+Q(T)-W(T)\ , \tag{3.1}$$

where κ is the thermal conductivity, $\delta(x)$ is the delta function, and G is the specific heat generated (absorbed) at $T=T_c$ if the system manifests a first-order phase transition.

Consider a domain wall propagating at a constant velocity v. Then $T=T(x-vt)$, and in the comoving frame of reference Eq. (3.1) takes the form $[T(0)=T_c]$

$$\frac{d}{dx}\kappa\frac{dT}{dx}+\nu v\frac{dT}{dx}+Q-W+vG\,\mathrm{sgn}\left[\frac{dT}{dx}\right]\delta(x)=0\ . \tag{3.2}$$

This equation, describing the domain wall, has a solution only at a specific value of v. The objectives of this section are to find the temperature distribution $T=T(x-vt)$ and to analyze the velocity v as a function of specimen parameters.

This problem can be traced back, presumably, to the pioneer paper by Kolmogorov, Petrovsky, and Piskunov

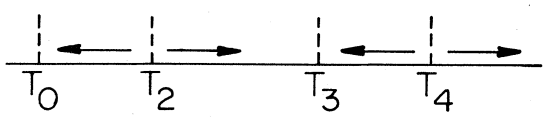

FIG. 11. The direction of temperature relaxation in the case of uniform perturbations.

(1937). Its various mathematical aspects were later discussed by a large number of authors, such as Kametaka (1976), Aronson, and Weinberger (1978), Fife (1979), and some others. The same problem was also analyzed in the framework of various physical phenomena, such as combustion waves (Frank-Kamentsky, 1967; Zeldovich *et al.*, 1980), switching waves in the gas or semiconductor plasma (Volkov and Kogan, 1968; Scott, 1970; Bonch-Bruevich *et al.*, 1972; Bass and Gurevich, 1975), optical gas discharge (Raizer, 1980), thermal breakdown of superconductivity in a current-carrying conductor (Maddock, James, and Norris, 1969), etc. (other examples are given in the reviews of Büttiker and Landauer, 1982; Gurevich and Mints, 1984a). Here we give the main conclusions formulated in these papers, to the extent that they will be necessary for the subsequent description of thermal switching waves in homogeneous and inhomogeneous normal metals and superconductors.

In order to make sure that Eq. (3.2) indeed has a solution describing the domain wall, it will be convenient to make use of an illustrative qualitative analogy with the equation of motion of a classical particle of mass κ, subjected to an external force $f=W-Q$ and frictional force $-\nu v\,dT/dx$. At a point $T=T_c$ the particle undergoes an impact which changes its momentum by $-vG\,\mathrm{sgn}(dT/dx)$ (here T and x play the roles of "coordinate" and "time"). Multiplying (3.2) by $\kappa\,dT/dx$ and then integrating from x to ∞, we arrive at the conservation laws for "energy" and "momentum":

$$\frac{1}{2}\left[\kappa\frac{dT}{dx}\right]^2-v\int_x^\infty \nu\kappa\left[\frac{dT}{dx}\right]^2dx-S(T)=\frac{vG\kappa}{2}\left[\left|\frac{dT}{dx}\right|_{+0}+\left|\frac{dT}{dx}\right|_{-0}\right],\quad x<0\,, \tag{3.3}$$

$$\kappa\frac{dT}{dx}\bigg|_{+0}-\kappa\frac{dT}{dx}\bigg|_{-0}=-vG\,\mathrm{sgn}\left[\frac{dT}{dx}\right]_{x=0}. \tag{3.4}$$

The first term in Eq. (3.3) represents the kinetic energy of the particle, the second the work of the friction force, and the third the potential energy $S(T)$ corresponding to a force $f(T)$,

$$S(T)=\int_{T_1}^{T}(W-Q)\kappa\,dT\,. \tag{3.5}$$

A typical $S=S(T)$ curve of a bistable system is shown in Fig. 12 for three values of current. The domain wall corresponds to a trajectory $T=T(x)$ in the potential $-S(T)$, on which the particle leaves point 1 at an infinitely low initial velocity, and then arrives at point 3 at zero final velocity. For such a trajectory to exist, it is necessary that the energy difference $\Delta U=S(T_3)$ be compensated for by the work done by the friction force and by the change in the kinetic energy of the particle upon impact at the point $T=T_c$. This condition prescribes the velocity v of the domain wall. Assuming in Eq. (3.3) $x=-\infty$, one finds

$$v=-\frac{S_3(j)}{\int_{-\infty}^{\infty}\kappa\nu\left[\frac{dT}{dx}\right]^2dx+\frac{G\kappa}{2}(T_c)\left[\left|\frac{dT}{dx}\right|_{+0}+\left|\frac{dT}{dx}\right|_{-0}\right]}\,, \tag{3.6}$$

where the notation $S_3(j)\equiv S[T_3(j),j]$ is used. Figure 12 shows that the function $S_3(j)$ decreases with increasing j, passing through zero at some $j=j_p$. The velocity $v(j)$, therefore, increases with increasing j, and vanishes at $j=j_p$ ($v>0$ for $j>j_p$ and $v<0$ for $j<j_p$). The domain wall is thus a switching wave which transforms the bistable conductor from one stable state, $T=T_1$, to another, $T=T_3$, or vice versa, depending on the relation between j and j_p.

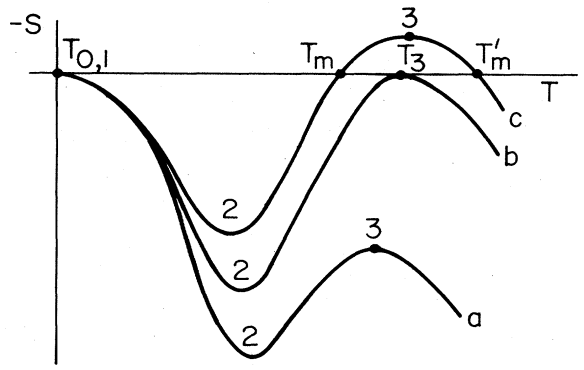

FIG. 12. $S=S(T)$ for a, $j<j_p$; b, $j=j_p$; and c, $j>j_p$.

The reversal in the sign of $v(j)$ at $j=j_p$ points to the metastability of the homogeneous state $T=T_1$ at $j>j_p$ and of $T=T_3$ at $j<j_p$. As a result, a sufficiently large "seed" domain of the $T=T_3$ phase expands at $j>j_p$ and collapses at $j<j_p$. At $j=j_p$ the interface between the $T=T_1$ and $T=T_3$ phases is in neutral equilibrium ($v=0$). The quantity j_p is found from the equation $S_3(j_p)=0$ or from

$$\int_{T_1}^{T_3}[W(T)-Q(T)]\kappa(T)dT=0\,, \tag{3.7}$$

where $T_1=T_1(j_p)$ and $T_3=T_3(j_p)$. If the dependence of κ on T is negligible, Eq. (3.7) transforms to

$$\int_{T_1}^{T_3}(W-Q)dT=0\,. \tag{3.8}$$

This relation is usually called the "equal areas theorem" (the relevant areas are shadowed in Fig. 1).

Equation (3.6) is not closed for $v(j)$ because it contains in its denominator a v-dependent derivative dT/dx. An explicit expression for v can only be derived in the interval $|j-j_p|\ll j_p$, where the velocity $v(j)$ is low. In this case dT/dx can be found from Eq. (3.3), whose solution

describes a domain wall at rest if we assume $v=0$:

$$x=\int_T^{T_c}(2S)^{-1/2}\kappa\,dT\ . \tag{3.9}$$

Here the origin of coordinates is placed at the point $T=T_c$. Consequently,

$$v(j)=\frac{(j-j_p)2^{-1/2}}{\int_{T_1}^{T_3}\nu S^{1/2}dT+GS_c^{1/2}}\left|\frac{\partial S_3}{\partial j}\right|_{j_p}, \tag{3.10}$$

where $S_c\equiv S(T_c,j)$. The sign of $v(j)$ is reversed at $j=j_p$, corresponding to the propagation of the "hot" phase $T=T_3$ at $j>j_p$ and to its collapse at $j<j_p$.

In the general case, $v(j)$ can be found for arbitrary j only numerically. It is then convenient to rewrite Eq. (3.2) for a new variable $s=\kappa\,dT/dx$. Neglecting, for the sake of simplification, the latent heat G of the phase transition, one finds

$$s\frac{ds}{dT}+\nu vs=\kappa f\ . \tag{3.11}$$

The solution of this equation, describing the switching wave, satisfies the necessary boundary conditions $s(T_1)=s(T_3)=0$ only for a specific value of v. The corresponding integral curve $s=s(T)$ in the phase plane is a separatrix connecting the points $T=T_1$ and $T=T_3$ (Fig. 13).

In the opposite limiting case, when the latent heat of the transition

$$G\gg\int_{T_1}^{T_3}\nu\,dT\ ,$$

the general form of the expression for v can be obtained. The term $\nu v\,dT/dx$ in Eq. (3.2) can now be neglected, after which the first integral in (3.3) is evaluated in a straightforward manner. Substituting the thus obtained values of $dT/dx\mid_{\pm 0}$ into the boundary condition (3.4), one finally arrives at

$$v(j)=\frac{\sqrt{2}}{G}\{S_c^{1/2}(j)-[S_c(j)-S_3(j)]^{1/2}\}\ . \tag{3.12}$$

As might be expected, in the limit $G\gg(T_3-T_1)\nu$ and $S_3\ll S_c$ Eq. (3.12) transforms into (3.10) derived for the cases of $|j-j_p|\ll j_p$, if one takes into account that

$$S_3(j)\approx(j-j_p)\left|\frac{\partial S_3}{\partial j}\right|_{j_p}\ .$$

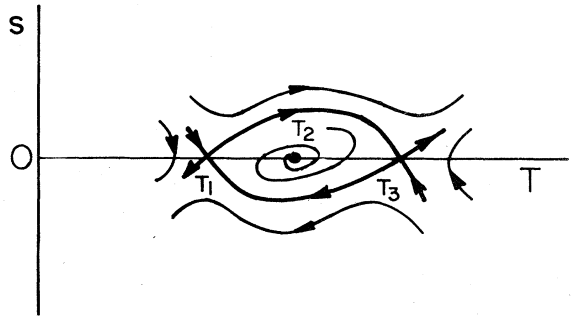

FIG. 13. Phase plane of Eq. (3.11).

A. Normal metals

Let us consider the propagation of switching waves in current-carrying normal metals. We begin with the case of bistability due to the transition to film boiling in the coolant. Then the specimen has at $j_*<j<j^*$ two allowed stable homogeneous states corresponding to either the nucleate ($T=T_1$) or film boiling ($T=T_3$) regime. If a conductor in the state $T=T_1$ is subjected to a sufficiently strong local perturbation, a region covered by vapor film is formed on the conductor surface. If $j>j_p$, the vapor film region widens and finally covers the whole specimen. Such phenomena were experimentally observed at liquid-helium (Altov *et al.*, 1977), liquid-nitrogen (Ivanchenko *et al.*, 1983), and room temperatures (Zhukov *et al.*, 1979, 1983). As an illustration, Fig. 14 shows the typical patterns of the transition from the nucleate to film boiling regime on a platinum current-carrying filament cooled by water at $T_0\approx 90$–$100\,^{\circ}$C.

It is not easy to derive an analytical expression for the velocity of propagation $v(j)$ of the vapor region boundary, mostly because of a complicated nonlinear function $W(T)$ at the boiling regime transition. For this reason we choose a simple model in which the velocity $v(j)$ is found exactly (Zhukov *et al.*, 1979). The real $W(T)$ curve is approximated in this model by two straight lines, and $\rho(T)$ and $\kappa(T)$ are independent of T (Fig. 15). Then Eq. (3.2)

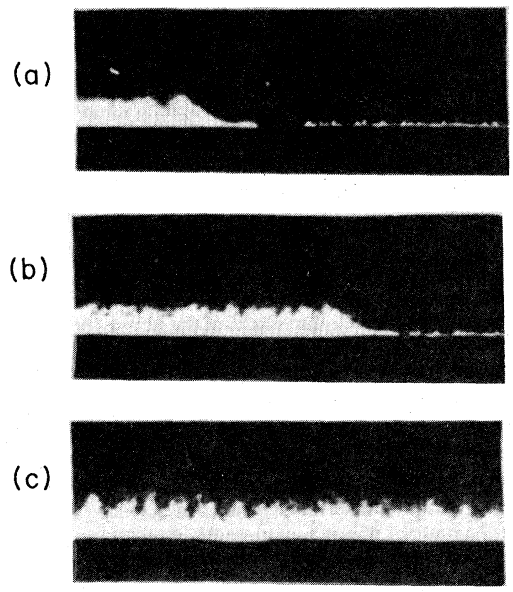

FIG. 14. Propagation of vapor film on the surface of water-cooled platinum wire heated by current. $T_0=371$ K, $I=2.96$ A, $v=1.1$ cm/s (Zhukov, Barelko, and Merzhanov, 1979).

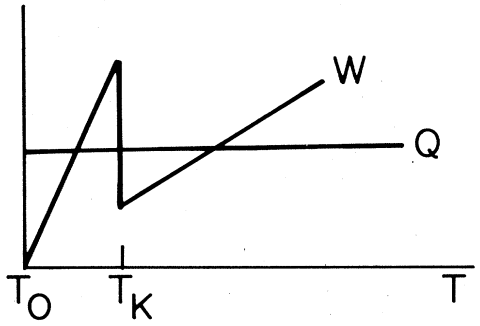

FIG. 15. Model functions $Q(T)$ and $W(T)$ used for calculating the velocity of switching waves for the transition from nucleate to film boiling regime.

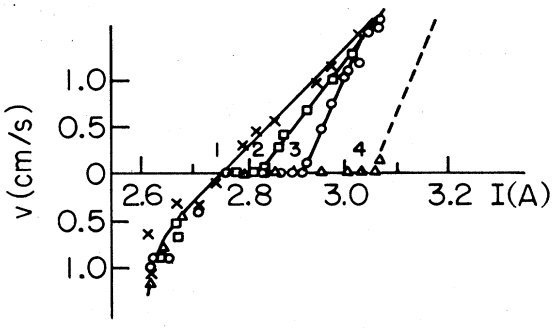

FIG. 16. Velocity $v(I)$ of vapor film propagation along the surface of platinum wire, 1 mm in diameter, water-cooled at four different temperatures: (1) $T_0=371$ K; (2) $T_0=369.5$ K; (3) $T_0=368$ K, (4) $T_0=366$ K (Zhukov, Barelko, and Merzhanov, 1979).

can be written in the following dimensionless form:

$$\begin{aligned}&\theta''+c\theta'-\theta+i^2=0, \quad \theta<1\ ,\\ &\theta''+c\theta'-\theta\delta_h+i^2=0, \quad \theta>1\ ,\end{aligned} \tag{3.13}$$

where $\theta=(T-T_0)/(T_k-T_0)$, $\delta_h=h_f/h_b$ is the ratio of the heat transfer coefficients of the nucleate (h_b) and film boiling (h_f) regimes, T_k is the boiling regime transition temperature, $i=j/j^*$, j^* is given by (2.22), $c=v/v_h$, and $v_h=L/t_h$, where L and t_h are the characteristic thermal length and time,

$$L=\sqrt{d\kappa/h_b}, \quad t_h=\frac{\nu d}{h_b}\ . \tag{3.14}$$

The quantities L and t_h have the following physical meaning: L is the length over which temperature decays from the value produced by a steady-state point heater, and t_h is the time necessary for the cooling of a conductor heated by a uniform thermal pulse. The piecewise-linear equation (3.13) is solved exactly, and the following expression for v is obtained:

$$v=v_h\frac{(i^4-\delta_h)}{i[(1-i^2)(i^2-\delta_h)]^{1/2}}\ , \tag{3.15}$$

$$v_h=\frac{1}{\nu}\sqrt{h_b\kappa/d}\ . \tag{3.16}$$

As follows from Eqs. (2.22) and (3.15),

$$j^*=\left[\frac{(T_k-T_0)h_b}{d\rho}\right]^{1/2}, \tag{3.17}$$

$$j_*=j^*\delta_h^{1/2}, \quad j_p=j^*\delta_h^{1/4}\ . \tag{3.18}$$

In this model the velocity $v(j)$ monotonically increases as j increases, goes through zero at $j=j_p$, and tends to minus and plus infinity at $j=j_*$ and $j=j^*$, respectively. Typical experimental curves $v=v(j)$ are plotted in Fig. 16. Note that the experiment reveals a finite current interval in which the wave does not propagate ($v=0$). This effect will be discussed in Sec. VI.

The characteristic width L_W of the wave front in the selected model depends on c as follows:

$$L_W=\frac{L}{\left[\frac{c^2}{4}+1\right]^{1/2}-\frac{c}{2}}+\frac{L}{\left[\frac{c^2}{4}+\delta_h\right]^{1/2}+\frac{c}{2}}\ . \tag{3.19}$$

The function $L_W=L_W(c)$ is plotted in Fig. 17. If $\delta_h\ll 1$, the curve $L_W(c)$ is essentially nonsymmetrical. In the limit $\delta_h\to 0$ the minimum value $L_W=3\sqrt{3}L/2$ is reached at $c=2/\sqrt{3}$, i.e., for $j=\sqrt{2}j^*/\sqrt{3}=0.82j^*$.

Let us evaluate the characteristic values of the parameters of switching waves under the conditions of the transition to film boiling of helium ($T_0=4.2$ K, $\delta_h=0.025$). Taking typical characteristics, say, of commercial copper, $\kappa=1$ W/cm K, $\nu=10^{-3}$ J/cm^3, and assuming $h_b=1$ W/cm^2 K, $d=0.01$ cm, we obtain $j_*=0.16j^*$, $j_p=0.4j^*$, $L=0.1$ cm, $t_h=10^{-5}$ s, $v_h=100$ m/s.

Another example of switching waves is found in the waves generated in the phase transition that is accompanied by a jump in $\rho(T)$. This situation arises, for instance, when metals are melted by intensive Joule heating, so that at $j_*<j<j^*$ a boundary separating the solid and the liquid phases can propagate through the conductor. In order to describe thermal switching waves in conduc-

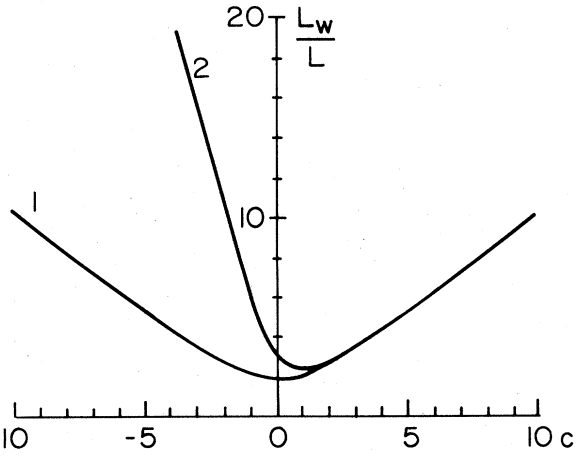

FIG. 17. $L_w=L_w(c)$ for (1) $\delta_h=1$, and (2) $\delta_h=0.2$.

tors with a first-order phase transition, let us analyze the Stefan problem under the following assumptions (Abramov *et al.*, 1985): $\rho(T)=\rho_1+(T-T_0)\rho'$, $\kappa(T)=\kappa_-$ for $T<T_c$, and $\rho(T)=\rho_2+(T-T_0)\rho'$, $\kappa(T)=\kappa_+$ for $T>T_c$, where $\kappa_\pm$, $\rho_{1,2}$, ρ', ν, and h are independent of T. The heat conduction equation (3.2) is then piecewise linear and is easily solved. Assuming that $G \ll (T_c-T_0)\nu$, and that κ and ρ at $T=T_c$ are related by the Wiedemann-Franz law, we obtain

$$v=v_h\frac{(i^4-\delta_r)(k-i^2)^{1/2}}{i[(1-i^2)(i^2-\delta_r)]^{1/2}}, \tag{3.20}$$

$$v_h=\frac{1}{\nu}\sqrt{\kappa_- h/kd}, \quad k=1+\frac{\rho_1}{(T_c-T_0)\rho'}, \tag{3.21}$$

where $i=j/j^*$, and $\delta_r=\rho_-/\rho_+<1$ is the ratio of resistivities of the solid (ρ_-) and liquid (ρ_+) phases at the phase transition point. In qualitative terms, the function $v(j)$ is similar to that realized in the case of the boiling crisis [see Eq. (3.15)]. The critical current density j^* is found from Eq. (2.23), and j_* and j_p from Eq. (3.18) with $\delta_h\to\delta_r$. The width of the phase transition wave front is

$$L_W=\frac{L}{(k-i^2)^{1/2}}\left[\left[\frac{c^2}{4}+1\right]^{1/2}+\left[\frac{c^2}{4}+\delta_r\right]^{1/2}\right], \tag{3.22}$$

where $c(i)$ is given by Eq. (3.20). If $k\gg 1$, the length L_W monotonically increases with increasing $|c|$ (see Fig. 17).

In the other limiting case, $G\gg(T_c-T_0)\nu$, the general formula (3.12) yields for $v(j)$

$$v=\frac{v_h k}{g}\left[\frac{1}{\sqrt{\delta_r}}+1\right]\frac{(i^2-\delta_r^{1/2})}{(k-i^2)^{1/2}}, \tag{3.23}$$

where $g=G/(T_c-T_0)\nu$. If $g\gg 1$, the wave velocities $v(j^*)$ and $v(j_*)$ remain finite, in contrast to the case $G=0$, in which the model under consideration gives $v(j^*)=\infty$ and $v(j_*)=-\infty$ [see Eq. (3.20)].

In most pure metals at room temperatures the parameters k and g are of the order of unity (Zinoviev, 1984). Thus, in air-cooled aluminum wire ($T_0=300$ K) 0.3 mm in diameter, the thermal length is $L\simeq 1$ cm, and $k\simeq 1.3$ (Abramov *et al.*, 1985). Assuming $\kappa_-=2.3$ W/cm K and $\nu=2.5$ J/cm^{3}K (Schulze, 1967), we obtain $t_h\sim L^2\nu/\kappa\sim 1$ s, $v_h\sim 1$ cm/s.

B. *N-S* interface in current-carrying superconductors

1. Minimum normal-zone propagating current

The propagation of thermal switching waves in current-carrying superconductors occurs at $j_p<j<j_c$. At $j>j_p$ the superconducting state is metastable and can be destroyed by a sufficiently large local perturbation which results in nucleation and subsequent propagation of the normal zone across the whole specimen (Breemer and Newhouse, 1958; Newhouse, 1964; Maddock, James, and Norris, 1969; Altov *et al.*, 1977; Wilson, 1983). Consequently, a normal zone created by some factor has to expand if $j>j_p$ and to collapse if $j<j_p$. The *N-S* interface between the normal ($T=T_3$) and the superconducting phase ($T=T_0$) is at equilibrium at the current $I_p=j_pA$ referred to as the minimum normal-zone propagating current (Maddock, James, and Norris, 1969).

In the general case the quantity j_p is found from Eq. (3.7). Unfortunately, actual functions $Q(T)$, $W(T)$, and $\kappa(T)$ in superconductors are too complex to permit the analytical derivation of j_p directly from Eq. (3.7). Consider, therefore, a simple model in which j_p is calculated exactly (Keilin *et al.*, 1967). This model assumes that $j_c(T)$ decreases linearly with increasing T, and κ, ρ, and h are independent of T. In this case

$$j_p=\frac{j_c}{2\alpha}(\sqrt{1+8\alpha}-1). \tag{3.24}$$

As follows from Eq. (3.24), $\alpha\geq 1$ implies $j_p\leq j_c$. Therefore normal-zone propagation in the interval $j_p<j<j_c$ is then possible only if $\alpha>1$, which coincides with the condition of thermal bistability. In the limit $\alpha\gg 1$ Eq. (3.24) gives $j_p=(2/\alpha)^{1/2}j_c$, so that the interval of currents $I_p<I<I_c$ in which the thermal propagation of the normal zone is possible becomes wider as the Stekly parameter increases.

Despite the simplicity and the lucidity of this model, it neglects certain important features of the temperature dependences $Q(T)$, $W(T)$, and $\kappa(T)$ in superconductors. First of all, the boiling crisis drastically reduces the heat transfer, $W(T)$, at $T\gtrsim T_k$ (Figs. 6 and 15). Correspondingly, we turn to a more realistic model that takes this factor into account (see, for example, Cesnak, 1983).

Assume again that κ and ρ are independent of T, and $j_c(\theta)=(1-\theta)j_c$, where $\theta=(T-T_0)/(T_c-T_0)$ is the dimensionless temperature. Then the heat generation is $Q(\theta)=\rho j_c^2 i^2 r(\theta)$, where $i=j/j_c$ and

$$r(\theta,i)=\begin{cases}0, & \theta<1-i,\\ \dfrac{\theta-1+i}{i}, & 1-i<\theta<1,\\ 1, & \theta>1.\end{cases} \tag{3.25}$$

For $W(T)$ the piecewise-linear approximation can be used:

$$W(T)=\frac{h_b}{d}(T-T_0), \quad T<T_k,$$
$$W(T)=[q_0+h_f(T-T_k)]d^{-1}, \quad T>T_k, \tag{3.26}$$

where h_b, h_f, and q_0 are independent of T. Substituting Eq. (3.25) into (3.7), we arrive at the following equation for $i_p=j_p/j_c$:

$$\alpha_f^2 i_p^4-2\alpha_f i_p^2(1+\omega_m-\theta_k)+\omega_m^2-\theta_k^2\delta_h^{-1}=-\alpha_f i_p^3, \tag{3.27}$$

$$\omega_m=\frac{q_0}{(T_c-T_0)h_f},\quad \theta_k=\frac{T_k-T_0}{T_c-T_0},\quad \alpha_f=\frac{\rho j_c^2 d}{(T_c-T_0)h_f}, \tag{3.28}$$

where $\delta_h=h_f/h_b<1$.

In the limit $\alpha_f\gg 1$, $\max(\omega_m^2,\delta_h^{-1}\theta_k^2)\ll 1$, the solution of Eq. (3.27) is

$$i_p=\sqrt{2/\alpha_f}\ . \tag{3.29}$$

In this case the value of i_p is not very sensitive to the detailed shape of the $W(T)$ curve and is mostly determined by the heat-transfer coefficient h_f in the film boiling regime. If, however, $(\omega_m^2,\theta_k^2\delta_h^{-1})\gg\alpha_f^{-1/2}$, we can neglect the right-hand side of Eq. (3.27). This yields

$$i_p=\frac{1}{\alpha_f^{1/2}}\{1+\omega_m-\theta_k+[(1+\omega_m-\theta_k)^2+\theta_k^2\delta_h^{-1}-\omega_m^2]^{1/2}\}^{1/2}\ . \tag{3.30}$$

Let us estimate the parameters of this formula in the case of composite superconductors. Assuming $h_f=0.025$ W/cm^2 K, $\rho=3\times10^{-8}$ Ω cm, $T_c-T_0=5$ K, $d=10^{-2}$ cm, $j_c=10^5$ A/cm^2, we obtain $\alpha_f=240$. The quantities δ_h and T_k-T_0 are $\delta_h=\frac{1}{45}$, $T_k-T_0=0.6$ K, whence $\theta_k=0.12$ and $\omega_m=1.2$. Substituting these quantities into Eq. (3.30), we find $j_p=0.13j_c$. The normal-zone propagation then takes place already at $j\ll j_c$, which is characteristic of superconducting composites (Brechna, 1973; Altov *et al.*, 1977; Wilson, 1983).

The current j_p in thin superconducting films and microbridges is often calculated using the model with stepwise heat production, i.e., with $Q(T)=0$ at $T<T_c$ and $Q(T)=\rho j^2$ at $T>T_c$ (Skocpol, Beasley, and Tinkham, 1974a). This model neglects the temperature dependence of the parameters h, ν, κ, and ρ, and also the heat generation in the resistive state $[T_r(j)<T<T_c]$. As a result, the formula for j_p takes a simple form:

$$j_p=\left[\frac{2hT_c}{\rho d}\right]^{1/2}\left[1-\frac{T_0}{T_c}\right]^{1/2}. \tag{3.31}$$

Here the quantity j_p is greater by a factor of $\sqrt{2}$ than the minimum current density of normal phase existence, j_m [see Eq. (2.16)].

The dependence of h on T can also prove to be significant in superconducting films. This was demonstrated by Yamasaki and Aomine (1979), who calculated j_p in the model with stepwise heat production, having replaced the linear heat transfer $W(T)\propto(T-T_0)$ by a more realistic expression $W(T)=(T^4-T_0^4)Y/d$, where $Y=$const. In this case the equation for j_p becomes

$$5J_p^2\theta_c+4\theta_0^5=4(J_p^2+\theta_0^4)^{5/4}\ , \tag{3.32}$$

where $\theta_0=T_0/T_c$, $\theta_c=T_r(J_p)/T_c$, $J_p^2=j_p^2\alpha_0/j_0^2$, $\alpha_0=\rho d j_0^2/YT_c^4$, and j_0 is the critical current density at $T=0$. At $\theta_c=1$ Eq. (3.32) coincides with the equation derived by Yamasaki and Aomine. The factor θ_c in Eq. (3.32) appears because the derivation of Eq. (3.32) takes into account heat generation in the resistive state, assuming approximately that $Q(T)=0$ at $T<T_r(j)$ and $Q(T)=\rho j^2$ at $T>T_r(j)$. In narrow films, where pair breaking is typically uniform, $j_c\simeq(1-T/T_c)^{3/2}j_0$ (Ginzburg, 1958) and $\theta_c=1-J_p^{2/3}\alpha_0^{-1/3}$. And if j_c is determined by the surface barrier for the magnetic flux tubes, then $j_c(T)\simeq(1-T^2/T_c^2)j_0$ (see, for example, Huebener, 1979), and therefore $\theta_c=(1-J_p\alpha_0^{-1/2})^{1/2}$. We have mentioned already that the typical values of the parameter α_0 for thin films are of order 10^2–10^3, so that the difference between θ_c and unity is negligibly small everywhere except in a narrow temperature range close to T_c, where $j_p\sim j_c$.

Figure 18 plots J_p as a function of T_0, found by numerically solving Eq. (3.32) with $\theta_c=1$. In the range of $T_0\approx T_c$ it is clearly not necessary to take into account the temperature dependence of h. Thus at $T_0=0$ one finds $j_p=\frac{25}{16}j_0\alpha_0^{-1/2}$, which is 0.55 of the value yielded by the simple formula (3.31), assuming the coefficient h to be taken at $T=T_c$, i.e., $h=4T_c^3Y$.

2. Propagation velocity of the *N*-*S* interface

Let us consider the propagation of thermal switching waves from the superconducting (S) into the normal state (N), that is, propagation of N-S boundaries. Such waves were first observed by Breemer and Newhouse (1958) in thin superconducting films. The propagation of N-S boundaries in thin films was later analyzed by numerous authors (e.g., Broom and Rhoderick, 1960; Cherry and Gittleman, 1960; Newhouse, 1964; Overton, 1971; Gray *et al.*, 1983); in thin wires of type-I superconductors it was studied by Posada and Rinderer (1975a, 1975b). Studies were carried out at the same time of normal-zone dynamics in composite superconductors, in view of the problem of stabilization of superconducting magnetic systems (e.g., Brechna, 1973; Altov *et al.*, 1977; Wilson,

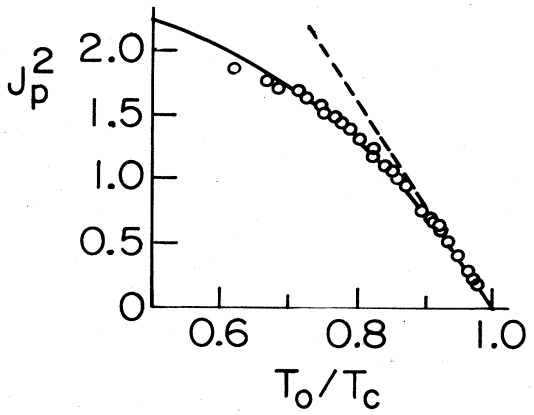

FIG. 18. J_p as a function of temperature for granulated aluminum films: solid curve, Eq. (3.32); dashed curve, Eq. (3.31) (Yamasaki and Aomine, 1979).

1983). In this section we review the main qualitative results on the velocities of thermal waves, $v(j)$, in current-carrying superconductors.

As has been mentioned above, a general expression for $v(j)$ can be derived only for $j \simeq j_p$, or if G is sufficiently large. For other values of current, $v(j)$ has to be found numerically. A qualitative description of thermal propagation of the N-S interface in superconductors can be obtained by using a simple model that was introduced in the early papers devoted to calculating $v(j)$ (Broom and Rhoderick, 1960; Cherry and Gittleman, 1960; Whetstone and Ross, 1965; Keilin *et al.*, 1967; Overton, 1971). Following these papers, we assume that h, κ, and ν are independent of T. Equation (3.2) can then be written in the form

$$\theta''+c\theta'-\theta+\alpha i^2 r(\theta,i)=0 , \tag{3.33}$$

where $\theta=(T-T_0)/(T_c-T_0)$, $i=j/j_c$, $c=v/v_h$ is the dimensionless velocity of the S-N interface, v_h is the thermal velocity [see Eq. (3.16)], $r(\theta,j)=1-j_c(\theta)/j$ at $T>T_r$ and $r(\theta,j)=0$ at $T<T_r$, and a prime stands for differentiation with respect to a dimensionless coordinate $(x-vt)/L$.

Equation (3.33) includes a function $r(\theta,i)$, which is the ratio of the specimen resistance at a given temperature θ to its resistance in the normal state ($\theta>1$). Two forms of the function $r(\theta,i)$ are typically chosen (Keilin *et al.*, 1967). In the first of them $r(\theta,i)$ jumps from zero to unity at the temperature of the transition from the superconducting to the resistive state, $\theta=\theta_r$, where $\theta_r=[T_r(j)-T_0]/(T_c-T_0)$ [Fig. 19(a)]. The corresponding model will be referred to throughout this paper as the stepwise heat production model. The other form of $r(\theta,i)$ [Fig. 19(b)] leads to a more consistent description of heat generation in the resistive state. It is then assumed that $j_c(T)$ linearly decreases with increasing T. This gives $\theta_r=1-i$, and the function $r(\theta,i)$ is given by Eq. (3.25). Hereafter we refer to this model as the resistive model.

Both these models very much simplify the actual situation, but make it possible, nevertheless, to analyze analytically the main qualitative feature of thermal propagation of the normal zone in superconducting composites and thin films. In the stepwise heat generation model the solution of Eq. (3.33), which describes the moving N-S interface, is

$$\theta(z)=\theta_r \exp\left[\frac{k_- z}{L}\right], \quad z>0 , \tag{3.34}$$

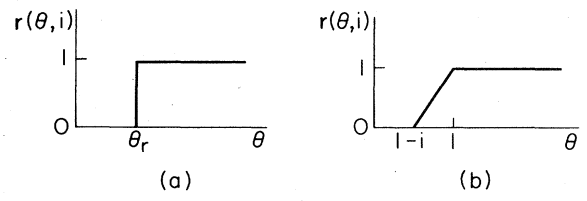

FIG. 19. $r(\theta)$ in (a) stepwise heat production model, and (b) resistive model.

$$\theta(z)=\alpha i^2+(\theta_r-\alpha i^2)\exp\left[\frac{k_+ z}{L}\right], \quad z<0 , \tag{3.35}$$

$$k_\pm=-\frac{c}{2}\pm\left[\frac{c^2}{4}+1\right]^{1/2} , \tag{3.36}$$

where $z=x-vt$. The characteristic width of an N-S interface, $L_W=L/k_+ + L/|k_-|$, is given by the formula

$$L_W=L(c^2+4)^{1/2} , \tag{3.37}$$

which coincides with Eq. (3.19) for $\delta=1$. Let us estimate the quantities t_h, L, and v_h in composite superconductors, assuming $h=250$ W/m^2 K, $d=10^{-3}$ m, $\kappa=10^3$ W/m K, and $\nu=2\times10^3$ J/m^3 K. This gives $L\simeq 6$ cm, $t_h=8\times10^{-3}$ s, and $v_h=8$ m/s. Likewise, in granular aluminum film [$d=1.5\times10^{-6}$ cm, $T_0=1.5$ K, $\nu=10^{-4}$ J/cm^3 K, $h=4YT_0^3=0.04$ W/cm^3 K, $\kappa=2\times10^{-4}$ W/cm K (Yamasaki and Aomine, 1979)], we obtain $L\approx 1$ μm, $t_h=4\times10^{-9}$ s, and $v_h=250$ m/s.

In the stepwise heat production model the velocity $v(j)$ is calculated exactly (Broom and Rhoderick, 1960; Cherry and Gittleman, 1960; Keilin *et al.*, 1967; Turck, 1980):

$$v(i)=v_h\frac{\alpha i^2-2\theta_r(i)}{\{[\alpha i^2-\theta_r(i)]\theta_r(i)\}^{1/2}} . \tag{3.38}$$

In this model the dependence of v on j is similar to the dependences $v(j)$ indicated in the preceding sections for switching waves in normal metals. The velocity of the N-S interface monotonically increases as j increases, passing through zero at $j=j_p$ and going to minus and plus infinity at $j=j_m$ and $j=j_c$, respectively. The quantity v_h determines the characteristic value of v for moderately large values of the Stekly parameter α. In the limit $\alpha\gg1$, Eq. (3.38) implies that $v(i)=v_h\alpha^{1/2}i/\sqrt{\theta_r(i)}$ in the whole range of current $0<i<1$, except for a narrow range close to $i=0$, with width $\sim\alpha^{-1/2}\ll1$. If $j_c(\theta)=(1-\theta)j_c$, then $\theta_r=1-i$ and

$$v(i)=v_0\frac{i}{\sqrt{1-i}}, \quad i\gg\alpha^{-1/2} . \tag{3.39}$$

The characteristic velocity $v_0=v_h\sqrt{\alpha}$, is

$$v_0=\frac{j_c}{\nu}\left[\frac{\kappa\rho}{T_c-T_0}\right]^{1/2}\gg v_h . \tag{3.40}$$

Equations (3.39) and (3.40) are thus valid for a thermally insulated superconductor ($h\to0$) when the velocity of the N-S interface is independent of the heat-transfer coefficient h, and $j_p\to0$. For the characteristic value $\alpha\sim10^2$, we find in the above-described examples that $v_0\simeq80$ m/s in composite superconductors and $v_0\simeq2500$ m/s in thin films. This last value is of the order of the sound velocity v_s. In this case the simple theory of thermal propagation of the normal zone is invalidated because heat diffusion definitely cannot be faster than the ballistic phonon propagation (Overton, 1971). In what follows we always assume that $v\ll v_s$.

In the stepwise heat production model the formula for

i_p is found from the conduction $v(i_p)=0$ (Keilin *et al.*, 1967):

$$i_p=\frac{1}{\alpha}(\sqrt{1+2\alpha}-1)\ . \tag{3.41}$$

In the case $\alpha\gg 1$ this formula gives $i_p=(2/\alpha)^{1/2}$, in agreement with Eq. (3.24) derived from the resistive model. At the same time, however, Eq. (3.41) implies that $i_p<1$ for any α, including $\alpha<1$. This conclusion contradicts the condition for thermal bistability of superconductors, $\alpha>1$, and thus points to the inconsistency of the stepwise heat production model if $\alpha\sim 1$. Physically, this paradox stems from the overestimation of heat production in the resistive state (see also Aomine and Miyake, 1979; Dharmadurai, 1980b). It can be avoided by renormalizing the quantity θ_r. If, for example, j_c is a linear function of T, then an assumption $\theta_r=1-i/2$ (Dresner, 1979) yields a qualitatively correct behavior of $v(j)$ in the whole range of transport current.

Consider now the velocity of the N-S interface in the resistive model. The temperature distribution across the N-S interface is described by Eq. (3.33), where $r(\theta,i)$ is given by Eq. (3.25). This equation is piecewise linear and is easily solved (Altov *et al.*, 1977). Nevertheless, the velocity $c(i)$ is the root of a fairly cumbersome transcendental equation, which is solved only numerically (Dresner, 1979). A number of $c=c(i)$ curves are plotted in Fig. 20 for different values of α. In contrast to the model with stepwise heat production, in the resistive model the velocities $c(i_m)$ and $c(1)$ remain finite (Altov *et al.*, 1973):

$$c(i_m)=-2(\alpha^{1/2}-1)^{1/2},\quad c(1)=2\sqrt{\alpha-1}\ . \tag{3.42}$$

Only approximate analytical formulas can be derived for $c(i)$ in the intermediate current range $j_m\lesssim j\lesssim j_c$. Thus Dresner (1979) suggested the following relation:

$$c(i)=(1+0.561\alpha^{-1.45})(M-1)/\sqrt{M}\ ,$$
$$M=\left[\alpha i^2-1+\frac{i}{2}\right]\Big/\left[1-\frac{i}{2}\right]\ , \tag{3.43}$$

which is accurate to about 1%. This formula qualitatively corresponds to an "effective" stepwise heat production model in which the resistive state is taken into account by a temperature shift $\theta_r\to 1-i/2$. Other approximation formulas that take into account heat production in the resistive state and the boiling crisis in the coolant were suggested by Turck (1980) and Lvovsky (1984).

In principle, the thermal propagation velocity of the N-S interface can be calculated numerically if the temperature dependences of all parameters in Eq. (3.2) are known. Detailed numerical calculations of $v(j)$ for composite superconductors and comparison with the available experimental data were carried out, for example, by Altov *et al.* (1973, 1977), Dresner (1976, 1979, 1980), Ishibashi *et al.* (1979), Tsukamoto and Miyagi (1979), and some others (Fig. 21). It was found that despite the good qualitative agreement between theory and experiment, significant quantitative discrepancies are observed in a number

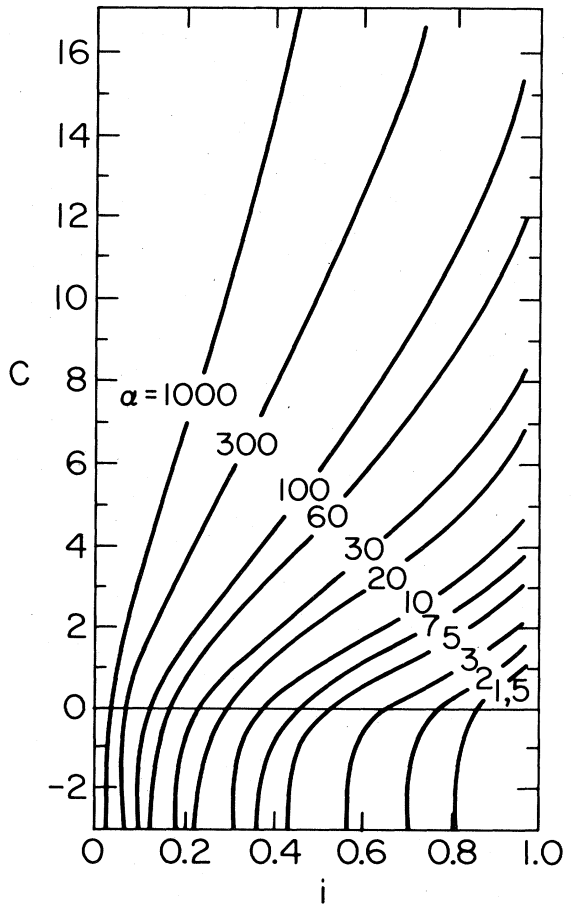

FIG. 20. $c=c(i)$ for various values of α in the resistive model (Dresner, 1979).

of cases. This indicates that the above-described scheme for calculating the normal-zone propagation velocity neglects some important features of superconducting materials. Let us discuss the peculiarities in some detail.

The analysis outlined above invariably assumed that the heat production Q and heat transfer W were determined only by the instantaneous temperature distribution. This is true only if the distribution $T(x,t)$ is quasistationary. Otherwise one has to take into account the time of current redistribution t_m over the superconductor cross section (Hartlin, Wertheimer, and Graham, 1964), as well as the time of buildup of stationary heat transfer to the coolant. These effects may prove to be appreciable; thus, the transient heat-transfer coefficient h in nonstationary conditions may differ substantially from its steady-state value (Grigor'iev *et al.*, 1977; Iwasa and Apgar, 1978; Giarratano and Frederick, 1980; Kirichenko and Rusanov, 1983).

For composite superconductors, the contribution to $Q(T)$ due to a lag in current redistribution over the cross section is small only if the composite is far from the boundary of stability of the critical state with respect to magnetic flux jumps. The corresponding criteria are

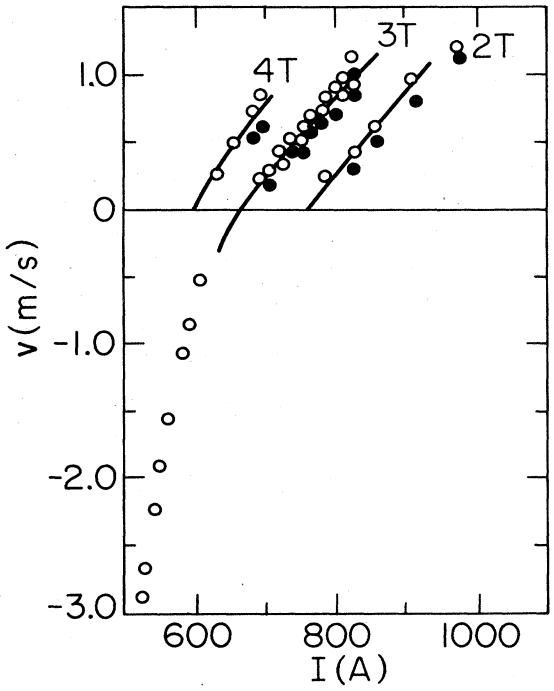

FIG. 21. Typical dependence $v=v(I)$ in a composite superconductor. Solid curve represents numerical calculations (Dresner, 1979).

found, for example, in Mints and Rakhmanov (1981, 1984). Many papers were devoted to studying the transient heat transfer W [detailed bibliography can be found in the monograph by Kirichenko and Rusanov (1983)]. At moderate values of $\partial T/\partial t$ the following empirical relation is valid in some cases (Iwasa and Apgar, 1978):

$$q_t = q(T) + a(T)\frac{\partial T}{\partial t} , \tag{3.44}$$

where $q(T)=h(T)(T-T_0)$ is the steady-state heat flux per unit surface area of the specimen, and q_t is the nonstationary heat flux. Typical values of the constant $a(T)$ in the film boiling regime in helium II are of the order of 1—10 J/m^2 K (Iwasa and Apgar, 1978).

Consequently, taking transient heat transfer into account results, in the first approximation, in the appearance of an additional term, proportional to $\partial T/\partial t$, in the heat conduction equation. This is equivalent to introducing, instead of $\nu(T)$, some effective heat $\nu_0(T)$ taking into account the heat required for evaporation in helium:

$$\nu_0(T) = \nu(T) + a(T)d^{-1} . \tag{3.45}$$

The effect of nonstationarity of external cooling can be characterized by a dimensionless parameter $\delta_W = a/\nu d$. Assuming $a = 5$ J/m^2 K, $d = 10^{-3}$ m, $\nu = 3\times 10^3$ J/m^3 K, we find $\delta_W \sim 1$. Nonstationary cooling can thus prove to be significant for the calculations of normal-zone propagation velocities in composite superconductors (Dresner, 1976, 1979; Ishibashi *et al.*, 1979; Tsukamoto and Miyagi, 1979; Lvovsky and Lutset, 1982; Funaki *et al.*, 1985; etc.).

Furthermore, the thermal propagation of the normal phase is affected by the latent heat of the superconducting transition, released at the N-S interface in a magnetic field (Overton, 1971), by the diffusion of nonequilibrium excitations in thin films (Eru, Peskovatsky, and Poladich, 1979), by thermoelectric effects (Gurevich and Mints, 1980, 1981b), and by the flow of the coolant along a superconductor (Altov *et al.*, 1977; Hoenig, 1980; Hoffer *et al.*, 1977). As a rule, these effects are relatively weak, but the last two effects produce a difference between the velocity of propagation of an N-S interface parallel to (v_+) and antiparallel to (v_-) the current direction.

Let us analyze in detail the asymmetry of $v(j)$ due to thermoelectric effects. With these effects taken into account, the heat conduction equation (3.2) takes the form

$$\frac{d}{dx}\kappa\frac{dT}{dx} + (\nu v - j\Pi)\frac{dT}{dx} + Q - W = 0 , \tag{3.46}$$

where Π is the effective thermoelectric constant (Landau and Lifshitz, 1982). If j and E are related by Eq. (2.8), then (Gurevich and Mints, 1980, 1981b)

$$\Pi = T\frac{\partial}{\partial T}\left[\pi(T)\left[1-\frac{j_c}{|j|}\right]\right]\eta(j-j_c) , \tag{3.47}$$

where $\eta(x)=0$ if $x<0$, $\eta(x)=1$ if $x\geq 0$, and $\pi(T)$ is the Seebeck coefficient. Equation (3.47) contains, in addition to the ordinary term $(1-j_c/j)T\partial\pi/\partial T$ representing the Thomson effect, the term $-T\pi(T)(\partial j_c/\partial T)/j$, which takes into account the electric field gradient in that part of the N-S interface which is in the resistive state. This effect can be treated as an analog of the Peltier effect. Its clearest manifestation is found in composite superconductors, where the difference between the resistivities of the normal matrix and the superconducting filaments in the resistive state is such ($\rho_f \gg \rho_n$) that the value of $\pi(T)$ in Eq. (3.47) is determined by the Seebeck coefficient of the normal matrix. In this case the Peltier heat is generated when current penetrates from the superconductor into the normal metal, and is deposited at the interface between them.[2]

The change in the velocity of the N-S interface caused by the reversal in current direction appears because, in contrast to the Joule heat production, the thermoelectric heat production $Q_T = -j\Pi\partial T/\partial x$ reverses its sign. For $j = j_p$ the expression for the difference $\Delta v = v_+ - v_-$ is

$$\Delta v(j_p) = 2j_p\frac{\int_{T_0}^{T_3}\Pi S^{1/2}dT}{\int_{T_0}^{T_3}\nu S^{1/2}dT} . \tag{3.48}$$

In the stepwise heat generation model a formula for $\Delta v(j)$ can be obtained in the whole range $j_m < j < j_c$:

$$\Delta v = \frac{j\Pi}{\nu} , \tag{3.49}$$

[2]In this sense the statement of Clem and Bartlett (1983) that Eq. (3.47) ignores the Peltier effect is not correct.

where Π is the thermoelectric constant which at $T > T_r$ was assumed, for simplification, independent of T. This asymmetry of the velocities of N-S interfaces in composite superconductors was discovered by Bartlett, Carlson, and Overton (1979). Setting $\nu_0 \sim 3\times10^{-3}$ J/cm^{3}K, $j = 5\times10^4$ A/cm^2, and $\Pi \sim 10^{-7}$ V/K, we obtain $\Delta v \sim 1-10$ cm/s. Both this estimate and the linear dependence of Δv on j are in good qualitative agreement with experiment (see Fig. 22). A more detailed comparison between theory and experimental data was given by Clem and Bartlett (1983).

We conclude this section with one more remark. For the sake of simplification, we have discussed only the case of three intersection points of the curves $Q(T)$ and $W(T)$, and hence of a single type of switching wave which transforms a specimen from the superconducting ($T = T_0$) to the normal state ($T = T_3$), or vice versa. If the number of intersection points is greater, several types of such waves can arise (e.g., this occurs in composite superconductors coated by a layer of thermal insulation). For instance, in the situation shown in Fig. 10 such waves result in the following transitions: (1) $T_0 \rightleftarrows T_3$, (2) $T_0 \rightleftarrows T_5$, (3) $T_3 \rightleftarrows T_5$. The number of switching wave types here is three. Figure 10(a) shows that the interface between the $T = T_3$ and T_5 phases propagates along the normal specimen, and the transition $T_3 \rightleftarrows T_5$ entails not the destruction of superconductivity but the formation of a vapor film on the superconductor surface.

Along with the superconducting-normal state switching waves in composite superconductors, thermal switching waves can also be generated in the normal matrix. It has been mentioned above that this effect can also be caused by sufficiently steep temperature dependence $\rho(T)$ in the low-temperature range. The propagation of such a thermal wave destroys the superconducting state $T = T_3$ and heats up the specimen to $T = T_5 \sim T_D$. This effect can also be observed in cryoresistive systems in which the current-carrying elements are made of a normal high-conductivity metal. This and a number of similar cases can be treated by analogy to the above-described example of the $T_1 \rightleftarrows T_3$ transition.

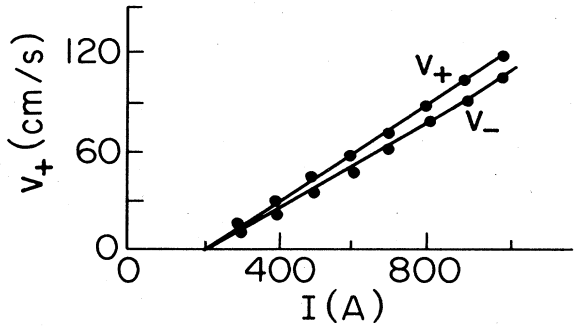

FIG. 22. Asymmetry of the velocity of N-S interfaces in a composite superconductor with bronze matrix and niobium stannide filaments. Solid curves represent numerical calculations (Clem and Bartlett, 1983).

IV. ELECTROTHERMAL DOMAINS

Another situation possible in bistable current-carrying conductors is the formation of steady-state domains (electrothermal domains) in which the Joule heat production is mostly concentrated. The temperatures and electric fields in these domains are considerably higher than those in the rest of the conductor.

These domains are formed because at $j_* < j < j^*$, two phases, one at $T = T_1$ and the other at $T = T_3$, can coexist in a specimen, the $T = T_1$ phase being metastable in the range $j > j_p$. In this case there exists a steady-state nonuniform distribution $T(x)$ which describes the critical nucleus of the $T = T_3$ phase. This nucleus is what is called the electrothermal domain. The corresponding distribution $T(x)$ is a solitary thermal wave [Fig. 2(b)].

Let us consider the solutions of the heat conduction equation (3.2) which describes an electrothermal domain in an infinite conductor. The qualitative analysis of such solutions is conveniently carried out by using the analogy between Eq. (3.2) and the equation of motion of a particle in a potential $-S(T)$ (Fig. 12). A domain corresponds to such a trajectory $T(x)$ on which the particle starts its motion from the point $T = T_0$ at infinitesimal velocity, reaches the point $T = T_m$, reverses its velocity, and ultimately returns to the starting point $T = T_0$ at zero final velocity. Figure 12 shows that such solutions exist for $S_3(j) \equiv S_3(T_3, j) < 0$, i.e., $j > j_p$. Furthermore, it is necessary that the work done by friction on the selected trajectory be zero; hence, in this case, the domain velocity $v_d = 0$.[3]

The temperature distribution $T(x)$ in an electrothermal domain can be found by integrating Eq. (3.3) with $v = 0$, which yields

$$|x| = \frac{1}{\sqrt{2}} \int_T^{T_m} \kappa S^{-1/2} dT \,. \tag{4.1}$$

Here the function $S(T)$ is given by Eq. (3.5), and T_m is the maximum temperature within the domain. Figure 12 also shows that T_m is a root of the equation

$$S(T_m, j) = 0 \,. \tag{4.2}$$

Hence the temperature T_m decreases with increasing current. Indeed, differentiation of Eq. (4.2) with respect to j yields

$$\frac{\partial T_m}{\partial j} = \frac{1}{\kappa (W - Q)_{T_m}} \int_{T_1}^{T_m} \kappa \frac{\partial Q}{\partial j} dT \,.$$

The numerator of this expression is always positive because $\partial Q/\partial j > 0$. At the same time, $W(T_m) < Q(T_m)$ because $T_2 < T_m < T_3$ (see Fig. 12). From this, $\partial T_m/\partial j < 0$, and the above statement follows immediately.

[3]The situations in which a domain can move along the specimen will be treated in Sec. VII.

A. Resistive domains in composite superconductors

Electrothermal domains in composite superconductors are stationary domains heated by current to a temperature above $T_r(j)$. The whole voltage applied to the superconductor drops across these domains, hence the name resistive domains (Gurevich and Mints, 1980).

Let us analyze the length $D(j)$ of the nonsuperconducting part of the domain as a function of j (Fig. 23). Substituting $T=T_r$ into Eq. (4.1), we obtain

$$D(j)=\sqrt{2}\int_{T_r}^{T_m}\kappa S^{-1/2}dT\ . \tag{4.3}$$

When $j\to j_p$, the temperature $T_m\to T_3$, and the curve $S(T)$ comes in contact with the abscissa axis at the point $T=T_3$ (Fig. 12). In this case the main contribution to the integral (4.3) is made by the interval $T\simeq T_3$ in the neighborhood of the minimum of $S(T)$, where $S(T)$ can be expanded into a series:

$$S(T)=S_3(j)+\tfrac{1}{2}(T-T_3)^2\left.\frac{\partial^2 S}{\partial T^2}\right|_{T_3}\ .$$

The substitution of this relation into (4.3) gives a logarithmically divergent integral as $j\to j_p$, ($S_3\to 0$):

$$D(j)\sim L(T_3)\ln\frac{j_p}{j-j_p}\ , \tag{4.4}$$

where $L(T_3)$ is the thermal length at $T=T_3$. Equation (4.4) holds in the interval $j-j_p\ll j_p$, when $D(j)\gg L$. In the intermediate region, $j_p\lesssim j\lesssim j_c$, the domain length $D\sim L$, and $D(j)\to 0$ as $j\to j_c$. This last characteristic arises because $T_m\to T_r(j)$ as $j\to j_c$. The resistive domain length thus increases with decreasing current, and in the limit $j\to j_p$ it becomes much greater than the domain boundary width, which is $\sim L$ [as $j\to j_p$, the normal part of the domain grows while the length of the resistive part remains fixed ($\sim L$)].

The voltage $U(j)$ across the domain is

$$U(j)=\int_{-D/2}^{D/2}(j-j_c)\rho\,dx\ .$$

Changing to the integration variable T by using Eq. (4.1), one arrives at the current-voltage characteristic of the superconductor with a resistive domain:

$$U(j)=\sqrt{2}\int_{T_r}^{T_m}\kappa\rho(j-j_c)S^{-1/2}dT\ . \tag{4.5}$$

As an illustration, we shall consider the stepwise heat production model. The solution of Eq. (3.33) gives the following expressions describing a resistive domain in an infinite specimen:

$$\theta(x)=\alpha i^2-(\alpha i^2-\theta_r)\frac{\cosh(x/L)}{\cosh(D/2L)},\quad 2|x|<D\ , \tag{4.6}$$

$$\theta(x)=\theta_r\exp[(D-2x)/2L],\quad 2x>D\ , \tag{4.7}$$

$$\theta_m=\alpha i^2-[\alpha^2 i^4-2\alpha i^2\theta_r(i)]^{1/2}\ , \tag{4.8}$$

$$D(i)=L\ln\frac{\alpha i^2}{\alpha i^2-2\theta_r(i)}\ , \tag{4.9}$$

where $\theta_m=(T_m-T_0)/(T_c-T_0)$. In this model $U(j)=\rho jD(j)$, whence

$$U(i)=U_0 i\ln\frac{\alpha i^2}{\alpha i^2-2\theta_r(i)}\ , \tag{4.10}$$

where $U_0=L\rho j_c$. Figure 24 plots the main characteristics of the resistive domain as functions of current. According to Eqs. (4.8) and (4.9), the length $D(i)$ increases from zero to infinity as i diminishes from 1 to i_p, while the temperature θ_m grows from zero to $2\theta_r(i_p)$. In the current range $i_t<i<1$ the quantity θ_m is below unity, $\theta_m<1$, so that the domain is completely resistive. But if $i_p<i<i_t$, the center of the domain contains a normal "interlayer" (Fig. 23). The expression for i_t in the resistive model is

$$i_t=\alpha^{-1/3}\ . \tag{4.11}$$

The current-voltage characteristic of a superconductor with a resistive domain is plotted in Fig. 25. The curve $U=U(j)$ is decreasing, i.e., a specimen with a resistive domain has negative differential resistance $R(I)=dU/dI$. This fact indicates that domains in the fixed-current regime are unstable.

A resistive domain, constituting a critical nucleus of the normal phase, can thus exist in a current-carrying su-

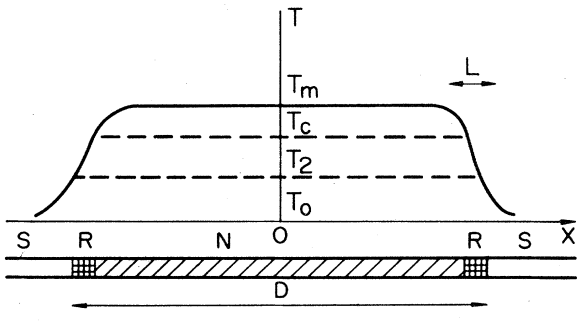

FIG. 23. Distributions of temperature and of normal, resistive, and superconducting phases in a specimen with a resistive domain.

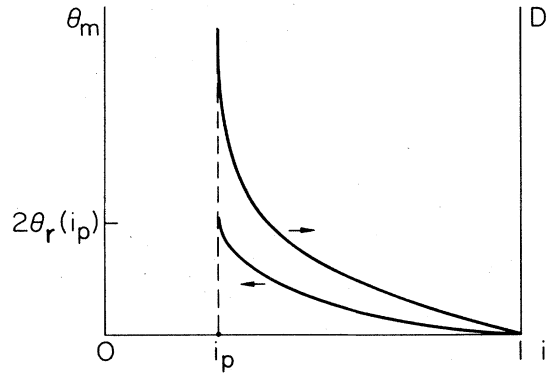

FIG. 24. $\theta_m=\theta_m(i)$ and $D=D(i)$ curves in the stepwise heat production model.

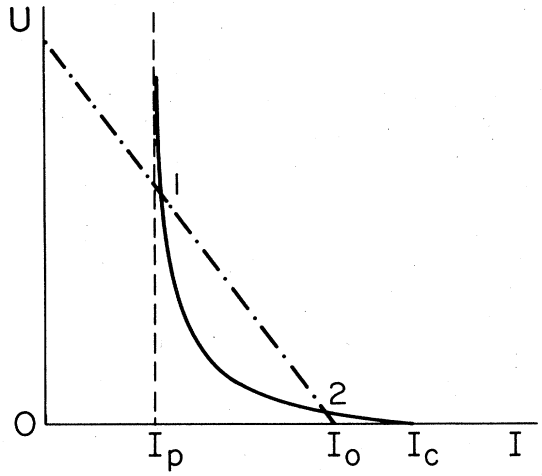

FIG. 25. *I-V* characteristic of an infinitely long superconductor with a resistive domain. The dot-dashed line is the loading curve.

perconductor at $j > j_p$. The formation of this domain produces the transition of the superconducting state $T = T_0$, which at $j > j_p$ is metastable, to the normal state $T = T_3$. Indeed, owing to the domain instability, any small perturbation producing a temperature drop in the domain results in its disappearance. Likewise, small perturbations raising the domain temperature cause the domain to expand, i.e., to occupy the whole specimen. The energy necessary to form a resistive domain thus characterizes the amount of perturbation which will initiate the thermal destruction of superconductivity by transport current (Martinelli and Wipf, 1973; Wilson and Iwasa, 1978; Wipf, 1979).

B. "Hot spots" in superconducting microbridges and in thin films

Resistive domains occur not only in superconducting composites but also in other superconductors at high critical current density, namely, in thin films, point contacts, superconducting microbridges, etc. Usually such domains are localized in the range of maximum current concentration, determining the shape of the appearing normal domain. For example, in long superconducting microbridges the domain appears at the center of the bridge [Fig. 26(a)]. The temperature distribution in this case is one dimensional. In short thin-film bridges and in weak links the resistive domain is typically a "hot spot" [Fig. 26(b)]. And finally, the normal region in three-dimensional point contacts is "mushroom shaped" [Fig. 26(c)]. Traditionally, resistive domains in thin films are called "hot spots" regardless of concrete geometry (Breemer and Newhouse, 1958; Skocpol, Beasley, and Tinkham, 1974a; etc.).

The treatment of a hot spot in a long superconducting microbridge differs from that of the preceding section only in that one has to take into account the finite length

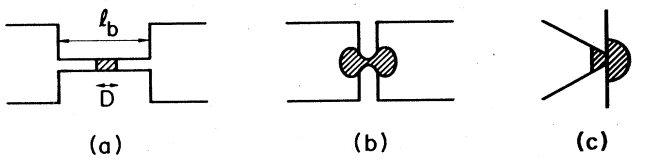

FIG. 26. Distribution of normal phase (hatched) in superconducting weak links under Joule self-heating: (a) long microbridge; (b) short microbridge; (c) point contact.

of the bridge at whose ends $T = T_0$. In this case the temperature distribution in the superconductor is

$$|x(T)| = \frac{1}{\sqrt{2}} \int_T^{T_m} \kappa(T') S_m^{-1/2}(T') dT' , \tag{4.12}$$

$$S_m(T) = \int_{T_m}^{T} \kappa(W - Q) dT . \tag{4.13}$$

The temperature at the hot spot center T_m is found from the condition $T(\pm l_b/2) = T_0$, which gives the following equation for T_m:

$$l_b = \sqrt{2} \int_{T_0}^{T_m} \kappa(T) S_m^{-1/2}(T) dT , \tag{4.14}$$

where l_b is the bridge length. The current-voltage characteristic of a bridge with a hot spot is described by Eq. (4.5) after the substitution $S(T) \to S_m(T)$.

Let us use the stepwise heat production model to illustrate the application of the general formulas (4.12)–(4.14). This was first done by Skocpol, Beasley, and Tinkham (1974a), who analyzed in detail the formation of hot spots in superconducting microbridges. This subject was later studied by Huebener (1975), Yamasaki and Aomine (1979), Dharmadurai (1980a, 1980b, 1981), and some others [a detailed bibliography can be found in the review by Dharmadurai (1980a) and Skocpol (1981)].

In the stepwise heat production model the following equation gives the hot spot length D as a function of current:

$$\frac{\alpha i^2}{\theta_r(i)} = 1 + \left[\frac{\kappa_s}{\kappa_n}\right]^{1/2} \coth\left[\frac{D}{2L_n}\right] \coth\left[\frac{l_b - D}{2L_s}\right] , \tag{4.15}$$

where $i = j/j_c$; $L_n = (d\kappa_n/h)^{1/2}$ and $L_s = (d\kappa_s/h)^{1/2}$ are the respective thermal lengths in the normal and superconducting states. The derivation of Eq. (4.15) assumed that $\kappa(T) = \kappa_n$ at $T > T_c$ and $\kappa(T) = \kappa_s$ at $T < T_c$, and that κ_n and κ_s are independent of T.

Equation (4.15) differs from the similar expression obtained by Skocpol, Beasley, and Tinkham (1974a) in the factor $\theta_r^{-1}(i)$ in the left-hand side, taking into account the dependence of the superconducting transition temperature on current. This factor becomes significant for $j \simeq j_c$ [as $j \to j_c$, the quantity $\theta_r(j) \to 0$, and the length $D(j)$ is either zero or equals l_b].

Figure 27 plots the hot spot length D as a function of current in the superconducting microbridge. For $\kappa_s = \kappa_n$, the curve $D(j)$ is symmetrical with respect to the point $D = l_b/2$, so that the quantity $j_r = j(l_b/2)$ is the

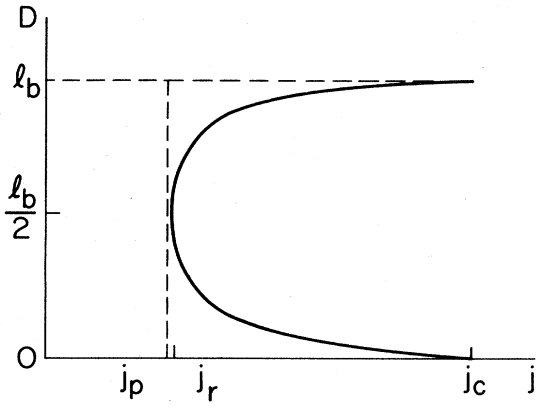

FIG. 27. $D=D(j)$ of a long microbridge for $l_b \gg L$, $\kappa_n=\kappa_s$.

minimum current density at which a hot spot can exist in a microbridge. The equation for j_r, can thus be written in the form

$$\alpha_{\text{eff}} i_r^2 = 2\theta_r(i_r) , \tag{4.16}$$

$$\alpha_{\text{eff}} = \frac{2\alpha}{1+\coth^2(l_b/4L)} . \tag{4.17}$$

The quantity α_{eff} is the effective Stekly parameter obtained when the additional cooling at the microbridge end points is taken into account. In thin films the parameter α_{eff} is typically much greater than unity, so that $i_r \sim \alpha_{\text{eff}}^{-1/2}$ and we can set $\theta_r=1$ in Eq. (4.16). This yields

$$i_r = (2/\alpha_{\text{eff}})^{1/2} . \tag{4.18}$$

The parameter α_{eff} of a long microbridge ($l_b \gg 4L$) equals α and the current i_r coincides with i_p of the infinite specimen [see Eq. (3.41) for $\alpha \gg 1$]. This behavior is caused by a logarithmic growth in the length of the resistive domain as $j \to j_p$ [see Eq. (4.4)].

In the case $\alpha_{\text{eff}} \sim 1$ the expression for i_r is determined by the specific form of the function $\theta_r(i)$. For example, if j_c linearly decreases with increasing T, then $\theta_r = 1-i$ and

$$i_r = \left[\frac{1}{\alpha_{\text{eff}}^2} + \frac{2}{\alpha_{\text{eff}}}\right]^{1/2} - \frac{1}{\alpha_{\text{eff}}} . \tag{4.19}$$

The two-valuedness of the hot spot length $D(j)$ in microbridges has a simple physical meaning. Indeed, as was pointed out in the preceding section, the resistive domain length in the infinite specimen decreases as current increases. The same is true for microbridges when the hot spot length $D(j)$ is less than $l_b/2(\kappa_n=\kappa_s)$. Owing to the efficient cooling of the bridge ends, further decrease of j does not result in enhancing $D(j)$. The heat dissipation at the bridge ends can be compensated by increasing the production of heat in the hot spot. The result is a rising branch of $D(j)$, corresponding to an increase in the length $D(j)$ with increasing current. At $j=j_c$ the microbridge completely transforms to the normal state ($D=l_b$).

The above-described behavior of hot spots in microbridges is clearly seen on the bridge I-V characteristic (Fig. 28). Each branch of the $D=D(j)$ curve in Fig. 27 has a corresponding branch of $U=U(j)$. Thus a microbridge has negative differential resistance at low voltage. As voltage increases, the current density passes through the minimum j_r, and at still greater values of U the I-V characteristic becomes practically linear. In this case the hot spot length is close to l_b regardless of the value of j.

The I-V characteristic of a microbridge with a hot spot manifests a hysteresis: in the absence of external perturbations the increasing current destroys superconductivity at $j=j_c$, while with the subsequent decrease of j superconductivity recovers at $j=j_r \ll j_c$. In actual experimental conditions, however, a specimen is invariably subjected to some perturbations [e.g., in the case of boiling helium cooling, the local temperature fluctuations may reach ~ 1 K (Efferson, 1969; Smirnov and Fedorov, 1971)]. As a result, thermal destruction of superconductivity usually occurs not at $I=I_c$ but at a much lower current $I \sim I_p$ whose temperature dependence is different from that of I_c [see, for example, Eq. (3.31)]. Another result is a substantial hysteresis. Such behavior was often observed in the studies of superconductivity breakdown in current-carrying thin films, whiskers, and superconducting weak links (Breemer and Newhouse, 1959; Kolchin *et al.*, 1961; Newhouse, 1964; Smirnov *et al.*, 1965; Wyatt, 1969; Gubankov, Likharev, and Margolin, 1972; Nad' and Polyansky, 1973; Eru *et al.*, 1973a, 1975; Fulton and Dunkleberger, 1974; Skocpol, Beasley, and Tinkham, 1974a; Huebener, 1975; Meyer, 1975; Smith and Bohner, 1975; Gray, 1976; Jahn and Kao, 1976; Volotskaya *et al.*, 1976; Decker and Palmer, 1977; Tinkham, Octavio, and Skocpol, 1977; Aomine and Miyake, 1979; Ivanchenko *et al.*, 1979, 1981, 1982; Yamasaki and Aomine, 1979; Dharmadurai, 1980a; Mizuno and Aomine, 1980; Feuer and Prober, 1981; Skocpol, 1981; Tinkham, 1981; Schulze and Keck, 1983; etc.).

We have discussed above the simplest situation of the ideal cooling of microbridge ends [$T(\pm l_b/2)=T_0$]. More complicated cases are possible, when the hot spot

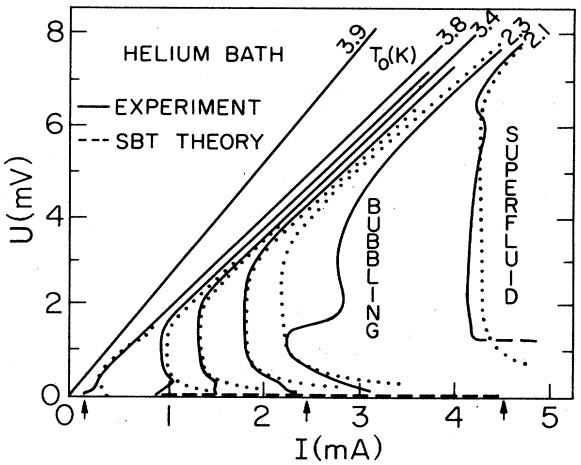

FIG. 28. I-V characteristic of a tin microbridge with a "hot spot" (Skocpol, Beasley, and Tinkham, 1974a).

reaches the end point of the bridge and starts propagating over the banks [Fig. 26(b)]. This situation was treated by Iwanyshin and Smith (1972) and Skocpol, Beasley, and Tinkham (1974a). Volkov and Kogan (1974) considered a hot spot in a closed l_b-long ring. In this case the equation for D is

$$\frac{\alpha i^2}{\theta_r(i)}=1+\left[\frac{\kappa_s}{\kappa_n}\right]^{1/2}\coth\left[\frac{D}{2L_n}\right]\tanh\left[\frac{l_b-D}{2L_s}\right]. \tag{4.20}$$

The current-voltage characteristic of a hot spot in a ring is shown in Fig. 29. In contrast to the case in a microbridge, a hot spot in a ring can survive down to the minimum current I_m of normal-zone existence. A detailed analysis of steady-state thermal structures that can build up in the framework of the stepwise heat production model within a microbridge or a closed ring was carried out by Mazur and Bedeaux (1981).

Rigorously speaking, the above-presented one-dimensional model of a hot spot is valid only for narrow films, of width $b \ll L$. Nevertheless, the one-dimensional model was shown by Huebener (1975) and Ivanchenko and Mikheenko (1983a) to give a qualitatively acceptable description of experimental data for films with $b \sim L$, when the variation of $j(y)$ over the film width becomes significant. The results obtained by Ivanchenko and Mikheenko (1983a) demonstrated that the hot spot temperature in indium and lead films with $b \approx 6$–7 mm changes mostly along the current flow direction (Fig. 30). The data obtained by scanning electron microscopy lead to a similar conclusion (see Huebener's review, 1984).

The effects of the Joule self-heating in three-dimensional point contacts were studied by Gubankov, Likharev, and Margolin (1972), Jahn and Kao (1976), Tinkham, Octavio, and Skocpol (1977), and some others [see also the reviews by Likharev (1979) and Tinkham (1981)]. The characteristic temperature at the contact center can be evaluated by using the formula derived by Tinkham, Octavio, and Skocpol (1977) for $h=0$:

$$T_m=[T_0^2+3(eU/2\pi k_B)^2]^{1/2}, \tag{4.21}$$

where U is the applied voltage, k_B is the Boltzmann constant, and e is the electron charge. For $T_0=4.2$ K and $U=15$ mV, Eq. (4.21) gives $T_m \approx 48$ K. In the papers cited above, the self-heating at point contacts is shown to result in hysteresis, in enhanced intensity of the thermal electric noise, and in the appearance of the voltage limit in the nonstationary Josephson effect.

Self-heating may also be important in microwave irradiation of thin superconducting films. Thus Latyshev and Nad' (1976), as well as Pals and Doben (1979), observed thermal hysteresis in microwave stimulation of superconductivity. Eru *et al.* (1974) observed a hysteresis in superconductivity destruction by microwave irradiation. In such experiments the thermal bistability may be caused by a sharp increase in the absorption coefficient at $T \approx T_c$ if the microwave irradiation is sufficiently intensive.

To conclude this section, we note that simple Joule heating becomes unimportant as $T_0 \to T_c$. In this temperature range the important factors are various nonequilibrium effects, which result, among other things, in the creation of phase-slip centers in narrow superconducting microbridges and whiskers (Skocpol, Beasley, and Tinkham, 1974b), inhomogeneous states in laser irradiation and tunnel injection (Eckern *et al.*, 1979; Elesin and Kopaev, 1981), etc. As temperature decreases, the Joule heating of the phase-slip center transforms it into the above-described macroscopic hot spot (Skocpol, Beasley, and Tinkham, 1974b; Ivanchenko and Mikheenko, 1983b; Stuivinga *et al.*, 1983). Furthermore, the destruction of superconductivity in thin films by current or by microwave radiation may be caused by electron overheating (Shklovsky, 1975; Kashchei and Shklovsky, 1976). This overheating can also lead to bistability and formation of resistive domains, as well as to switching waves (Kashchei, 1977, 1978).

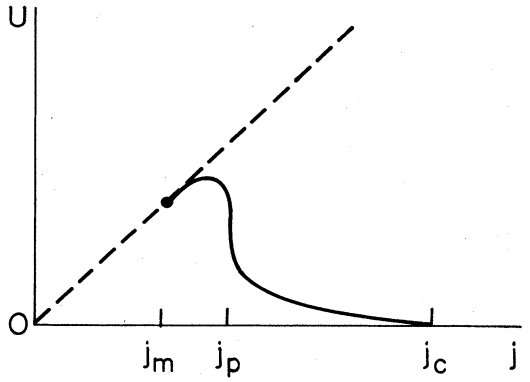

FIG. 29. I-V characteristic of "hot spot" in a closed ring (Volkov and Kogan, 1974).

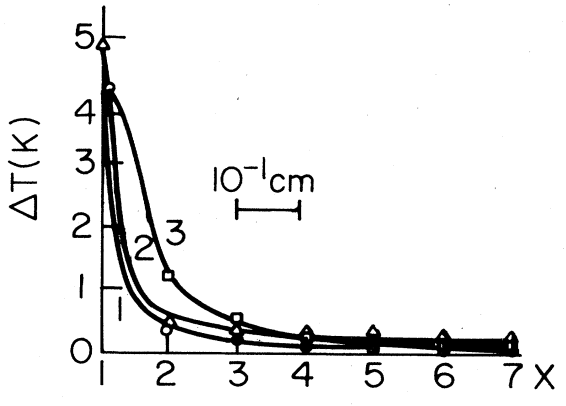

FIG. 30. Temperature distribution in a resistive domain for a lead film 6 mm wide: (1) $T_0=2.92$ K (liquid helium); (2) $T_0=2.2$ K (liquid helium); (3) $T_0=2.92$ K (helium vapor) (Ivanchenko and Mikheenko, 1983a).

C. Electrothermal domains in normal metals

In normal metals electrothermal domains can exist in the range of metastability of the low-temperature ($T=T_1$) state, $j_p<j<j^*$. As mentioned in the Introduction, numerous mechanisms are known for this behavior, but among the factors causing it the best investigated by now are (1) boiling crisis of the coolant (Petukhov and Kovalev, 1963; Zhukov, Barelko, and Merzhanov, 1979; Zhukov, Bokova, and Barelko, 1983); (2) sufficiently steep dependence $\rho(T)$ at low temperatures (Kadigrobov and Slutskin, 1978; Boiko, Podrezov, and Klimova, 1982a, 1982b, 1984; Tzyan and Logvinov, 1982; Kadigrobov *et al.*, 1984; Abramov *et al.*, 1983, 1985); (3) a jump in $\rho(T)$ at melting (Abramov *et al.*, 1983, 1985) or at some other structural transition (Barelko *et al.*, 1981).

Typical I-V characteristics of the three enumerated mechanisms are qualitatively similar to those shown in Fig. 31. Ohm's law holds at low voltages, but as U increases, the differential conductivity $\partial I/\partial U$ begins to decrease owing to the heating of the specimen. Then the current I decreases abruptly at $U=U^*$ and $I=I^*$, after which the differential conductivity becomes negative. As U further increases, the current I in a sufficiently long conductor continues to decrease, tending asymptotically to a constant value I_p. The subsequent decrease of voltage results in a hysteresis which depends on the specimen length. Such current-voltage characteristics were observed in a number of metals (aluminum, copper, indium, platinum, tin, iron) at liquid-helium, liquid-nitrogen, and room temperatures.

An electrothermal domain forms at $U>U^*$. In other words, a region appears in the current-carrying conductor where the maximum temperature T_m and electric field E_m are substantially greater than their respective values in the remaining part of the specimen. For instance, a molten light-emitting segment in a peculiar oxide film "hose" is formed in an air-cooled aluminum wire ($T_0\approx 300$ K) at $U>U_m$ (Abramov *et al.*, 1983). The domain length in a conductor 237 mm in length and 1 mm in diameter at $I=33.7$ A was $\simeq 50$ mm, and the electric fields outside (E_1) and inside the domain (E_m) were 34 and 111 mV/cm, respectively.

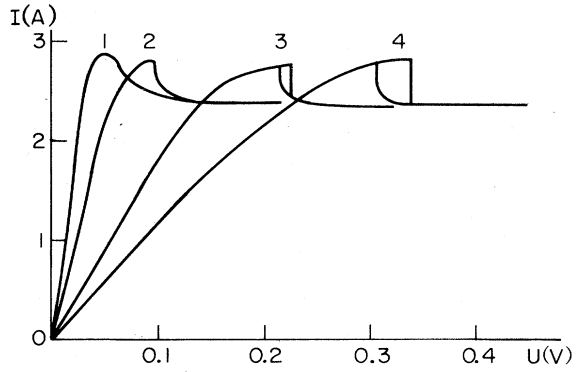

FIG. 31. I-V characteristic of platinum wire 0.1 mm in diameter cooled by helium vapor ($T_0=4.2$ K): (1) $L_c=50$ mm; (2) $L_c=105$ mm; (3) $L_c=255$ mm; (4) $L_c=410$ mm (Abramov *et al.*, 1985).

The distributions $E(x)$ and $T(x)$ in a conductor containing a domain are substantially less uniform at low temperatures ($T_0=4.2$ K) than at $T_0=300$ K. Thus Boiko, Podrezov, and Klimova (1982a, 1982b) reported $E_m/E_1\approx 200$ for copper wire 0.05 mm in diameter, cooled by liquid helium.

In studying electrothermal domains caused by the slope of the $\rho(T)$ curve, obvious difficulties are produced by the pool cooling of the specimen, that is, by additional bistability effects due to boiling crisis. For this reason Abramov *et al.* (1983, 1985) and later Boiko *et al.* (1984) made use of specimen cooling by air or helium vapor, i.e., of heat transfer by free convection whose $W(T)$ is a monotone function of T.

Table I lists the main characteristics of electrothermal domains in a number of gas-cooled metals (Abramov *et al.*, 1985). Domains due to steep $\rho(T)$ dependence were studied in platinum, copper, and indium at low temperatures ($T_0\approx 4.2$ K), and domains due to the jump in $\rho(T)$ at melting were studied in aluminum ($T_0=300$ K). In the former case the temperature and electric field in the domain exceeded the respective values in the rest of the specimen by more than an order of magnitude. In aluminum the distributions $E(x)$ and $T(x)$ were more uniform, in this sense, although T_m, for instance, was greater than the melting point by a factor of 1.5.

A domain-containing conductor has a negative differential conductivity (Fig. 31), so that electrothermal domains are stable in the fixed-voltage regime. This conclusion is familiar for electric field domains in semiconductors (Knight and Peterson, 1967; Volkov and Kogan, 1968; Bonch-Bruevich, Zvyagin, and Mironov, 1972). In this case the formation of an electrothermal domain in a metal specimen can be described as follows. The spontaneous transition of the conductor from one homogeneous state ($T=T_1$) to another ($T=T_3$) in the fixed-current regime takes place at $j=j^*$ (Fig. 1). If, however, the fixed quantity is not current but voltage, this transition becomes impossible, because it is accompanied by a strong increase in electric resistance and a drop in j below j_*, which eliminates the possibility of equilibrium at $T=T_3$. Consequently, only a part of the specimen is transformed into the high-temperature state, this part constituting the electrothermal domain.

This transition is especially clear-cut if the domain length D is much greater than the thermal length $L=(d\kappa/h)^{1/2}$. In this case the domain temperature is T_3 everywhere except within relatively narrow boundaries of width L, and the length $D(U)$ is found from the conduction of domain wall equilibrium, $I=I_p$. This behavior explains the stabilization of current in a conductor at high U, when the electrothermal domain length grows in direct proportion to the applied voltage:

$$D(U)=[U-L_c j_p\rho(T_1)]/j_p[\rho(T_3)-\rho(T_1)]\ . \quad (4.22)$$

In the general case, $T(x)$ in a domain-containing con-

TABLE I. The main characteristics of electrothermal domains in metals (Abramov *et al.*, 1985).

Metal characteristics	Pt $d_0=0.1$ mm $T_0=4.2$ K	Cu $d_0=0.12$ mm $T_0=4.2$ K	In $d_0=0.5$ mm $T_0=4.2$ K	Al $d_0=0.3$ mm $T_0=300$ K
$j^*\times10^{-4}$ A/cm^2	3.56	13.1	2.95	1.02
$j_p\times10^{-4}$ A/cm^2	3.0	7.2	1.0	0.92
T^*, K	27	30	6	920
T_m, K	160	260	70	1420
T_i, K	25	25	4.5	610
E_m, mV/cm	155	93	15.6	28.9
E_i, mV/cm	5.9	1.0	0.024	64.5

ductor is described by a general formula (4.12), and the temperatures T_m at the center and T_l at the end of the specimen are found from the system of equations

$$S_m(T_m,T_l)=2h_l(T_l)(T_l-T_0)\ , \tag{4.23}$$

$$L_c=\sqrt{2}\int_{T_l}^{T_m}\kappa S_m^{-1/2}dT\ . \tag{4.24}$$

Here L_c is the conductor length, and the thermal boundary conditions at the specimen edges are chosen in the form

$$(T_l-T_0)h_l(T_l)=-\kappa\frac{\partial T}{\partial x}\bigg|_{\pm L_c/2}\ ,$$

where h_l is the heat-transfer coefficient for conductor end faces. The expression for the current-voltage characteristic is given by (4.5) for $j_c=0$, $T_r=T_l$.

As an illustration we shall consider an electrothermal domain due to the jump in $\rho(T)$ at the melting point. We shall make use of the model presented in Sec. IV.A (see Fig. 7). The simplest is the case of adiabatic cooling of specimen ends ($\partial T/\partial x\mid_{\pm L_c/2}=0$). Here the I-V characteristic has two branches (Abramov *et al.*, 1985):

$$u(i)=\frac{iL_0}{k-i^2},\quad u<u^*\equiv u(1)\ , \tag{4.25}$$

$$u(i)=\frac{i}{k-i^2}\left[L_0+\left(\frac{1}{\delta_r}-1\right)D_0\right],\quad u>u^*\ , \tag{4.26}$$

$$D_0=\frac{1}{(k-i^2)^{1/2}}\operatorname{arctanh}\left[\frac{(1-i^2)\delta_r^{1/2}}{i^2-\delta_r}\right]. \tag{4.27}$$

Here $i=j/j^*$, j^* is given by Eq. (2.23), $u=U/U_0$ is the dimensionless potential difference, $U_0=2\rho_-(\kappa_-k/\rho')^{1/2}$, k is given by Eq. (3.21), $L_0=L_c/L$, $D_0=D/L$, and D is the length of the molten fragment of the conductor.

If $L_0\gg1$, the I-V characteristic given by Eqs. (4.25)—(4.27) is plotted in Fig. 32. Equation (4.25) describes the $0a$ branch of the specimen without domains, and (4.26) and (4.27) describe the *acd* branch of the domain-containing specimen. In a sufficiently long specimen the current-voltage characteristic has a hysteresis. As follows from Eq. (4.26), this occurs if

$$L_c>3.8L\left[\frac{k}{k-1}\right]^{1/2}. \tag{4.28}$$

In aluminum $\delta_r=\rho_-/\rho_+=0.455$ (Zinoviev, 1984). Let us estimate the parameters L and k in Eqs. (4.25)—(4.28). Assuming $\rho_1=1.7\times10^{-6}$ Ω cm, $\rho'=1.4\times10^{-8}$ Ω cm/K, and $d=0.25$ mm, we find $k=1.27$, $j^*=10^4$ A/cm^2. The thermal length L will be found by rewriting the expression $j^*=(h/\rho' dk)^{1/2}$ in the form $j^*=(\kappa_-/\rho' k)L^{-1}$, whence

$$L=\frac{1}{j^*}\left[\frac{\kappa_-}{k\rho'}\right]^{1/2}.$$

Assuming $\kappa_-=2.25$ W/cm K and using the above-given values of ρ', k, and j^*, we obtain $L=1.1$ cm. This value determines the characteristic length of electrothermal domains in aluminum at the moment of current jump on the I-V characteristic at $U=U^*$. The critical electric field strength $E^*=U^*/L_c$ is

$$E^*=\rho_-j^*\ . \tag{4.29}$$

In air-cooled ($T_0=300$ K) aluminum wire 1 mm in diameter, $j^*\simeq10^4$ A/cm^2 and $\rho_-=1.2\times10^{-5}$ Ω cm, so that $E^*=0.12$ V/cm.

D. Stability of electrothermal domains and switching waves. Effect of external electric circuit

An electrothermal domain in a homogeneous conductor is unstable in the fixed-current regime, as follows, for example, from the descending current-voltage characteristic

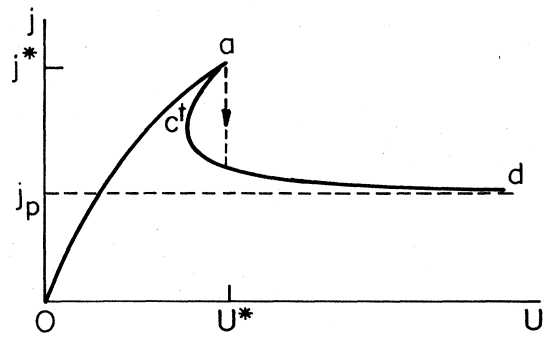

FIG. 32. Theoretical I-V characteristic of metal containing an electrothermal domain [see Eqs. (4.25)—(4.27)].

of the domain-containing specimen (Figs. 25 and 32). This instability is of the same nature as the well-known instability of electric field domains in semiconductors with negative differential conductivity (Knight and Peterson, 1967; Volkov and Kogan, 1968; Bonch-Bruevich, Zvyagin, and Mironov, 1972).

The fixed-current regime is a limiting case because a conductor is usually an element of some electric circuit. The parameters of this circuit may affect the stability of an electrothermal domain, for instance, may bring about its stabilization at certain conditions. Then a steady-state "hot" region, not expanding over the whole conductor, is formed in the specimen.

Let us analyze the domain stability in more detail, presenting the solution of Eq. (3.1) in the form

$$T(x,t)=T(x)+\kappa^{-1}\sum_{n=0}^{\infty}\psi_n(x)e^{\gamma_n t},$$

where $T(x)$ is the steady-state temperature distribution in the domain and the second term describes a small perturbation $\delta T(x,t)\ll T(x)$ with increments γ_n ($n=0,1,2,\ldots$). The equation for $\psi_n(x)$ in the fixed-current regime is

$$\frac{d^2\psi_n}{dx^2}-\frac{\psi_n}{\kappa}\left[\nu\gamma_n+\frac{\partial f}{\partial T}\right]=0\,, \tag{4.30}$$

$$\psi_n(\pm\infty)=0\,, \tag{4.31}$$

where $f=W-Q$, and the dependence of the functions $f(T)$, $\kappa(T)$, and $\nu(T)$ on x is determined by the distribution $T(x)$, which is to be analyzed for stability. The instability of $T(x)$ means that there exists at least one eigenvalue with $\mathrm{Re}\gamma_n>0$. If the ratio ν/κ is independent of T, then Eq. (4.30) is an analog of the one-dimensional Schrödinger equation with the energy $\varepsilon_n=-\gamma_n\nu/\kappa$. The potential $\kappa^{-1}\partial f/\partial T$ depends on the specific form of $T(x)$; for instance, in the case of the domain, the potential has two "wells" (Fig. 33).

One of the solutions of Eq. (4.30) is

$$\psi_n(x)\propto\kappa(T)\frac{dT}{dx}(x)\,. \tag{4.32}$$

This perturbation corresponds to a small shift of the distribution $T(x)$ as a whole. In a homogeneous medium, this shift corresponds to $\gamma=0$ (owing to translational invariance: the domain is in "neutral" equilibrium).

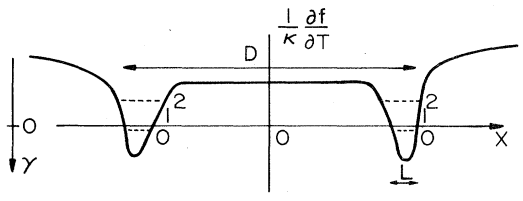

FIG. 33. Effective potential $\kappa^{-1}\partial f/\partial T$ for an electrothermal domain. Dashed curves mark the "energy levels" corresponding to eigenvalues γ_n.

The stability of an arbitrary solution $T(x)$ of Eq. (3.2) can be deduced from the Sturm-Liouville theorem, which states that the perturbation with maximum increment γ_0 corresponds to a function $\psi_0(x)$ without zeros at $|x|<\infty$ (Morse and Feschbach, 1953). This is a very convenient method, first used to study the stability of combustion waves (see, for example, Zeldovich *et al.*, 1980).

The function $\psi_0(x)$ for the switching wave is determined by Eq. (4.32) ($\gamma_0=0$), because in this case the derivative $dT(x)/dx$ vanishes only when $|x|=\infty$. By virtue of the Sturm-Liouville theorem, all other perturbations $\psi_n(x)$ with $n=1,2,3,\ldots$ damp out ($\gamma_n<0$), so that the switching wave is stable in the fixed-current regime.

For the electrothermal domain the function dT/dx is equal to zero at $x=0$, so that the eigenvalue $\gamma=0$ is not the greatest one here. There is in this case a perturbation $\psi_0(x)$ increasing with an increment $\gamma_0>0$, corresponding to the expansion or contraction of the domain in the fixed-current regime.

The quantity γ_0 of a long domain ($D\gg L$) can be estimated by regarding Eq. (4.30) as analogous to the Schrödinger equation. The wave functions $\psi(x)$ are then localized, to high accuracy, in the wells of the potential $\kappa^{-1}\partial f/\partial T$ (Fig. 33). Each such function corresponds to the ground state in an isolated well and describes the most "dangerous" perturbations with $\gamma=0$, resulting in a displacement of domain boundaries. When $D\gg L$, a weak overlapping of these functions produces an exponentially small splitting of the doubly degenerate level $\gamma=0$ into two levels: $\gamma=\gamma_1=0$, $\gamma=\gamma_0>0$ (see, for example, Landau and Lifshitz, 1974). This yields

$$\gamma_0\sim t_h^{-1}\exp[-D(j)/L]\,. \tag{4.33}$$

When a domain-containing conductor is in an electric circuit, the above analysis must be modified, taking into account the current perturbations in the specimen. Let us consider the differential impedance $Z(\omega)$ which determines the linear response of a domain-containing conductor to a small current perturbation $\delta I\propto\exp(i\omega t)$ at a frequency ω:[4]

$$Z(\omega)=\int_0^{L_c}\frac{\delta E(x,\omega)}{\delta I(\omega)}dx\,, \tag{4.34}$$

where $\delta E(x,\omega)$ is the electric field fluctuation in the specimen due to a fluctuation $\delta I(\omega)$. We restrict the analysis to long domains ($D\gg L$), when $t_h\gamma_0\ll 1$. The domain stability can then be analyzed by using the expression for $Z(\omega)$ at low frequencies ($\omega t_h\ll 1$). In this case (see Appendix A),

[4]Although the dimensionless current i and $i=\sqrt{-1}$ are denoted here by the same symbol, no confusion will arise because hereafter the imaginary unit appears only in the combination $i\omega$.

$$Z(\omega)=R_m(j)+\frac{R(j)-R_m(j)}{1-i\omega/\gamma_0}\ , \tag{4.35}$$

$$R_m=\left[1+\frac{2\frac{\partial Q}{\partial T}}{\frac{\partial W}{\partial T}-\frac{\partial Q}{\partial T}}\right]_{T_3}\frac{\rho(T_3)D}{A}$$

$$+\left[1+\frac{2\frac{\partial Q}{\partial T}}{\frac{\partial W}{\partial T}-\frac{\partial Q}{\partial T}}\right]_{T_1}\frac{\rho(T_1)(L_c-D)}{A}\ , \tag{4.36}$$

where $R(I)=dU/dI$ is the static differential resistance of the domain-containing specimen, γ_0 is the increment of the most "dangerous" perturbation $\psi_0(x)$, and $R_m(j)$ is the sum of differential resistances of two regions of the conductor, D and L_c-D long, heated to T_3 and T_1, respectively [obviously, the second term in Eq. (4.36) vanishes for superconductors]. For $\omega t_h \ll 1$ the equivalent electric circuit of an electrothermal domain-containing conductor is shown in Fig. 34, where $R_d=R-R_m<0$ and $C_d=-[(R-R_m)\gamma_0]^{-1}>0$.

Let us consider, using Eq. (4.35), the stability of a domain in a conductor connected to an electric circuit. For example, let a specimen be shunted by a resistance r and an inductance $\mathscr{L}$, and the whole circuit be connected to a dc power supply unit at $I=I_0$. Then

$$Z_c^{-1}(\omega)=Z^{-1}(\omega)+(r+i\omega\mathscr{L})^{-1}\ ,$$

where $Z_c(\omega)$ is the total impedance of the system, the poles of $Z_c(\omega)$ determining the spectrum of eigenfrequencies of the circuit under consideration. The corresponding function $\omega=\omega(I_0,r,\mathscr{L})$ takes the form

$$i\omega=\frac{1}{2\mathscr{L}}\{\mathscr{L}\gamma_0-R_p+[(\mathscr{L}\gamma_0-R_p)^2+4\gamma_0\mathscr{L}(R+r)]^{1/2}\}\ ,$$

$$|\omega|t_h\ll 1\ , \tag{4.37}$$

where $R_p(I)=r+R_m(I)$, and the current I through the specimen is found from the expression

$$U(I)=(I_0-I)r\ . \tag{4.38}$$

Here $U(I)$ is given by Eq. (4.5). Figure 25 shows a graphic solution of Eq. (4.38) for a resistive domain in an infinite superconductor; the load line $(I_0-I)r$ is traced by the dot-dashed line.

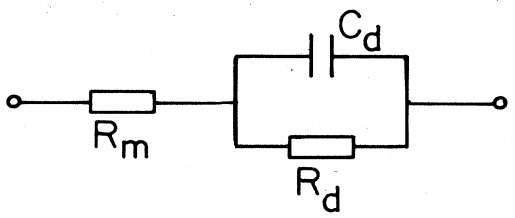

FIG. 34. Equivalent electric circuit of a conductor with an electrothermal domain.

An electrothermal domain is stable if $\mathrm{Im}\omega>0$. If $\mathscr{L}=0$, the stability condition takes a simple form (see, for example, Knight and Peterson, 1967; Volkov and Kogan, 1968; Bonch-Bruevich, Zvyagin, and Mironov, 1972):

$$r<\left|\frac{dU}{dI}\right|\ . \tag{4.39}$$

This condition holds not only in the above-discussed case $D\gg L$ but also for arbitrary-length domains. The inequality (4.39) has a simple physical meaning, because it reduces to the requirement that the total differential resistance of the circuit, consisting of the conductor that contains the electrothermal domain and a resistor r in parallel to it, be positive, i.e.,

$$\frac{Rr}{R+r}>0\ .$$

In superconductors, condition (4.39) holds for the state denoted by point 1 in Fig. 25. Consequently, shunting the superconductor stabilizes the resistive domain. The same is true for electrothermal domains in normal metals.

When the inequality (4.39) is satisfied, the domain is stable at sufficiently low inductances $\mathscr{L}<\mathscr{L}_k$. Otherwise, the domain stability breaks down under perturbations, oscillating at a frequency ω_k. The expressions for $\mathscr{L}_k$ and ω_k, for $D\gg L$, are

$$\mathscr{L}_k=[r+R_m(I)]\gamma_0^{-1}(I)\ , \tag{4.40}$$

$$\omega_k^2=[\,|R(I)|-r]\gamma_0(I)\mathscr{L}_k^{-1}(I)\ . \tag{4.41}$$

The domain instability at $\mathscr{L}>\mathscr{L}_k$, resulting in self-sustained current oscillations in the conductor, will be discussed in detail in Sec. VII.

Now let us turn to the details of the behavior of a resistive domain in a shunted superconductor. If $D\gg L$, the length $D(I_0)$ of this domain is found from the condition of equilibrium of its boundaries, $I=I_p$. This yields

$$D(I_0)=\frac{rA}{\rho(T_3)}\left[\frac{I_0}{I_p}-1\right]\ . \tag{4.42}$$

This solution corresponds to point 1 in Fig. 25. The substitution of Eq. (4.42) into the relation $U(I_0)=\rho ID/A$ leads to the following expression for the current-voltage characteristic of a shunted superconductor:

$$U(I_0)=(I_0-I_p)r\ . \tag{4.43}$$

In addition to this branch, the I-V characteristic also has an unstable descending branch represented by point 2 in Fig. 25. The complete I-V characteristic of a shunted superconductor is plotted in Fig. 35, where the superconductivity recovery current I_r corresponds to merging of points 1 and 2 in Fig. 25. In this case the quantity I_p plays the role of excess current at sufficiently high U.

In this section we have discussed the stability of domains and switching waves described by a single nonlinear heat conduction equation (3.1). In more complicated situations, such waves in bistable conductors are analyzed by supplementing Eq. (3.1) with equations

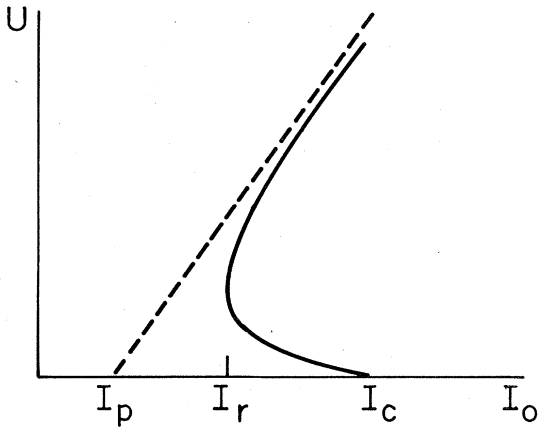

FIG. 35. I-V characteristic of a shunted superconductor with a resitive domain.

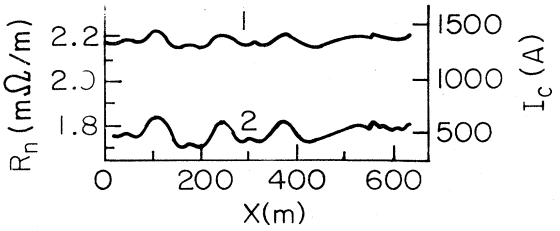

FIG. 36. $R_n(x)$ (curve 1) and $I_c(x)$ (curve 2) along a commercial composite superconductor (Genevey *et al.*, 1983).

describing, for example, particle diffusion, nonstationary effects in external cooling, the influence of front curvature on T_c, etc. Thus, in treating the propagation of crystallization waves in binary alloys, one has to add to Eq. (3.1) the equation of diffusion of one of the alloy components. An analysis of this problem shows that under certain conditions the planar crystallization interface becomes unstable with respect to interface bending. The result is the buildup of periodic concentration and temperature superstructures at the crystallization interface (Mullins and Sekerka, 1963, 1964; Langer, 1980; Kerzberg, 1983; McFadden and Coriel, 1984).

The retardation effects in the external cooling can also affect the stability of switching waves. Thus Zhukov, Bokova, and Barelko (1983) studied the heating of water-cooled platinum wire by electric current and observed oscillations of the propagation velocity of the switching wave which transforms nucleate boiling to film boiling.

V. LOCALIZATION OF DOMAINS AND SWITCHING WAVES IN INHOMOGENEOUS CURRENT-CARRYING CONDUCTORS

A. Typical inhomogeneities in composite superconductors and thin superconducting films

Real superconductors are inevitably somewhat inhomogeneous. In composite superconductors an obvious cause is the fabrication technology (Hillman, 1981; Roberge, 1981; Suenaga, 1981). As a result, such characteristics of composites as j_c, ρ, κ, the chemical composition of superconducting filaments, transverse dimensions, etc. may vary along specimens (Genevy *et al.*, 1983; Kumakura *et al.*, 1985). Figure 36 plots the variation of $I_c(x)$ and of the resistance in the normal state, $R_n(x)$, along a commercial superconducting cable. In this case the nonuniformity in I_c and R_n reach $\sim 10\%$. The same level is typical for the inhomogeneity of the chemical composition of most niobium-titanium alloys (West *et al.*, 1983), and for the local variation of transverse dimensions of superconducting filaments in composites (Hillman, 1981).

In addition to the above-described technological inhomogeneities, inhomogeneity is found in the surroundings of composite superconductors. We mean, for example, nonuniform distribution of magnetic field along the superconductor, nonidentical conditions of cooling along the specimen, etc. (Brechna, 1973). Such nonuniformity may exist even when the superconducting composite is perfectly homogeneous from the technological standpoint.

Thin superconducting films are characterized by such nonuniformities as local variation of thickness, or of the surface barrier for vortex penetration, etc. In the former case the transport current has variable density $j(x)$, and in the latter the critical current $I_c(x)$ varies along the specimen (see, for example, Jones *et al.*, 1967). Another important factor may be nonuniform heat transfer from the film to helium, or nonuniform thermal resistance between the film and its substrate. The former nonuniformity is caused by the imperfections of the film surface, and the latter by the method of film deposition. Such nonuniformities resist quantitative monitoring and arise even when the film material has perfectly uniform parameters.

Nonuniformity in heat production $Q(x)$ or in heat transfer $W(x)$ can stem from the superconductor geometry as well. This is especially true for superconducting weak links with high current concentration: point contacts, microbridges, variable-thickness bridges, etc. [see, for example, a review by Likharev (1979)]. Thus a hot spot in a superconducting microbridge can also be treated as a resistive domain localized within an inhomogeneity, namely, in the weak link itself.

Nonuniformities in bistable current-carrying conductors affect the propagation of switching waves and result in their localization in a certain current range (Gurevich and Mints, 1984a). This creates in the conductor localized resistance domains that are stable even in the fixed-current regime. The next section deals with the properties of such localized domains and with the related hysteresis effects.

B. Localization of resistive domains in inhomogeneous superconductors

1. Smooth inhomogeneities

The static distribution of the normal, resistive, and superconducting phases in an inhomogeneous current-carrying superconductor is described by the heat conduction equation,

$$\frac{d}{dx}\kappa(T,x)\frac{dT}{dx}+Q(T,x)-W(T,x)=0\ , \tag{5.1}$$

in which all parameters may explicitly depend not only on T but also on x. Let us consider the solutions of Eq. (5.1) describing a resistive domain localized on an inhomogeneity in an infinite superconductor. Such solutions cannot be obtained in the general form if the parameters are arbitrary functions of T and x; for this reason we shall restrict the analysis to two limiting cases: a smooth inhomogeneity ($l \gg L$) and a point inhomogeneity ($l \ll L$), where l is the characteristic size of inhomogeneities along the specimen.

We begin with the case $l \gg L$, in which the parameters of a superconductor vary slowly over the thermal length L (Gurevich, 1982; Gurevich and Mints, 1984a). The equation describing the motion of the N-S interface in such superconductors takes the form

$$\frac{dX}{dt}=v(X)\ ,$$

where $X(t)$ is the coordinate of the N-S interface and $v(X)$ is its local velocity at each point of the specimen. The equilibrium positions of the N-S interface follow from the condition $v(X)=0$, which can be rewritten in the form

$$I=I_p(X)\ . \tag{5.2}$$

Here $I_p(X)$ is the local value of the minimum current of normal-zone propagation. The quantity $I_p(X)$ is found from Eq. (3.7) with X-dependent parameters. The function $I_p=I_p(X)$ is the most important characteristic for describing localized resistive domains in superconductors with smooth ($l \gg L$) inhomogeneities.

Let us consider a normal zone of length $D \gg L$, arising in the part of the specimen with $I > I_p(x)$. This zone will expand until the N-S interfaces reach those areas of the superconductor whose $I_p(x) > I$. The expansion of the normal zone then stops and a resistive domain is formed, whose size is given by Eq. (5.2). In the simplest situation, when the curve $I_p(x)$ has a single minimum, the domain length $D(I)$ monotonically increases as I increases (Fig. 37). Obviously, such domains are stable.

A nonmonotonic dependence $I_p(x)$ results in a hysteresis. Indeed, let a resistive domain appear originally at the center of the deepest "well" in Fig. 38. As I increases, the domain length gradually increases up to the current $I=I_+$ at which the right-hand N-S interface "jumps" into the neighboring inhomogeneity and the domain length increases abruptly by D_2-D_1. Further growth in I results in a monotonic increase of D until one of the N-S interface penetrates another adjacent inhomogeneity, and so forth. The corresponding dependence $D=D(I)$ is steplike; in Fig. 38(b) it is traced by upward arrows.

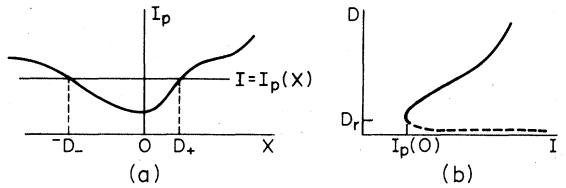

FIG. 37. (a) Graphic solution of Eq. (5.2); (b) the corresponding dependence $D=D(I)$, for $I_p(x)$ having a single minimum.

When current decreases, the length of a localized resistive domain monotonically decreases [downward arrows in Fig. 38(b)]. At $I=I_+$ the domain breaks in two, and at $I=I_-$ the right-hand domain of these two vanishes. Consequently hysteresis is obeyed in the range $I_- < I < I_+$.

We have considered the simplest case of not more than two domains coexisting in a specimen at a fixed current I. Their number may be substantially higher if the horizontal line $I=I_p$ in Fig. 38(a) intersects several "wells." In this case the $D=D(I)$ curve has no hysteresis-free segments.

The current-voltage characteristic of a superconductor with smooth inhomogeneities is qualitatively similar to the $D(I)$ curve plotted in Fig. 38(b). The localization of stable resistive domains that do not expand to occupy the whole specimen can thus produce steps in I-V characteristics of inhomogeneous superconductors (Mints, 1979; Gurevich and Mints, 1981a, 1984a; Gurevich, 1982). Each such step marks the appearance of a new resistive domain or the stepwise extension of the length of the existing domains due to an increase in I (see Fig. 38). Stable localized hot spots in thin films were observed by a number of direct techniques, e.g., by arranging potential contacts along the superconductor (Ivanchenko *et al.*, 1979, 1981, 1983; Schulze and Keck, 1983), by scanning electron microscopy (Huebener, 1984), etc.

A stepwise breakdown of superconductivity in a current-carrying conductor and a strong hysteresis under Joule self-heating were observed both in thin films (Breemer and Newhouse, 1959; Kolchin *et al.*, 1961; Smirnov

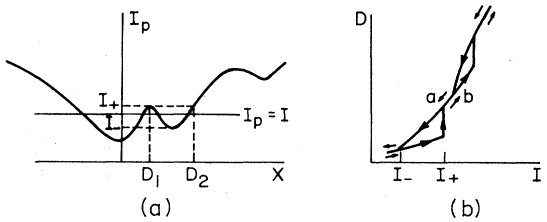

FIG. 38. (a) Graphic solution of Eq. (5.2); (b) the corresponding dependence $D=D(I)$, for $I_p(x)$ having several minima.

et al., 1965, 1968; Volotskaya *et al.*, 1976; Aomine and Miyake, 1979; Dharmadurai and Ratnam, 1979; Ivanchenko *et al.*, 1979, 1981; Skocpol, 1981; Ivanchenko and Mikheenko, 1982; Schulze and Keck, 1983, 1984; Golovashkin *et al.*, 1984) and in composite superconductors (Purcell and Brooks, 1968; Cesnak and Kokavec, 1969; Altov *et al.*, 1977; Tsuchiya and Suenaga, 1985). The corresponding I-V characteristics are shown in Figs. 39 and 40. Aomine and Miyake (1979) demonstrated that the I-V characteristics of thin films are considerably affected by inhomogeneities. Dharmadurai and Ratnam (1979) reported that specially introduced inhomogeneities such as holes and notches produced steps in I-V characteristics.

Let us illustrate the above arguments using the stepwise heat production model. Let the Stekly parameter $\alpha(x)$ and the local critical temperature $\theta_r(x)$ in Eq. (3.33) depend on x. If $\theta_r(x)=\theta_r(-x)$, and $\alpha(x)=\alpha(-x)$, then the equation for the length D of the nonsuperconducting part of the resistive domain is (Gurevich, 1982)

$$2\theta_r(i,D)=i^2\exp\left[-\frac{D}{2L}\right]\int_{-D/2L}^{D/2L}\alpha(x)\cosh x\,dx\ . \qquad (5.3)$$

Consider now the simplest case of a parabolic "well":

$$\alpha(x)=\left[1-s_1\left[\frac{x}{L}\right]^2\right]\alpha(0)\ ,$$

$$\theta_r(i,x)=\left[1+s_2\left[\frac{x}{L}\right]^2\right]\theta_r(i)\ ,$$

where $s_1\sim s_2\sim(L/l)^2\ll 1$, $\theta_r\equiv\theta_r(i,0)$. Such an inhomogeneity corresponds to a region with enhanced heat production. Then

$$\exp\left[-\frac{D}{L}\right]+s\left[\frac{D}{L}\right]^2+2\xi(i)-1=0\ . \qquad (5.4)$$

Here $\xi(i)=\theta_r(i)/\alpha(0)i^2$, $4s=s_1+s_2\xi(i)$. Equation (5.4) has two roots with substantially different values of D:

$$D_1\approx L\ln\frac{1}{1-2\xi},\quad D_2\approx L\left[\frac{1}{s}(1-2\xi)\right]^{1/2}\ .$$

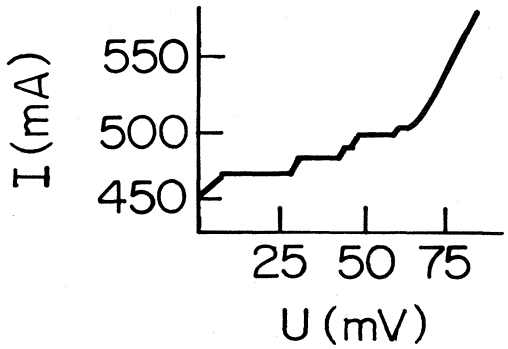

FIG. 39. Stepwise destruction of superconductivity in 3-nm-thick tin film ($T_0=1.8$ K) (Schulze and Keck, 1983).

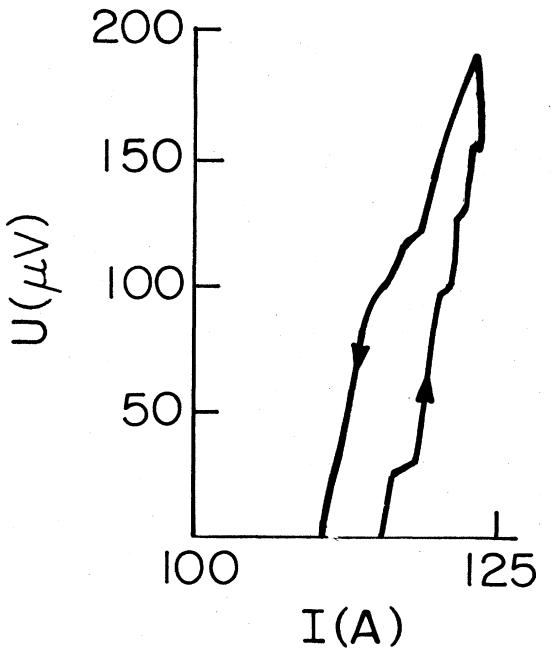

FIG. 40. Stepwise destruction of superconductivity in a composite superconductor (Bindari and Bernert, 1968).

The two branches $D=D_{1,2}(I)$ merge at $I=I_r\approx I_p(0)$, where $D(I_r)\sim L\ln 1/s\gg L$. The function $D=D(I)$ is schematically plotted in Fig. 37(b). The upper (solid) branch $D=D_2(I)$ corresponds to the above-discussed stable localized domain whose length is given by Eq. (5.2). The other solution, $D=D_1(I)$, corresponds, in fact, to an unstable resistive domain in a homogeneous superconductor whose parameters correspond to the point $x=0$ [dashed curve in Fig. 37(b)]. The reason for this is the fact that $D_1\sim L$, so that in view of $l\gg L$ the parameters of the specimen remain almost unchanged over the domain length. As I decreases, the unstable domain grows, absorbing gradually "colder" peripheral regions of the inhomogeneity. As a result, the domain vanishes stepwise at $I=I_r$ for the same reasons that a hot spot vanishes in a superconducting microbridge (Fig. 27), which can be treated as an inhomogeneity producing a rectangular "well" in $I_p(x)$.

The I-V characteristic of an infinite superconductor containing an inhomogeneity is shown in Fig. 41, where $I_p(0)$ and $I_c(0)$ are the values assumed by $I_p(x)$ and $I_c(x)$ at the center of the inhomogeneity, and $I_p(\infty)$ is the minimum propagating current far from the inhomogeneity. Two cases are possible, depending on the parameters: $I_p(\infty)<I_c(0)$ [Fig. 41(a)] and $I_p(\infty)>I_c(0)$ [Fig. 41(b)]. In the first of them the specimen transforms completely to the normal state at $I>I_c(0)$. In the subsequent decrease of current the reverse transition takes place beginning with $I=I_p(0)<I_p(\infty)$. A stable domain is localized in the superconductor in the interval $I_p(0)<I<I_p(\infty)$. The quantity $I_p(0)$ here is the current of complete recovery of superconductivity.

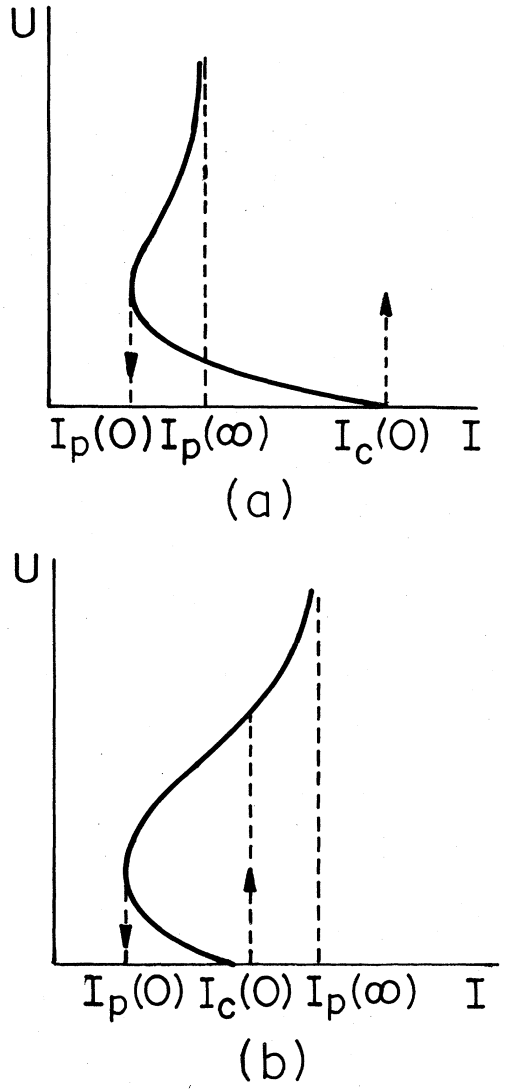

FIG. 41. I-V characteristics in the case of resistive domain localization on a smooth inhomogeneity: (a) $I_p(\infty)<I_c(0)$; (b) $I_p(\infty)>I_c(0)$.

In the second case [$I_c(0)<I_p(\infty)$; see Fig. 41(b)] a jump to the upper (stable) branch of the I-V characteristic takes place at $I=I_c(0)$, and a localized resistive domain appears at the center of the inhomogeneity. The rest of the specimen remains superconducting because $I_c(0)<I_p(\infty)$. Superconductivity completely recovers beginning with $I=I_p(0)$. Hysteresis occurs in both these cases, in the current interval $I_p(0)<I<I_c(0)$.

Figure 41 corresponds to domain localization on a single isolated inhomogeneity. Several inhomogeneities in one superconductor may result in steps appearing on its I-V characteristic. This behavior is caused by successive creation of resistive domains inside these inhomogeneities at the appropriate values of $I=I_c(X_n)$ where X_n is the coordinate of the nth inhomogeneity. As a result, we come to qualitatively the same picture of stepwise destruction of superconductivity by transport current that we discussed in connection with Fig. 38. The difference here lies only in the mechanism of normal phase propagation with increasing I: in the case shown in Fig. 41(b) the resistive domains begin to appear within inhomogeneities, and then grow and merge as I increases. It is also possible, however, that the earlier-outlined situation is realized: the breakdown of superconductivity starts at some "weak" point [$x=0$, $I>I_c(0)$ in Fig. 38(a)] and proceeds by successive jumps of N-S interfaces to the adjacent inhomogeneities where $I<I_c(X_n)$.

2. Point inhomogeneities

Let us consider another limiting case, namely, that of point inhomogeneities ($l \ll L$), which can also be analyzed in the general form (Mints, 1979; Gurevich and Mints, 1981a, 1984a). Local inhomogeneities are classified under two groups, regardless of their concrete nature. The first group is that of inhomogeneities with a reduced value of critical current. These inhomogeneities are the "weak" points at which the resistive domains first appear as I increases. All other inhomogeneities are classified under the second group. In the thermal problem of interest here these are the regions of elevated effective heat production or heat transfer. It is therefore possible to rewrite Eq. (5.1) in the form

$$\frac{d}{dx}\kappa\frac{dT}{dx}-f(T)+F(T)\delta(x)=0\ , \tag{5.5}$$

where $f(T)=W-Q$, the inhomogeneity is presented as a point heat source (heat sink) $F(T)\delta(x)$, and all other parameters are not explicit functions of x.

Let us consider the solutions of Eq. (5.5) describing a resistive domain localized on an inhomogeneity. The distribution $T=T(x,T_m)$ in a domain-containing specimen is given by Eq. (4.1); it essentially depends on the temperature at the inhomogeneity, $T_m(j)$.

In order to find an equation for T_m, we multiply Eq. (5.5) by $\kappa\,dT/dx$ and integrate in x from $+0$ to ∞. This gives

$$\frac{1}{2}\left[\kappa\frac{dT}{dx}\right]^2_{+0}=S(T_m)\ .$$

On the other hand, the derivative dT/dx has a jump at $x=0$:

$$\kappa\frac{dT}{dx}\bigg|_{-0}-\kappa\frac{dT}{dx}\bigg|_{+0}=F(T_m)\ . \tag{5.6}$$

Making use of the last two relations, and taking into account that within the domain $T(x)=T(-x)$, we find an equation for T_m:

$$S(T_m)=\tfrac{1}{8}F^2(T_m)\ . \tag{5.7}$$

An expression for the power of heat production $F(T)$ on the inhomogeneity can be found from the condition of continuity of $T(x)$ and $\kappa\,dT/dx$ at its boundaries. The result is

$$F^2(T_m)=\left[\int_{-l}^{l} f(T_m,x)dx\right]^2 - 8\kappa(T_m)f(T_m)\int_0^l \frac{dx}{\kappa(T_m,x)} \times \int_0^x f(T_m,x')dx' , \quad (5.8)$$

where $\kappa(T_m)$ and $f(T_m)$ are the values assumed by κ and f in the homogeneous part of the specimen, $|x|>l$. If f and κ are independent of x, then $F(T)\equiv 0$ and Eq. (5.7) reduces to $S(T_m)=0$, which determines T_m in a homogeneous superconductor.

The system of equations (5.7) and (5.8) makes it possible to analyze all allowed types of resistive domains that can be localized at a point inhomogeneity. Note that, owing to a substantial dependence of F on T, such an inhomogeneity is a self-consistent heat source (heat sink), which depends on the distribution $T(x)$ in the domain. Furthermore, this inhomogeneity differs from the steady-state microheater that is often used for the thermal diagnostics of superconducting composites (Stekly, 1966; Altov *et al.*, 1977).

Let us consider $F(T)$ for some typical inhomogeneities. Assume that the values of j_c and κ are reduced in the interval $|x|<l$, while that of ρ is increased. This inhomogeneity is both a "weak" point and a local heat source. If all parameters within the inhomogeneity are constant, then, for example, in the resistive model one finds

$$F_0(\theta)=0, \quad \theta<\theta_c ,$$
$$F_0^2(\theta)=\left[\frac{2l}{L}\right]^2 \alpha i\delta_r\delta_s(\theta-\theta_c) \times[(\delta_r-1)\theta+(\theta-\theta_c)\alpha i\delta_r\delta_s], \quad \theta_c<\theta<1-i , \quad (5.9)$$
$$F_0^2(\theta)=\left[\frac{2l}{L}\right]^2 \alpha i\delta_r\delta_s(\theta-\theta_c) \times[(\delta_r-1)\theta+\alpha i(1-\delta_s)(1-\theta)], \quad 1-i<\theta<1 ,$$
$$F_0^2(\theta)=\left[\frac{2l}{L}\right]^2 \delta_r(\delta_r-1)\alpha i^2\theta, \quad \theta>1 ,$$

where $F_0^2(\theta)=F^2(\theta)d/\kappa h(T_c-T_0)^2$, $\delta_r=\rho(0)/\rho$, $\delta_s=j_c(0)/j_c<1$, $\theta_c=1-i/\delta_s$ is the temperature of transition into the resistive state at the inhomogeneity, and $\rho(0)$ and $j_c(0)$ are the values of ρ and j_c within the inhomogeneity. For the sake of simplification it was assumed that $\alpha\gg 1$ and that κ and ρ at $T>T_c$ obey the Wiedemann-Franz law. The functions $F_0(\theta)$ are plotted in Fig. 42.

Let us discuss the possible types of resistive domains that can be localized at a point inhomogeneity. Their number is given by the number of roots T_m of the system of equations (5.7) and (5.8). A graphic solution of this system for an inhomogeneity due to $\rho(x)$ only, with $\delta_s=1$ and $\delta_r>1$ (local heat source), is shown in Fig. 43. Note

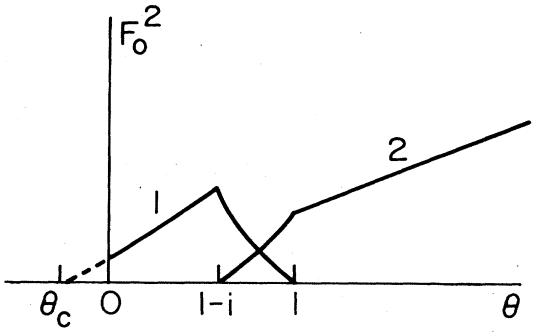

FIG. 42. Typical $F_0^2(\theta)$ dependence for (1) "weak" point and (2) "hot" point [local inhomogeneity with elevated $\rho(x)$].

that the number of different types of localized domains is a function of current. Thus, at $j>j_p$ one domain corresponding to point 1 in Fig. 43 can be localized on the inhomogeneity, at $j_r<j<j_p$ two domains of different types can be localized (points 1 and 2), and finally, at $j<j_r$ localized domains are impossible. The quantity j_r is found from the condition of tangency of the curves $S(T)$ and $F^2(T)/8$ in Fig. 43, that is,

$$S(T,j_r)=\tfrac{1}{8}F^2(T,j_r) , \qquad \frac{\partial}{\partial T}S(T,j_r)=\frac{1}{8}\frac{\partial}{\partial T}F^2(T,j_r) . \quad (5.10)$$

In terms of the mechanical analogy discussed above, a resistive domain localized on an inhomogeneity corresponds to the following trajectory of a particle in the potential $-S(T)$. The particle starts from the point $T=T_0$ at an infinitesimal velocity, is bounced back elastically at one of the points 1 or 2 in Fig. 43, and then returns to the point $T=T_0$. It is clear from these arguments that at $j>j_p$ the solution corresponding to point 2 is not realized because reaching point 2 is forbidden for a particle by the law of energy conservation.

The criterion of stability of localized resistive domains can be obtained with the following qualitative arguments. Let a small fluctuation of T_m arise in the domain. In the fixed-current regime the domain will be stable if an in-

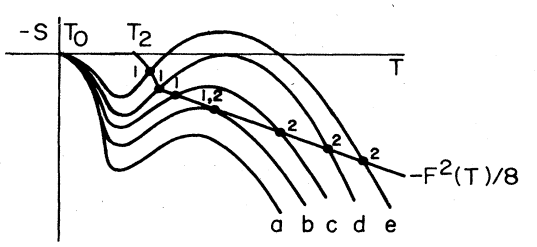

FIG. 43. Example of a graphic solution of Eq. (5.7) for a local inhomogeneity with elevated $\rho(x)$.

crease in T_m by δT_m makes the total heat transfer $\int_{-\infty}^{\infty} W\,dx$ exceed the total heat production $\int_{-\infty}^{\infty}[Q+F\delta(x)]dx$, i.e.,

$$\delta T_m \frac{\partial}{\partial T_m}\left[\int_{-\infty}^{\infty}(W-Q)dx - F(T_m)\right] > 0 .$$

Then the stability condition for a localized domain takes the form

$$\frac{\partial}{\partial T_m}\int_{-\infty}^{\infty} f(T,T_m)dx > \left.\frac{\partial F}{\partial T}\right|_{T_m} .$$

Taking into account that

$$f(T)=\frac{d}{dx}\kappa\frac{dT}{dx}$$

at $x\neq 0$, one finds

$$\frac{\partial}{\partial T_m}\int_{-\infty}^{\infty} f\,dx = 2^{3/2}\frac{\partial}{\partial T_m}S^{1/2}(T_m) = \frac{4}{F(T_m)}\left.\frac{\partial S}{\partial T}\right|_{T_m},$$

where we made use of Eqs. (5.6) and (5.7). As a result, we come to the stability condition for localized domains in the fixed-current regime

$$F\frac{\partial}{\partial T}\left[S-\frac{F^2}{8}\right]_{T_m} > 0 . \tag{5.11}$$

The physical meaning of this condition is that the temperature T_m in a stable domain increases with increasing current (such a domain corresponds to point 2 in Fig. 43). A rigorous analysis of stability of localized resistive domains was carried out by Gurevich and Mints (1981a, 1984a).

The current-voltage characteristic of a superconductor containing a localized resistive domain has the form

$$U(j)=\sqrt{2}\int_{T_r}^{T_m}(j-j_c)\kappa\rho S^{-1/2}dT + I\Delta R , \tag{5.12}$$

where $T_m(j)$ is one of the roots of Eq. (5.7) and

$$\Delta R = A^{-1}\int_{-\infty}^{\infty}[\rho(x,T_m)-\rho(T_m)]dx$$

is the excess resistance of the inhomogeneity. The I-V characteristic under discussion is multivalued, with Eq. (5.12) describing the branch corresponding to one of the domain solutions.

Figure 44(a) plots the I-V characteristic of an inhomogeneity due to an increase in $\rho(x)$. The ascending (stable) branch $U=U(I)$ corresponds to point 2 in Fig. 43, and the descending (unstable) branch to point 1. This branch can be stabilized by changing to the fixed-current regime. A stable resistive domain is thus localized on such inhomogeneities in the current range $I_r<I<I_p$. The quantity I_r is the current of complete recovery of superconductivity; it is lower than the minimum normal-zone propagation current I_p. The multivaluedness of the I-V characteristic produces a hysteresis in the destruction of superconductivity in current-carrying conductors.

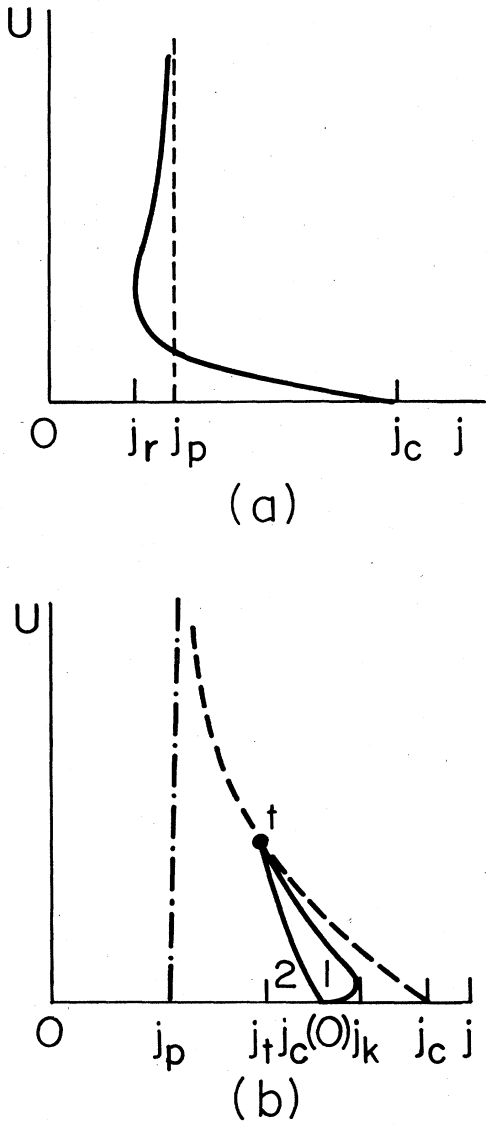

FIG. 44. I-V characteristics in the case of resistive domain localization on a point inhomogeneity: (a) with elevated $\rho(x)$; (b) with lowered $j_c(x)$.

An expression for I_r can be obtained from the system of equations (5.10). Thus, in the resistive model (Mints, 1979; Gurevich and Mints, 1981a),

$$i_r=\left[\frac{1}{4\alpha_r^2}+\frac{2}{\alpha_r}\right]^{1/2}-\frac{1}{2\alpha_r} , \tag{5.13}$$

where $\alpha_r=(1+\Gamma^2)\alpha$, $i_r=I_r/I_c$, $\Gamma=l\Delta\rho/L\rho$ is a parameter characterizing the inhomogeneity, and $\Delta\rho=\rho(0)-\rho$. By the order of magnitude, Γ is the ratio of the additional heat production on the inhomogeneity, $2l\Delta\rho j^2$, to the total heat production in the domain, which is $\sim L\rho j^2$.

The formula for Γ contains a small parameter l/L, so that $j_p-j_r\sim\Gamma^2 j_p \ll j_p$, unless the quantities $\Delta\rho/\rho$ or $A/A(0)$ are sufficiently high. The smallness of Γ is a result of the small contribution of a point inhomogeneity

into the total heat production within a resistive domain.

Figure 44(b) plots the I-V characteristic in the case when a resistive domain localizes at a "weak" point, i.e., in a region of reduced critical current. Here too there can be a stable branch at $j_c(0)<j<j_k$ and an unstable branch at $j_t<j<j_k$. At $j<j_t$ localized domains are impossible. In this case the temperature at the inhomogeneity T_m is greater than T_c, so that $F(T)=0$ (the inhomogeneity is "switched off"). For this reason at $j<j_t$ the I-V characteristic has the same form as the homogeneous superconductor characteristic [dashed curve in Fig. 44(b)].

In the resistive model j_t is given by Eq. (4.11), and the expression for j_k is

$$j_k=\left[1-\frac{\alpha l}{L}(1-\delta_s)\right]j_c,\quad \alpha l\ll L\ . \tag{5.14}$$

An increase in l or α may result in vanishing of the stable branch of the I-V characteristic [curve 2 in Fig. 44(b)]. This behavior arises if $j_k<j_c(0)$ or

$$\alpha j_c^2(0)l>Lj_c^2\ . \tag{5.15}$$

If this inequality is satisfied, heat production on the inhomogeneity is so intensive that the metastable superconducting state becomes absolutely unstable.

Figure 44(b) shows that the destruction of superconductivity in a current-carrying superconductor starts at the inhomogeneity: a stable resistive domain is localized on it at $I_c(0)<I<I_k$. As I further increases, this domain is destabilized at the thermal breakdown current,

$$I_j=\max[I_c(0),I_k]\ , \tag{5.16}$$

so that the normal zone grows to occupy the whole specimen. The localization of resistive domains on inhomogeneities thus reduces breakdown currents I_j and superconductivity recovery currents I_r as well. The decrease in I_j is caused by the presence of "weak" points in the superconductor, and the decrease in I_r is caused by inhomogeneities, which are the sources of additional heat production.

It was mentioned above that the creation of resistive domains localized on inhomogeneities leads to a stepwise destruction of superconductivity in current-carrying conductors. At the same time, steps on the I-V characteristics of thin films or narrow superconducting microbridges can be connected with the creation of moving magnetic tubes (Huebener, 1979), or with phase-slip centers (Skocpol, Beasley, and Tinkham, 1974b). These effects are especially pronounced at $T\approx T_c$, when self-heating becomes negligible. At lower temperatures macroscopic "hot" regions, i.e., resistive domains, begin to appear in the superconductor. As an illustration, Fig. 45 shows the I-V characteristic of indium film at various T_0; it demonstrates the transition to a multivalued function $U=U(j)$ typical of a resistive domain localized at low temperatures on an inhomogeneity (cf. Fig. 44). Phase-slip centers in inhomogeneous superconductors have been discussed by Ivlev, Kopnin, and Larkin (1983) and Kramer and Rangel (1984).

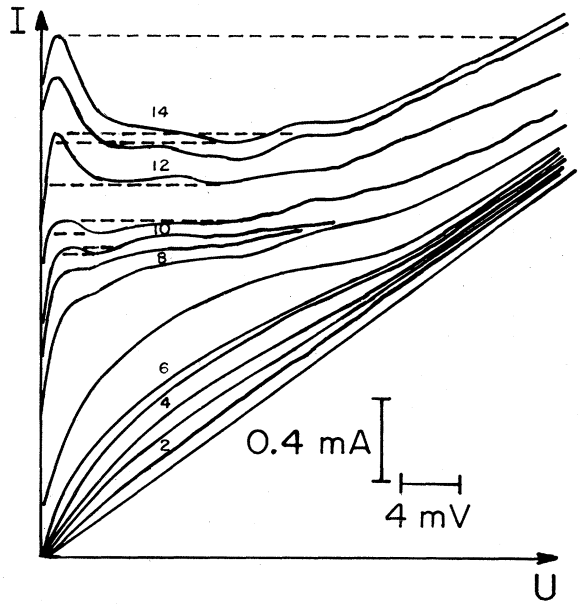

FIG. 45. I-V characteristic of an indium film at various temperatures $\zeta=1-T_0/T_c$: (1) 0; (2) 8×10^{-4}; (3) 4.7×10^{-3}; (4) 6.1×10^{-3}; (5) 7.5×10^{-3}; (6) 9.1×10^{-3}; (7) 1.19×10^{-3}; (8) 1.4×10^{-2}; (9) 1.46×10^{-2}; (10) 1.52×10^{-2}; (11) 1.63×10^{-2}; (12) 1.79×10^{-2}; (13) 1.9×10^{-2}; (14) 2.07×10^{-2} (Ivanchenko and Mikheenko, 1982).

C. Localization of N-S interfaces. Metastable dissipative structures

Consider now the localization of N-S interfaces on isolated point inhomogeneities (Gurevich and Mints, 1984a). The corresponding distributions $T=T(x,T_m)$ are conveniently classified using the analogy of Eq. (5.1) to the equation of motion of a particle in a potential $-S(T)$ (Fig. 12). At the instant of time $x=0$ an impact imparts to the particle an additional momentum $-F(T_m)$. The trajectories $T=T(x)$ begin at the point $T=T_0$ and end at $T=T_3$ (Fig. 12). The momentum $-F(T_m)$ is imparted to the particle so as to change its energy by a quantity $S_3(j)$ and so that it arrives at the point $T=T_3$ at zero final velocity. As $S_3(j)>0$ for $j<j_p$ and $S_3(j)<0$ for $j>j_p$, in the case of $j<j_p$ the particle under impact must be decelerated, and in the case of $j>j_p$ it must be accelerated. Hence the N-S interface can be localized only if the following conditions are met: $F>0, j<j_p$ or $F<0, j>j_p$. These conditions are a reflection of the fact that only "cold" inhomogeneities ($F<0$) can stop the normal-zone propagation ($j>j_p$), and only "hot" inhomogeneities ($F>0$) can stop the superconducting-zone propagation ($j<j_p$).

Let us analyze the case of $F>0$ ($j<j_p$). At low F (see below) the particle is somewhat decelerated by the impact but preserves the direction of motion. By virtue of the energy and momentum conservation law, we find the following equation for the temperature T_m of the inhomogeneity:

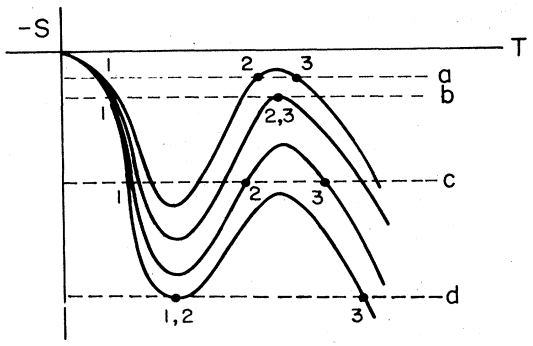

FIG. 46. Graphic solution of Eq. (5.17) for $F(T)=$const. Solid curves trace the functions $S(T)$, and dashed curves trace $\mathcal{F}$.

$$S^{1/2}(T_m)-[S(T_m)-S_3(j)]^{1/2}=F(T_m)/\sqrt{2}\ . \quad (5.17)$$

It has a solution only for $F^2<2|S_3|$ and $T_m<T_3$. As F further increases, the particle undergoes in the impact an "inelastic reflection," i.e., its direction of motion is reversed. In this case the impact can take place both at $T_m<T_3$ and at $T_m>T_3$, and the equation for T_m takes the form

$$S^{1/2}(T_m)=[S(T_m)-S_3(j)]^{1/2}=F(T_m)/\sqrt{2}\ . \quad (5.18)$$

This equation has a solution if $F^2>2|S_3|$. The two equations (5.17) and (5.18) are conveniently rewritten in the form

$$S(T_m,j)=\mathcal{F}(T_m,j) \equiv\frac{1}{2}\left[\frac{F(T_m,j)}{2}+\frac{S_3(j)}{F(T_m,j)}\right]^2 . \quad (5.19)$$

A graphic solution of Eq. (5.19) is shown in Fig. 46 for the simplest case of $F(T)=$const. If $F^2<2|S_3|$, the solutions of interest here correspond to points 1 and 2, and if $F^2>2|S_3|$ to points 1, 2, and 3. At these points the momentum of the particle changes by $-F(T_m)$. The corresponding temperature distributions across localized N-S interfaces are shown in Fig. 47.

If $F^2<2|S_3|$, the stability criterion for localized N-S interfaces can be obtained with the same qualitative arguments as in the case of localized domains. The result is[5]

$$F\frac{\partial}{\partial T}(\mathcal{F}-S)_{T_m}>0\ . \quad (5.20)$$

In the above example, where $F(T)=$const, only the temperature distribution $T=T(x,T_m)$ marked as curve 2 in Fig. 47(a) ($j_2<j<j_3$) and that marked as curve 3 in Fig. 47(b) ($j_3<j<j_p$) are stable. This situation corresponds to point 2 in Fig. 46 at $j_2<j<j_3$ and to point 3 at $j_3<j<j_p$.

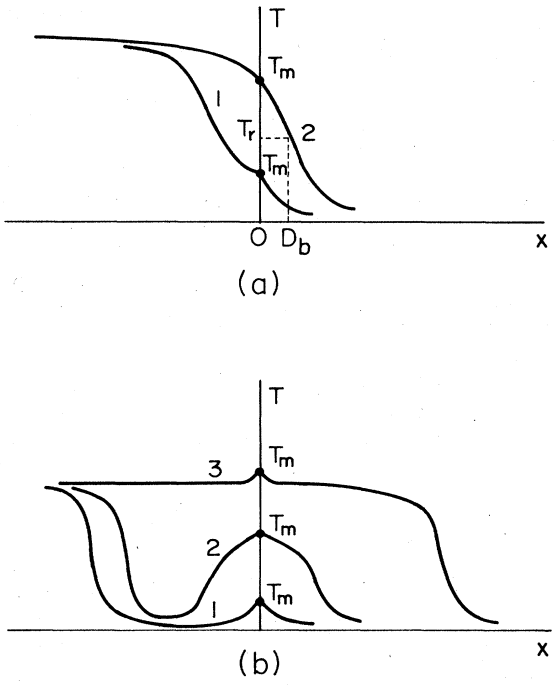

FIG. 47. Typical $T(x)$ distributions in localized N-S interfaces. The numbers correspond to the points of intersection of $S(T)$ and $\mathcal{F}$ in Fig. 46.

Equation (5.19) thus has two physically meaningful solutions in the interval $j_2<j<j_3$ and three in the interval $j_3<j<j_p$. The quantities j_2 and j_3 are found from the condition of tangency of the curves $S(T)$ and $\mathcal{F}(T)$ and give the least and the greatest roots of the system of equations

$$S(T,j)=\mathcal{F}(T,j)\ , \qquad \frac{\partial}{\partial T}S(T,j)=\frac{\partial}{\partial T}\mathcal{F}(T,j)\ . \quad (5.21)$$

At $j=j_3$ points 2 and 3 in Fig. 46 merge, and at $j=j_2$ points 1 and 2 merge. At $j<j_2$ Eq. (5.19) has no stable solutions $T_m(j)$. Physically this means that the localized N-S interface "breaks away" from the inhomogeneity and starts moving along the specimen.

The system (5.21) is substantially simplified if $\mathcal{F}(T)=$const. Then $T=T_2$ at $j=j_2$ and $T=T_3$ at $j=j_3$ (Fig. 46). As a result, we return to the equation $F^2(j_3)=2|S_3(j_3)|$ and obtain the following equation for j_2:

$$S_3(j_2)=F(j_2)[2S_2(j_2)]^{1/2}-\frac{F^2(j)}{2}\ , \quad (5.22)$$

where $S_{2,3}(j)=S[T_{2,3}(j),j]$.

The function $\mathcal{F}(T)$ can be calculated by using the solutions of Eqs. (5.1) inside and outside the inhomogeneity and matching the obtained distributions $T(x)$. This gives

$$\mathcal{F}(T_m)=\frac{F^2}{8}(T_m)+S_3(j)+\frac{S_3^2(j)}{2F_1^2(T_m,j)}\ , \quad (5.23)$$

[5]A detailed analysis of stability is given in the review of Gurevich and Mints (1984a).

$$F_1(T_m,j)=\int_{-l}^{l}\left[f(T_m,x)-\frac{f(T_m)\kappa(T_m)}{\kappa(T_m,x)}\right]dx\ , \qquad (5.24)$$

where $F^2(T_m)$ is given by Eq. (5.8). Equations (5.23) and (5.24) coincide with the expression for $\mathcal{F}(T_m)$ in (5.19), derived for a point inhomogeneity, provided $F=F_1$. This equality holds in the case of a strong inhomogeneity in $f(T,x)$ and a weak inhomogeneity in $\kappa(T,x)$.

We shall illustrate these general relations using the stepwise heat production model as an example. Let the N-S interface be localized at an inhomogeneity due to $\rho(x)$. Then the equation for the length D_b (see Fig. 47) has the form

$$2\theta_r(i)=i^2\int_0^{\infty}\alpha(x-D_b)\exp\left[-\frac{x}{L}\right]\frac{dx}{L}\ . \qquad (5.25)$$

For a point inhomogeneity, i.e., for $\alpha(x)=[1+\Gamma\delta(x/L)]\alpha$, $\Gamma=2l\Delta\rho/\rho L$, Eq. (5.25) yields

$$D_b=L\ln\frac{\Gamma}{2\xi(i)-1}\ , \qquad (5.26)$$

where $\xi(i)=\theta_r(i)/\alpha i^2$. A localized N-S interface exists if Γ and $(2\xi-1)$ are of like signs, i.e., either $\Gamma>0, i<i_p$ or $\Gamma<0, i>i_p$. As the current decreases, the length $D_b(i)$ decreases, and vanishes at $i=i_2$. Further decrease of i results in a delocalization of the N-S interface because $F(T)=0$ at $T<T_r$. This situation occurs when

$$2\xi(i)-1>\Gamma\ . \qquad (5.27)$$

As follows from Eq. (5.27), the current i_2 is given by Eq. (3.41), in which $\alpha\to(1+\Gamma)\alpha$. If $\alpha\gg1$ and $\Gamma\ll1$, then $i_p-i_2\simeq\Gamma i_p/2$, in contrast to the resistive domain, where $i_p-i_r\sim\Gamma^2 i_p$. Therefore, at $\Gamma\ll1$ the current interval in which N-S interfaces are localized is substantially wider than for the resistive domain. Consequently the superconductivity recovery current here is the quantity $I_r=j_2A$.

If a specimen contains several point inhomogeneities, a metastable resistive structure may be formed, consisting of individual "fragments," i.e., localized domains or N-S interfaces (Gurevich and Mints, 1984a, 1985). The formation of such a dissipative structure (Fig. 48) results in a stepwise destruction of superconductivity in a current-carrying conductor. This behavior occurs because steady-state normal regions, whose lengths D_n are determined only by the spacings between inhomogeneities, can exist in the specimen if N-S interfaces are localized in it.

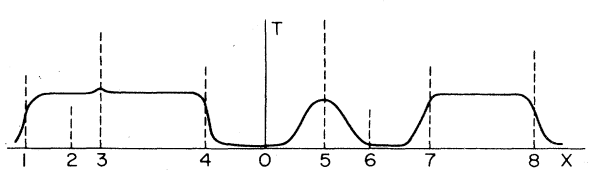

FIG. 48. An example of metastable dissipative structure in a nonhomogeneous medium. The lengths of dashed perpendiculars are proportional to the value of the parameter Γ_i.

If the localization condition is met for each N-S interface, the lengths D_n are nearly independent of j, and the I-V characteristic is nearly linear. When this condition is violated in the course of decreasing j, one of the N-S interfaces is delocalized. It can be subsequently localized on a stronger inhomogeneity (e.g., relocalization corresponds in Fig. 48 to the N-S interface's jumping from inhomogeneity 1 to inhomogeneity 3). This jumpwise restructuring can take place both as j diminishes and as a result of strong perturbations. When j is subsequently increased, hysteresis is produced because of a difference between j_2 and j_p. A similar jumpwise growth of electrothermal domains has also been observed in normal metals (Abramov *et al.*, 1985). The result is a sawtooth I-V characteristic in the range of current stabilization at $I=I_p$ in Figs. 31 and 32.

VI. DESTRUCTION OF SUPERCONDUCTIVITY BY EXTERNAL PERTURBATIONS

The superconducting state becomes metastable when $I>I_p$. This means that this state is stable with respect to small perturbations but can be quenched by a sufficiently strong perturbation which produces the nucleation of a normal zone and its subsequent propagation. In this section we consider the minimum energy Q_c of a perturbation initiating the thermal quench of superconductivity by current. To be more specific, we shall be discussing mainly superconducting composites, although the results presented below are equally true for thin films.

Characteristic perturbations acting on a composite superconductor are usually local and pulsed. Examples are the intermittent plastic strain, friction of the superconductor at the substrate, local magnetic flux jump, etc. (see, for example, Brechna, 1973; Altov *et al.*, 1977; Meuris, 1984). As a result, the destruction of superconductivity starts at a "weak" spot in the superconductor, which differs from the rest of the specimen either by the level of perturbations or by poorer mechanical, electrical, or thermal characteristics.

The problem of finding the critical energy Q_c is formulated as follows. At $t=0$ an external perturbation with specific power $\dot{Q}(x,t)$ starts to act on the superconductor. This perturbation results in local heating in the superconductor and the formation of a normal or resistive nucleus within it. If the perturbation energy $Q_p<Q_c$, this nucleus will disappear soon after the perturbation is over, owing to the heat transfer to the coolant. The quantity Q_c is the minimum quench energy; if $Q_p>Q_c$, the nucleated normal zone propagates over the whole superconductor because of Joule self-heating.

In order to find Q_c, one has to solve the nonstationary heat conduction equation (3.1). The functions $\nu(T)$, $Q(T)$, and $W(T)$ of composite superconductors are fairly complicated, so that only a numerical solution is possible. The relevant calculations have been carried out by a number of authors, who found the critical energy Q_c for actual temperature dependences of the parameters of super-

conductors and coolants (e.g., Chen and Purcell, 1978; Pasztor and Schmidt, 1978; Schmidt, 1978; Anashkin, Keilin, and Lyikov, 1979, 1981; Nick, Krauth, and Ries, 1979; Superczynski, 1979; Keilin and Romanovsky, 1982; Christianson and Boom, 1984; Meuris, 1984; Romanovsky, 1984a, 1984b; Ando *et al.*, 1985; Cornelissen and Hoogendoorn, 1985; Jüngst and Yan, 1985; Tsukamoto and Nakada, 1985). We shall return to discussing the results of these calculations and to comparing them with experimental data at the end of this section. Here we note that the Q_c thus obtained depends on a large number of parameters. Consequently it is impossible to derive a simple general relation between Q_c and j,α, or between Q_c and the characteristic time t_q and length L_q of the perturbation.

In view of this, we first consider a simpler approximate approach. It was mentioned in Sec. IV that the superconducting state which is metastable at $I > I_p$ can be destroyed by generating in the specimen a nucleus of normal phase, i.e., a resistive domain. Martinelli and Wipf (1973), Wilson and Iwasa (1978), and Wipf (1979) suggested that the enthalpy Q_d of formation of such a resistive domain be regarded as the energy of perturbation sufficient to initiate the thermal quench of superconductivity in a current-carrying superconductor. By definition,

$$Q_d = A \int_{-\infty}^{\infty} dx \int_{T_0}^{T(x)} \nu(T) dT ,$$

where $T(x)$ is the temperature distribution in a resistive domain. Changing to integration in T, we find through Eq. (4.1)

$$Q_d = A\sqrt{2} \int_{T_0}^{T_m} \kappa S^{-1/2} dT \int_{T_0}^{T} \nu(T') dT' , \tag{6.1}$$

where $S(T)$ is given by Eq. (3.5) and T_m is the maximum temperature in the domain $[S(T_m)=0]$. This approach, known as the minimum propagating-zone theory, makes it possible to estimate Q_c without solving the nonstationary heat conduction equation (3.1).

In the stepwise heat production model Eq. (6.1) yields

$$\frac{Q_d}{Q_0} = \alpha i^2 \ln \frac{\alpha i^2}{\alpha i^2 - 2\theta_r(i)} , \tag{6.2}$$

where $Q_0 = \nu A L (T_c - T_0)$ is the thermal unit of perturbation energy. We shall also give the expression for Q_d in the resistive model,

$$\frac{Q_d}{Q_0} = \frac{2\alpha i(1-i)}{\alpha i - 1}\left[1 + \frac{1}{\sqrt{\alpha i - 1}}\left[\frac{\pi}{2} + \arcsin\frac{1}{\sqrt{\alpha i}}\right]\right], \quad \alpha i^3 \geq 1 , \tag{6.3}$$

$$\frac{Q_d}{Q_0} = \frac{2\alpha i(1-i)}{\alpha i - 1}\left[1 + \frac{1}{\sqrt{\alpha i - 1}}\left[\arcsin\frac{\alpha i^2 - 1}{(1-i)\sqrt{\alpha i}} + \arcsin\frac{1}{\sqrt{\alpha i}}\right]\right] + \alpha i^2 \ln\frac{\alpha i^2 - 1 + (1-\alpha i^3)^{1/2}}{\alpha i^2 - 1 - (1-\alpha i^3)^{1/2}} - 2(1-\alpha i^3)^{1/2}\frac{\alpha i}{\alpha i - 1} . \tag{6.4}$$

The cases $\alpha i^3 > 1$ and $\alpha i^3 < 1$ correspond to the absence ($i_t < i < 1$) and presence ($i_p < i < i_t$) of a normal zone in the resistive domain (Fig. 23), with i_p and i_t determined by Eqs. (3.24) and (4.11). The functions $Q_d = Q_d(i)$ are qualitatively similar in the two selected models: they linearly vanish at $i=1$ and monotonically increase as i decreases, tending to infinity at $i = i_p$. This behavior has a simple physical meaning. Indeed, the size of the zone $\sim D(j)$, whose heating by $\Delta T \sim T_r - T_0$ initiates the propagation of the normal zone, decreases with increasing current.

In the general case the critical energy Q_c depends not only on the parameters of the superconductor and coolant, but also on the time dependence of the perturbation power, $\dot{Q}(x,t)$, and on its distribution along the specimen. The enthalpy Q_d is thus the critical energy for perturbations that produce in the superconductor an initial temperature distribution close to $T(x)$ in the resistive domain. The critical energy of an arbitrary perturbation can be lower or greater than Q_d. Nevertheless, the enthalpy Q_d is a convenient characteristic of critical perturbations, and hence is frequently used for estimating the maximum admissible perturbation not leading to irreversible destruction of superconductivity (see, for example, Chen and Purcell, 1978; Wilson and Iwasa, 1978).

The critical energy Q_c may be found by solving the nonlinear partial differential equation (3.1). First we shall consider the stepwise heat production model and the resistive model, where it is possible to derive in some cases simple expressions for Q_c, and to analyze the normal-zone dynamics after the application of strong nonstationary perturbations. We begin with a local heat pulse of length t_q applied to an L_q-long region of the superconductor, $t_q \ll t_h$ and $L_q \ll L$. Then $\dot{Q}(x,t) = Q_p \delta(x)\delta(t)$, where Q_p is the total perturbation energy. In the stepwise heat production model the length $D(t)$ of the normal zone generated by the heat pulse is described by a nonlinear integral equation given in Appendix B. The results of numerical solution of this equation are shown in Fig. 49. If $Q_p > Q_c$, the normal zone expands, and if $Q_p < Q_c$, it contracts. An equilibrium velocity of N-S interfaces is reached after a time $\sim \xi t_h \ln(Q_p/Q_c + 1)$ after the application of the pulse with $Q_p > Q_c$. A more detailed analysis of normal-zone dynamics under nonstationary conditions is given in Appendix B.

In the stepwise heat production model the critical energy of a pointlike heat pulse can be written in the form

$$Q_c = Q_0 \alpha i^2 \varphi(\xi) ,$$

where $\varphi(\xi)$ is a universal function of one dimensionless

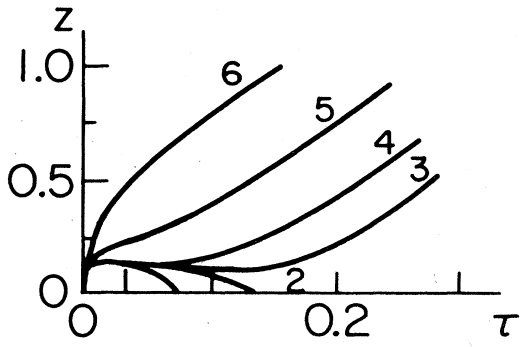

FIG. 49. Normal-zone length $Z(t)=D(t)/L$ as a function of $\tau=t/t_h$, in response to a pointlike heat pulse: (1) $Q_p=0.985Q_c$; (2) $Q_p=0.999Q_c$; (3) $Q_p=1.001Q_c$; (4) $Q_p=1.01Q_c$; (5) $Q_p=1.3Q_c$ (Gurevich, Kazantsev, and Parizh, 1983).

parameter

$$\xi(I)=\frac{\theta_r}{\alpha i^2}=\frac{hAP[T_r(I)-T_0]}{\rho I^2}\ , \tag{6.5}$$

which changes from 0 to 0.5 as I decreases from I_c to I_p. The results of numerical calculations are shown in Fig. 50. It was found that in the interval $0<\xi<0.475$ the function $\varphi(\xi)=2.3\xi^{3/2}(1-2\xi)^{-1/2}$, to an accuracy of at least 3%. Consequently the expression for Q_c is (Gurevich, Kazantsev, and Parizh, 1983)

$$Q_c=\frac{2.3\sqrt{\kappa}\nu A^2[T_r(I)-T_0]^{3/2}}{\{\rho I^2-2hAP[T_r(I)-T_0]\}^{1/2}}\ . \tag{6.6}$$

The thus calculated critical energy Q_c and the enthalpy Q_d grow from zero to infinity as current decreases from I_c to I_p. As $I\to I_c$, the quantity Q_c, being independent of external cooling, tends to zero as $(I_c-I)^{3/2}$ if $j_c(\theta)=(1-\theta)j_c$ (Pasztor and Schmidt, 1978; Schmidt, 1978; Anashkin, Keilin, and Lyikov, 1979). The reason

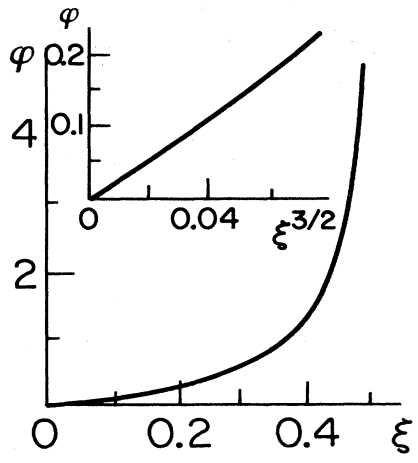

FIG. 50. The function $\varphi(\xi)$ (Gurevich, Kazantsev, and Parizh, 1983).

for this behavior is that at $I\approx I_c$ and $Q_p<Q_c$ the time of normal-zone existence $t_z\sim\xi t_h\ll t_h$, i.e., the external perturbation is mostly damped via heat conduction along the specimen while heat transfer to the coolant is negligible. As $I\to I_p$, the denominator in Eq. (6.6) vanishes, so that the critical energy $Q_c\propto(I-I_p)^{-1/2}$ essentially depends on h.

The critical energy for a pointlike heat pulse ($t_q\ll t_h$) can also be found for the resistive model (Dresner, 1985). If perturbation does not heat the superconductor above the critical temperature T_c, the expression for Q_c in the case of a thermally insulated specimen ($h=0$) takes the form

$$Q_c\approx\frac{\pi\nu A^2\sqrt{\kappa}(T_c-T_0)^{3/2}}{\rho^{1/2}I_c^{3/2}}\frac{(I_c-I)}{\sqrt{I}}\ . \tag{6.7}$$

If $L_q\gtrsim L$ and $t_q\gtrsim t_h$, the critical energy begins to depend on the form of the perturbation $\dot{Q}(x,t)$. As a result, an additional factor, approximately calculated by Dresner (1985), appears in Eq. (6.7).

Equations (6.6) and (6.7) for $h=0$ can be given the following physical interpretation. In a thermally insulated superconductor an external perturbation is damped out only by heat diffusion along the specimen. Hence Q_c can be estimated by

$$Q_c\sim\nu A\Delta Tl_c\ , \tag{6.8}$$

where $\Delta T\approx T_r(I)-T_0$ is the characteristic change in temperature necessary for normal-zone initiation and l_c is the critical length of this zone; if length exceeds l_c, the Joule heating exceeds heat transfer via heat conduction, i.e.,

$$\frac{\kappa\Delta T}{l_c^2}\sim\frac{\rho I^2}{A^2}r(\theta)\ , \tag{6.9}$$

where $r(\theta)$ is the factor (3.25) which takes into account the drop in heat production in the resistive state, $\theta\sim\Delta T/(T_c-T_0)$.

As $r(\theta)=1$ in the stepwise heat production model at $T>T_r$, we have $l_c\sim(\kappa\Delta T/\rho)^{1/2}j^{-1}$. Substituting this expression into Eq. (6.8), we obtain for $h=0$, to within a numerical factor, Eq. (6.6) (Pasztor and Schmidt, 1978). In the resistive model $r(\theta)\sim\Delta TI_c/(T_c-T_0)I$, so that here $l_c\sim[(T_c-T_0)\kappa/\rho jj_c]^{1/2}$; the substitution into Eq. (6.8) yields (6.7).

Comparing Eqs. (6.2)—(6.4) with (6.6) and (6.7), we find that the critical energy Q_c of a pointlike heat pulse may be greater or less than the enthalpy of formation of a resistive domain, Q_d. Thus, for $j\simeq j_c$, we find $Q_c\ll Q_d$, which is especially clear for $h\to0$, when the enthalpy $Q_d\sim\nu A\Delta TL\propto h^{-1/2}\to\infty$ and the energy Q_c tends to a finite limit. At the same time, at $j\approx j_p$ the reverse is valid, $Q_c\gg Q_d$, because $Q_c\propto(j-j_c)^{-1/2}$ and $Q_d\propto\ln(j-j_c)$.

An increase in the perturbation duration t_q results in increased critical energy Q_c because a fraction of Q_c is transferred to the coolant over the time t_q. For this reason the most "dangerous" perturbations, from the

standpoint of superconductor stability, are the "fast" ($t_q \ll t_h$) perturbations having minimum Q_c.

We first consider the case of "slow" local perturbation in which the total power $\dot{Q}_t$ is practically independent of time, and $t_q \gg t_h$, $L_q \ll L$. Finding Q_c then reduces to determining the critical perturbation power $\dot{Q}_c$, such that greater power results in an unstable quasistationary temperature distribution $T = T(x, T_m)$ described by Eq. (4.1) (T_m is the superconductor temperature in the region subjected to perturbation). This perturbation can be regarded as a pointlike steady-state heat source. This approach makes it possible to derive an equation for T_m by analogy to what we saw above in the case of local inhomogeneity [see Eq. (5.7)]. Then

$$S(T_m) = \tfrac{1}{8}\dot{Q}_t^2 . \tag{6.10}$$

Steady-state distributions $T = T(x, T_m)$ which are of interest here exist if Eq. (6.10) has solutions. This, however, takes place only at sufficiently low power $\dot{Q}_t$. An increase in power above the critical level $\dot{Q}_c$ heats the metastable superconducting state to a degree at which no thermal equilibrium is possible and the normal zone starts to propagate over the whole specimen (Stekly, 1966). This situation is illustrated in Fig. 51, which plots the graphic solution of Eq. (6.10). For small $\dot{Q}_t$ this equation has a stable solution corresponding to point a. The critical power corresponds to merging of points a and b. Hence

$$Q_c = 2^{3/2} A t_q S^{1/2}[T_2(j)] , \tag{6.11}$$

where the temperature T_2 corresponds to point 2 in Figs. 9 and 12. In the stepwise heat production model the general formula (6.11) gives

$$Q_c = 2A\nu L (T_c - T_0)\frac{t_q}{t_h}(1-i) . \tag{6.12}$$

In the resistive model the expression for Q_c is somewhat more complicated:

$$Q_c = 2A\nu(T_c - T_0)L\frac{t_q}{t_h}(1-i)\left[\frac{\alpha i}{\alpha i - 1}\right]^{1/2} . \tag{6.13}$$

If $t_q \gg t_h$, Eqs. (6.11)—(6.13) are valid in the whole range $j_p < j < j_c$, except a narrow neighborhood δj close to j_p (Romanovsky, 1984a). This behavior arises because the perturbation we consider will result in normal-zone propagation if, after a time t_q, its length exceeds the length $D(j)$ of the critical nucleus of normal phase (the resistive domain length), i.e.,

$$t_q \gtrsim \frac{D(j)}{2v(j)} \sim \frac{t_h j_p}{j - j_p}\ln\frac{j_p}{j - j_p} \gg t_h , \tag{6.14}$$

where $v(j)$ is the steady-state velocity of the N-S interface. With t_q fixed, the condition (6.14) ceases to hold for $j \simeq j_p$, so that a sharp increase in Q_c is observed in this current range in comparison with the predictions of Eqs. (6.12) and (6.13) (see Fig. 52).

The critical energy Q_c thus depends on the duration t_q of perturbations in the following manner. If $t_q \ll t_h \alpha^{-1/2}$, the value of Q_c tends to a finite limit, and if $0 < t_q \lesssim t_h \alpha^{-1/2}$, it is weakly dependent on t_q. As t_q increases, the energy Q_c increases and becomes linearly dependent on t_q in the interval $t_q \gtrsim t_h \alpha^{-1/2}$. A $Q_c = Q_c(t_q)$ curve typical of composite superconductors is plotted in Fig. 53.

Let us return to the most "dangerous" perturbations having $t_q \ll t_h$, and find Q_c as a function of the distribution of specific power $\dot{Q}(x,t)$ along the specimen. In the general case it would be necessary to solve the nonstationary heat conduction equation (3.1). If, however, $L_q \gg D(j)$, this stage is avoided because the general expression for Q_c can be derived.

It has been mentioned above that in order to destroy superconductivity at $I > I_p$, a critical nucleus of normal phase, i.e., a $D(j)$-long resistive domain, must be initiated

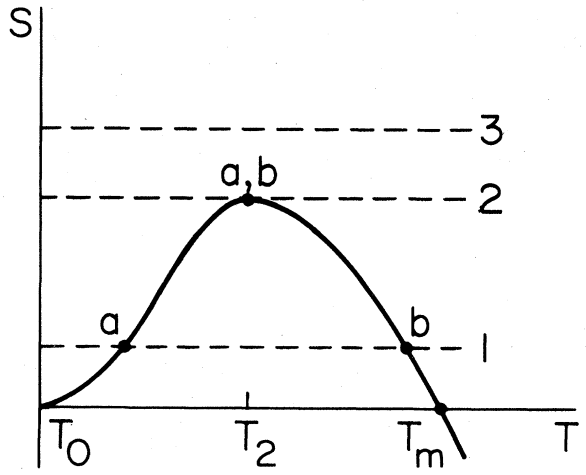

FIG. 51. Graphic solution of Eq. (6.10).

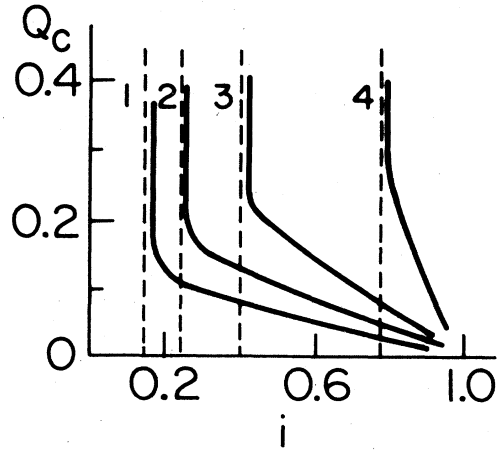

FIG. 52. $Q_c = Q_c(i)$ for the resistive model for various values of α and $T_q = 100 t_h/\alpha$: (1) $\alpha = 100$; (2) $\alpha = 30$ (the value of Q_c is found in units of $Q_0 \alpha^{-1/2}$((Romanovsky, 1984a).

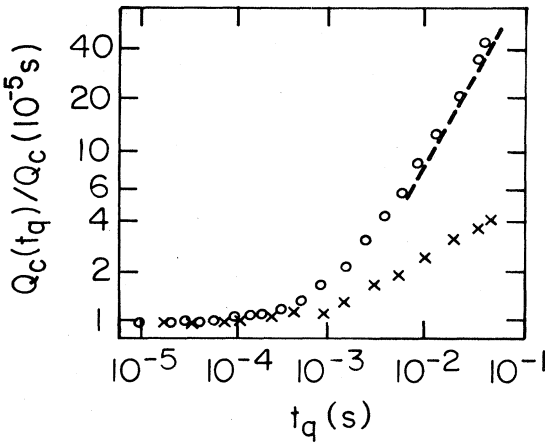

FIG. 53. $Q_c = Q_c(t_q)$ for a composite superconductor 1.17 mm in diameter ($x_{Cu}/x_{Nb\text{-}Ti} = 1$) for $B = 4$ T, $j = 6.33 \times 10^4$ A/cm^2, under different cooling conditions: ×, vacuum; ○, liquid helium (Schmidt, 1978).

in the specimen. This quantity, $D(j)$, determines the characteristic perturbation length, whose energy Q_c depends on the details of the distribution of $Q(x,t)$. If, however, $L_q \gg D(j)$, the superconductor is in fact uniformly heated. This case was discussed in Sec. II.B, where it was shown that to transform a homogeneous superconductor to the normal state ($T = T_3$) one must heat it to a temperature $T > T_2$. Consequently, for $t_q \ll t_h$ and $L_q \gg D(j)$, the quantity Q_c is the energy that must be deposited for an instantaneous homogeneous heating of an L_q-long region of the superconductor from $T = T_0$ to $T = T_2$, i.e.,

$$Q_c = AL_q \int_{T_0}^{T_2} \nu \, dT \, . \tag{6.15}$$

Explicit formulas for Q_c can be derived in the framework of the stepwise heat production model,

$$Q_c = A\nu L_q (T_c - T_0)(1-i) \, , \tag{6.16}$$

and also in the resistive model (Keilin and Romanovsky, 1982),

$$Q_c = A\nu L_q (T_c - T_0) \frac{\alpha i (1-i)}{\alpha i - 1} \, . \tag{6.17}$$

If $L_q \gg D(j)$, an expression for Q_c in the resistive model can be obtained in the form taking into account the perturbation length t_q. If, for example, a superconductor is subjected to a rectangular heat pulse, then (Keilin and Romanovsky, 1982)

$$Q_c = A\nu L_q (T_c - T_0) \frac{t_q}{t_h} \frac{(1-i)}{1 - \exp\left[\left(\frac{1}{\alpha i} - 1\right)\frac{t_q}{t_h}\right]} \, . \tag{6.18}$$

If $t_q(1/\alpha i - 1) \ll t_h$, we again arrive at Eq. (6.17). In the reverse case, i.e., $(1/\alpha i - 1)t_q \gg t_h$, the value of Q_c is directly proportional to t_q.

Beginning with $L_q \sim D(j)$, the critical energy Q_c depends on the specifics of the distribution $Q(x,t)$ along the specimen. The value of $Q_c(L_q)$ may then prove to be lower, for a certain class of perturbations, than that in the above-discussed limiting cases $L_q \ll D(j)$ and $L_q \gg D(j)$. This implies that the function $Q_c(L_q)$ has a minimum at $L_q \sim D(j)$ (Keilin and Romanovsky, 1982; Meuris, 1984). Thus such situations arise in the stepwise heat production model at $j \simeq j_p$. Here the quantity Q_c for the interval $0.45 < \xi < 0.5$ and pointlike perturbation is found to be greater than the enthalpy Q_d of resistive domain formation, pointing to a minimum of $Q_c(L_q)$ at $L_q \sim D(j)$. These conclusions are illustrated in Fig. 54, which shows typical $Q_c = Q_c(L_q)$ curves for the resistive model.

Now let us discuss some experimental data on quenching the superconductivity by thermal perturbations in a current-carrying conductor. Figure 55 plots $Q_c = Q_c(j)$ typical for composite superconductors for local pulse perturbations ($L_q \ll L$, $t_q \ll t_h$). In order to estimate Q_c, we set $T_c - T_c = 5$ K, $\kappa = 600$ W/m K, $d = 0.1$ cm, $\nu = 8 \times 10^3$ J/m^3 K, $h = 800$ W/m^2 K (Gall and Turowski, 1978). Then $L \simeq 1.5$ cm, whence $Q_c \sim Q_0 = \nu AL(T_c - T_0) \sim 10^{-3}$ J. This estimate is valid for $\alpha \gg 1$ and for the intermediate current range $I_p \ll I \ll I_c$.

A quantitative comparison of calculated and measured parameters is rather difficult because of insufficient information on the detailed temperature dependence of heat transfer, $W(T)$, and on the parameters characterizing the nonstationary behavior of W. As an illustration, Fig. 56 compares the results of numerical simulation of Chen and Purcell (1978) with the experimental data reported by Wilson and Iwasa (1978). Although calculations yielded qualitatively the same dependence $Q_c = Q_c(I)$ as the experiment, the discrepancy is fairly sensitive to the detailed form of the $W(T)$ curve.

The effect of nonstationary heat transfer on Q_c was analyzed by Ishibashi *et al.* (1979), Nick, Krauth, and

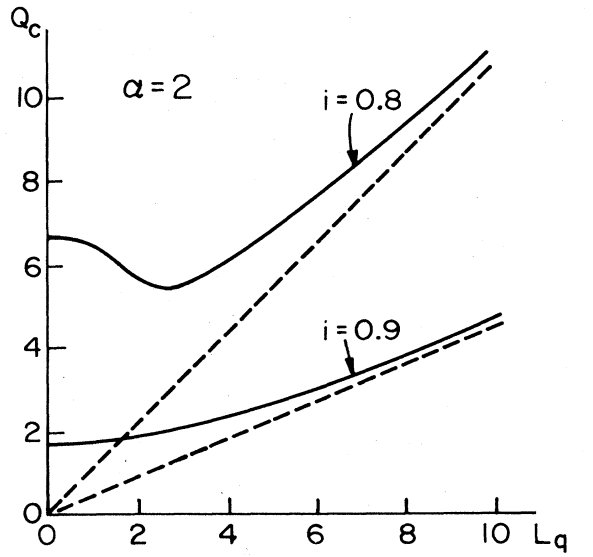

FIG. 54. $Q_c(L_q)$ for the resistive model (Keilin and Romanovsky, 1982); the units correspond with Fig. 52.

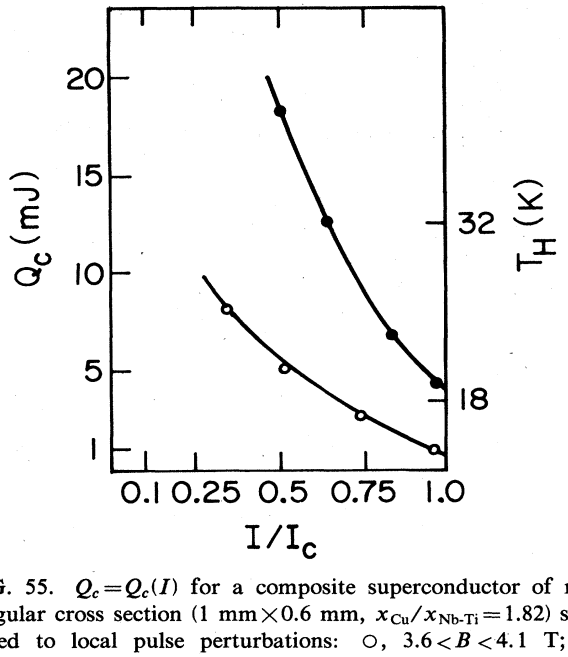

FIG. 55. $Q_c = Q_c(I)$ for a composite superconductor of rectangular cross section (1 mm×0.6 mm, $x_{Cu}/x_{Nb\text{-}Ti} = 1.82$) subjected to local pulse perturbations: ○, $3.6 < B < 4.1$ T; ●, $0.8 < B < 1.2$ T. The ordinate on the right shows the heater temperature (Gall and Turowski, 1978).

Ries (1979), Cornelissen and Hoogendoorn (1985), Tsukamoto and Nakada (1985), and some others. It was found that the resulting corrections are substantial, and taking them into account may result in a severalfold increase in the calculated values of Q_c (Fig. 57).

In concluding this section it should be noted that the nucleation of normal phase in current-carrying superconductors may also be caused by a local magnetic flux jump (Rakhmanov, 1983), thermal noise (Chechetkin, Levchenko, and Sigov, 1985), current pulses (Bezuglyj and Shklovij, 1984), etc.

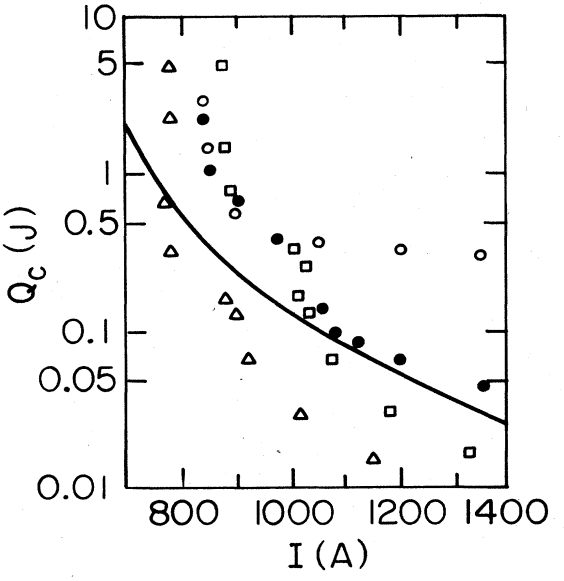

FIG. 56. Comparison of experimental data for Q_c (●,○) with the results of two numerical calculations (△,□) in which different functions $W(T)$ were used in the range of the boiling crisis. Solid line plots the enthalpy Q_d of resistive domain formation (Chen and Purcell, 1978).

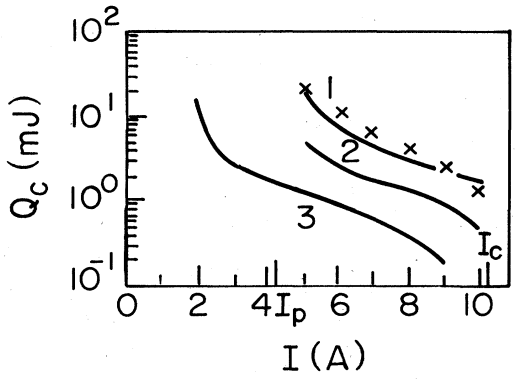

FIG. 57. Effect of nonstationary heat transfer on Q_c. Solid lines plot the results of numerical calculation of Q_c: (1) with the nonstationary part of W taken into account; (2) with only the steady-state part of W taken into account; (3) $W = 0$; ×, experimental data for superconducting composite of rectangular cross section (2.45×1.4 mm^2, $x_{Cu}/x_{Nb\text{-}TI} = 5$) (Nick, Krauth, and Ries, 1979).

VII. DYNAMIC PHENOMENA IN BISTABLE CURRENT-CARRYING CONDUCTORS

This section treats some dynamic phenomena in bistable current-carrying conductors, e.g., the motion of electrothermal and resistive domains, dynamics of localization of switching waves and domains on inhomogeneities, stability with respect to large perturbations, and self-sustained domain oscillations produced by connecting the conductor to an electric circuit.

A. Motion of domains. Analog of the Gunn effect

The motion of a resistive or electrothermal domain as a whole may be caused by thermoelectricity (Gurevich and Mints, 1980; Ausloos, 1981). In this case the temperature distribution within a domain is described by Eq. (3.46). The domain velocity v_d can be found as follows. Equation (3.46) is similar to the equation of motion of a classical particle in a potential $-S(T)$ (Fig. 12) in the presence of friction force $-(vv_d - j\Pi)dT/dx$. In this potential a domain corresponds to a trajectory $T(x)$ on which the particle begins its motion from the point $T = T_0$ at infinitesimal velocity and finally returns to the same point. This trajectory exists if the total work of friction force along it is zero, i.e.,

$$\int_{-\infty}^{\infty} (vv_d - j\Pi)\kappa \left[\frac{dT}{dx}\right]^2 dx = 0 . \tag{7.1}$$

Equation (7.1) implies that $v_d \sim j\Pi/v$. In composite su-

perconductors $\nu \simeq 3\times 10^{-3}$ J/cm^{3}K, $j \approx 10^5$ A/cm^2, $\Pi \approx 10^{-7}$ V/K, so that $v_d \sim 1$–10 cm/s. In thin films under the same conditions ($T_0 = 4.2$ K) $j \sim 10^7$ A/cm^2, so that $v_d \sim 10^2$–10^3 cm/s. The effect of thermoelectricity is thus to make resistive domains move at a velocity that is a function of current direction. This effect was observed in superconductors by Akhmetov, Baev, and Mints (1983). At liquid-helium temperatures the velocity v_d of electrothermal domains in normal metals is of the same order of magnitude as that in composite superconductors. If $T_0 \approx 300$ K and domain initiation is caused by a step in $\rho(T)$ at the melting point, then $v_d \sim 0.1$ mm/s (Abramov *et al.*, 1983, 1985).

The general expression for v_d can be obtained by treating the thermoelectric heat $Q_T = -j\Pi\, dT/dx$ as a small perturbation in comparison with Q. Then (Gurevich and Mints, 1980)

$$v_d = j\frac{\int_{T_0}^{T_m} \Pi S^{1/2} dT}{\int_{T_0}^{T_m} \nu S^{1/2} dT} . \tag{7.2}$$

An explicit dependence of v_d on j is found in the stepwise heat production model:

$$v_d = i\pi_0 \left[1 - \frac{2\xi^2}{2\xi - (1-2\xi)\ln(1-2\xi)}\right] v_h , \tag{7.3}$$

where $\xi(i) = \theta_r(i)/\alpha i^2$, $\pi_0 = j_c \Pi (d/\kappa h)^{1/2}$, $\Pi(\theta) = \Pi$ at $T > T_r$, and $\Pi(\theta) = 0$ at $T < T_r$. In this case the velocity v_d monotonically increases from $i_p \pi_0 v_h/2$ to $\pi_0 v_h$ as i increases from i_p to 1, and hence, as ξ decreases from 0.5 to zero.

The thermoelectric effect results in domain motion because at $\Pi > 0$ the Thomson heat $Q_T = -j\Pi\, dT/dx$ is released at the right-hand boundary of the domain and is absorbed at the left-hand boundary (Fig. 23). As a result, the distribution $T(x)$ is shifted to the warmer region, i.e., the domain travels rightward. The motion of a resistive or electrothermal domain is thus related to the appearing gradients of heat release or external cooling along the conductor. These gradients can be produced not only by thermoelectric effects but also by any smooth inhomogeneity of length $l \gg L$. Then the heat conduction equation can be written to first order in L/l in the form ($|x| \ll l$)

$$\frac{d}{dx}\kappa\frac{dT}{dx} + \nu v_d \frac{dT}{dx} - f(T,X) - (x - X)\left.\frac{\partial f}{\partial x}\right|_X = 0 , \tag{7.4}$$

where $X(t)$ is the coordinate of the domain center point and $v_d = dX/dt$ is its velocity (for the sake of simplification, here $\Pi = 0$). The last term, taking care of the inhomogeneity, is a small correction of the order of $L/l \ll 1$.

In order to find v_d, we multiply Eq. (7.4) by $\kappa\, dT/dx$ and integrate in x from $-\infty$ to ∞. Then the first and third terms in (7.4) vanish by virtue of boundary conditions $T(\pm\infty) = T_0$, $dT/dx\,|_{\pm\infty} = 0$. Assuming the specimen to be homogeneous, one can calculate the derivative dT/dx in Eq. (7.4) to first order in $\partial f/\partial x$. This leads to

$$v_d = \frac{dX}{dt} = -\int_{T_0}^{T_m} \kappa x(T) \left.\frac{\partial f}{\partial x}\right|_{X(t)} dT \Big/ \sqrt{2}\int_{T_0}^{T_m} \nu S^{1/2} dT , \tag{7.5}$$

where the function $x = x(T)$ is given by Eq. (4.1). Equation (7.5) describes a slow ($v_d \ll v_h$) motion of a domain through a conductor with smooth inhomogeneities. It shows that the domain travels toward the region of higher heat production or poorer external cooling, at a velocity

$$v_d \sim v_h \frac{D}{l} , \tag{7.6}$$

where v_h is the thermal velocity and D is the characteristic domain length.

The inhomogeneities may be caused, for example, by nonuniform distribution of magnetic field along the superconductor, by variable cross-sectional area of the conductor, etc. A similar situation arises in force-cooled composite superconductors with internal channels through which liquid helium is pumped (Brechna, 1973). Indeed, $W(x)$ is nonuniform here because helium flowing through cooling channels is gradually heating up as it moves along the normal zone. Let us analyze this case in some detail.

Assume for simplicity that the composite is not cooled externally; then the equation describing the temperature distribution $T_0 = T_0(x - v_d t)$ along the coolant flow takes the form, in the simplest case (Altov *et al.*, 1977; Hoenig, 1980),

$$(v_H - v_d)\nu_H \frac{dT_0}{dx} - \frac{hP_H}{A_H}(T_0 - T) = 0 , \tag{7.7}$$

where A_H and P_H are the area and perimeter, respectively, of all cooling channels, ν_H is the helium specific heat, and v_H is the velocity of helium flow. As follows from Eq. (7.7), the characteristic length l_H on which coolant temperature varies along the specimen is

$$l_H = L\frac{\nu_H}{\nu}\frac{v_H - v_d}{v_h}\frac{A_H}{A - A_H} , \tag{7.8}$$

where A is the cross-sectional area of the specimen, $v_h = L/t_h$, $L = (d_H\kappa/h)^{1/2}$, $t_h = \nu d_H/h$, $d_H = (A - A_H)/P$, ν and κ are the specific heat and thermal conductivity, respectively, averaged over the conductor cross section (neglecting the cooling channels). Note that in this case l_H is a function of domain velocity v_d; l_H is found to be much greater than L, even if $v_d \sim v_h$, owing to the high specific heat of liquid helium [$\nu_H(4\text{ K}) \approx 0.6$ J/cm^{3}K (Brechna, 1973), $\nu_H/\nu \approx 3\times 10^2$].

The substitution of Eq. (7.8) into (7.6) yields the following estimate for v_d, provided $v_d \ll v_h$, i.e., $l_H \gg D$:

$$\frac{v_d^{\pm}}{v_h} \simeq \frac{v_H}{2v_h} \pm \left[\left(\frac{v_H}{2v_h}\right)^2 - \frac{\nu}{\nu_H}\frac{D}{L}\left(\frac{A}{A_H} - 1\right)\right]^{1/2} . \tag{7.9}$$

The function $v_d = v_d(v_H)$ is two valued (see, for example, Altov *et al.*, 1977). In addition, there is a critical coolant

velocity v_{Hc}, below which no moving domains are possible (Fig. 58). As follows from Eq. (7.9),

$$v_{Hc}=2v_h\left[\frac{\nu}{\nu_H}\frac{D}{L}\left[\frac{A}{A_H}-1\right]\right]^{1/2}. \tag{7.10}$$

The ascending branch $v_d=v_d^+(v_H)$ in Fig. 58 is unstable even in the fixed-voltage regime. Indeed, an increase in the coolant velocity v_H improves heat transfer and reduces its nonuniformity along the superconductor. Consequently the domain velocity v_d must diminish as v_H increases, and this does take place for the descending branch $v_d=v_d^-(v_H)$ in Fig. 58. (In the limit $v_H\to\infty$ the coolant temperature T_0 is independent of x and we are returned to the above-discussed static domain in a homogeneous specimen at $\Pi=0$.) On the ascending branch $v_d=v_d^+(v_H)$ this condition is violated. The branch is, therefore, unstable. The same conclusion is reached when Eqs. (7.4) and (7.7) are analyzed for stability.

As follows from the above discussion, an increase in the domain velocity from v_d^- to $v_d<v_d^+$ due to some pulse perturbation will result in a reverse relaxation of $v_d(t)$ to the stable level v_d^-. In the opposite case, i.e., $v_d>v_d^+$, the resistive domain begins to accelerate. The quantity v_{Hc} is thus the maximum possible velocity of stationary motion of a resistive domain. Assuming for the sake of estimating v_{Hc} that $D\sim L$, $A\sim A_H$, $\nu/\nu_H\sim 10^{-2}$, we find from Eq. (7.10) that $v_{Hc}\sim 0.1v_h$.

A nonuniformity in heat transfer $W(x)$ can appear not only as a result of forced cooling but also as a result of the vertical orientation of the specimen. In this case heat production in an electrothermal domain causes convective flows of coolant along the specimen and, hence, the motion of the domain. An effect of this type was observed by Abramov *et al.* (1983) in studying electrothermal domains due to the jump in $\rho(T)$ at the melting point ($T_0=300$ K) in aluminum. The average domain velocity in these experiments was 0.63 and 0.47 mm/s for domains moving along and against the current, respectively. Presumably, the velocity of electrothermal domains is a function of current direction because of the thermoelectric effect. The motion of electrothermal domains in metals was also observed by Zhukov, Bokova, and Barelko (1983). In these experiments domains were initiated by the boiling crisis of the coolant.

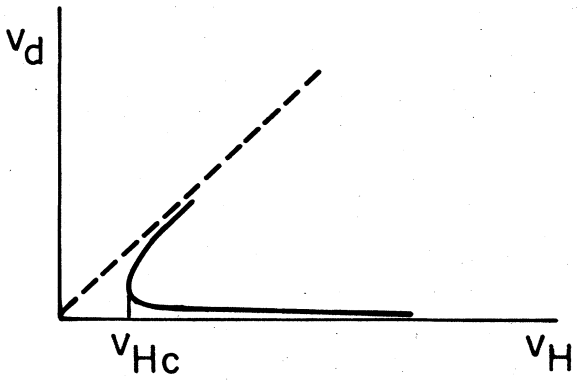

FIG. 58. Resistive domain velocity v_d as a function of helium flow velocity v_H along the superconductor.

In principle, the motion of stable electrothermal domains in conductors may generate current oscillations, by analogy with the Gunn effect (Gurevich and Mints, 1980). In this regime a domain is initiated at some "weak" point, travels some distance L_g, and disappears on entering a "colder" part of the specimen where $I<I_p$. Then the process repeats itself periodically, at a frequency v_d/L_g. Assuming for composite superconductors $v_d\sim(10^{-1}-10^{-2})v_h$, $v_h\sim 10$ m/s, $L_g\sim 10$ cm, we find the frequency of such self-sustained oscillations to be of order 1—10 Hz. Typical values for superconducting films are $v_h\sim 10^4$ cm/s, $L_g\sim 1$ μm, and thus $v_d/L_g\sim 10^5-10^6$ Hz.

Resistive or electrothermal domains can travel only in sufficiently homogeneous specimens, where they are not localized on inhomogeneities. If the motion of resistive domains is caused, say, by the thermoelectric effect, the condition of localization at $D\gg L$ is for the additional heat production on inhomogeneity, $j_p^2\Delta\rho l$, to exceed the characteristic Thomson heat $j_p(T_3-T_0)\Pi$ that is released at the N-S interface (Gurevich and Mints, 1981a). This is equivalent to the inequality $\Gamma>\Gamma_c$, where the parameter

$$\Gamma_c\sim\frac{T_3-T_0}{j_p\rho L}\Pi(T_3)$$

is the ratio of the characteristic Thomson heat production to the Joule heat. The localization of resistive domains has been analyzed in more detail, taking into account thermoelectric effects, by Ivanchenko, Medvedev, and Yarish (1985).

B. Dynamics of localization of domains and switching waves

In the general case the dynamic equations describing the localization of domains or switching waves are fairly unwieldy, even for simple models (see Appendix B). At the same time, as follows from Sec. IV, the localization on weak inhomogeneities occurs within a relatively narrow current interval around I_p, where the domain and switching wave velocities are small compared with the thermal velocity v_h. It is, therefore, possible to use the quasistationary approximation for an analytical description of localization dynamics (Gurevich and Mints, 1982, 1984a; Bezuglyj and Shklovskij, 1984; Gurevich, Leikin, and Mints, 1984; Kadigrobov, Slutskin, and Krivoshei, 1984).

We begin with the localization of a resistive domain on a point inhomogeneity. Let a normal zone be created in the neighborhood of the inhomogeneity as a result of external perturbation (Fig. 59). In this case slow motion ($v\ll v_h$) of its boundaries is described by a system of first-order differential equations. In the stepwise heat production model these equations are (Gurevich and Mints, 1982)

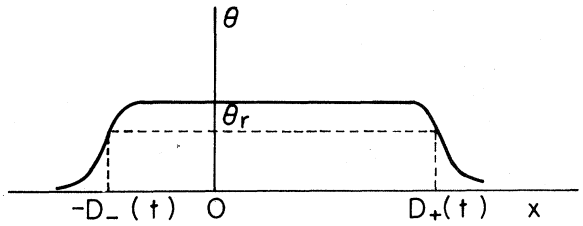

FIG. 59. Temperature distribution in a normal zone in the course of its localization on an inhomogeneity.

$$\frac{1}{2L}\dot{D}_{\pm}+\frac{2\dot{I}}{I}=\frac{c(i)}{2}+\Gamma\exp\left[-\frac{D_{\pm}}{L}\right]-\exp\left[-\frac{D_{\pm}+D_{\mp}}{L}\right], \tag{7.11}$$

where $D_+>0$, $D_->0$ (Fig. 59), $c(i)=v(i)/v_h\approx 2[1-2\xi(i)]$ is the dimensionless velocity of the N-S interface in a homogeneous superconductor at $|i-i_p|\ll i_p$, and overdots denote differentiation with respect to dimensionless time $\tau=t/t_h$.

The resistive domain localization dynamics at $\dot{I}=0$, $j_r<j<j_p$, is conveniently analyzed by using the phase plane of the system of equations (7.11) (Fig. 60). The singular points 1 (saddle) and 2 (node) in Fig. 60 correspond to the unstable and stable types of domains, respectively, localized at an inhomogeneity at $j_r<j<j_p$. If the external perturbation is such that at $t=0$ the point $[D_+(0),D_-(0)]$ is to the right of the separatrix $A\,1B$ in Fig. 60, it will move to point 2 as $t\to\infty$. This corresponds to domain localization at an inhomogeneity. If, however, the phase trajectory passes to the left of the curve $A\,1B$, the domain vanishes before it can be localized at the inhomogeneity. A localized domain is thus stable with respect to small perturbations that do not move the representing point to the left of the separatrix $A\,1B$.

Now we shall use Eqs. (7.11) to describe the dynamics of localization of the N-S interface. In this case we can

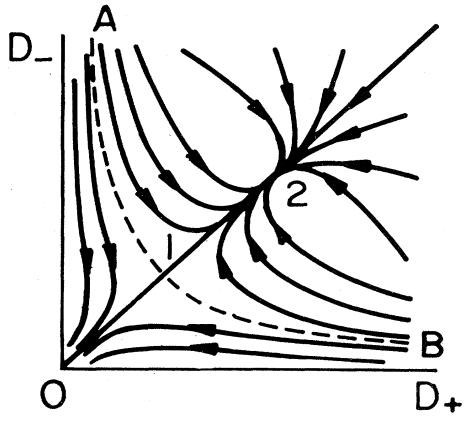

FIG. 60. Phase plane of Eqs. (7.11).

set $D_-=\infty$, so that

$$D_+(\tau)=L\ln\left[-\frac{2\Gamma}{c}+\left[\exp\frac{D_+(0)}{L}+\frac{2\Gamma}{c}\right]e^{c\tau}\right], \tag{7.12}$$

where $D_+(0)$ is the coordinate of the N-S interface at $t=0$. As follows from Eq. (7.12), at $\Gamma>0$ the interface gets localized if $c<0$ ($j<j_p$) and $2\Gamma>|c|$. The second of these inequalities coincides with the condition, derived in Sec. IV, for the existence of localized N-S interfaces.

The inequality $|c|<2\Gamma$ signifies that an N-S interface cannot move through an inhomogeneous superconductor at a velocity less than 2Γ. In the general case the localization condition reduces to the inequality $j_2<j<j_p$ ($\Gamma>0$), where j_2 is the solution of the system (5.19). Hence the critical velocity of switching waves in an inhomogeneous specimen is $v_c=v(j_2)$ where $v(j)$ is the velocity at $\Gamma=0$. Recalling that $j_p-j_2\sim\Gamma j_p\ll j_p$ (see Sec. IV), and thus $v_c<<v_h$, one can use Eq. (3.10) for determining v_c. Therefore

$$v_c=\frac{|j_p-j_2|\,2^{-1/2}}{\int_{T_1}^{T_3}\nu S^{1/2}dT+GS_c^{1/2}}\left|\frac{\partial S_3}{\partial j}\right|_{j_p}. \tag{7.13}$$

By the order of magnitude, $v_c\sim v_h|\Gamma|$. Switching waves with $v<v_c$ are localized at inhomogeneities. Such localization was observed, for example, by Zhukov, Barelko, and Merzhanov (1979), who studied thermal switching waves in water-cooled platinum wires and found the finite current interval where $v(j)=0$ (see Fig. 16).

A localization criterion for moving domains can be obtained in a similar manner. The procedure is the simplest if $D\gg L$ and the domain walls (switching waves) interact with the inhomogeneity independently of one another. Likewise, the equations describing the slow motion of domains or switching waves can be derived for an arbitrary weakly inhomogeneous medium. In the case of domains this result was obtained in the preceding section [Eq. (7.5)]. In the case of switching waves the relevant equation is (Gurevich, Leikin, and Mints, 1984)

$$\frac{dX}{dt}=v(j)-\Psi(X), \tag{7.14}$$

where $v(j)$ is the velocity of the switching waves in a homogeneous medium and $\Psi(X)$ is the effective potential produced by inhomogeneities:

$$\Psi(X)=\sum_{i=1}^{n}\int_{-\infty}^{\infty}G_i(x-X)\delta k_i(x)dx, \tag{7.15}$$

$$G_i(x)=\kappa(T)\frac{dT}{dx}\frac{\partial f}{\partial k_i}\Big/\left[\sqrt{2}\int_{T_1}^{T_3}\nu S^{1/2}dT\right]_{j_p,\langle k_i\rangle}, \tag{7.16}$$

where k_i is a parameter that, in an inhomogeneous specimen, is a function of x, $\delta k_i(x)$ is the derivation of $k_i(x)$ from the mean value $\langle k_i\rangle$ ($\delta k_i\ll\langle k_i\rangle$), and $T(x)$ is the temperature distribution in a fixed switching wave ($j=j_p$) described by Eq. (3.9).

If $v\gg\Psi$, inhomogeneities represent a weak perturba-

tion and result in a diffusional motion of the interface in the reference frame moving at the mean velocity of the wave (Mikhailov *et al.*, 1983). In the reverse case, $v \sim \Psi$, wave dynamics changes drastically: the wave is localized at the boundaries of those regions of the conductor in which $\Psi(X)=v$. Therefore the average length l_+ of the regions for which $v > \Psi(X)$ characterizes the mean free path of switching waves in a random potential Ψ. The expression for l_+ is

$$l_\pm = \pi(\sigma_F/\sigma_\varphi)[1 \pm \mathrm{erf}(v/v_F\sqrt{2})]\exp(v^2/2\sigma_F^2) , \quad (7.17)$$

where l_- is the average length of regions with $\Psi(X) > v$, $\sigma_F^2 = \langle \Psi^2 \rangle$, and $\sigma_\varphi^2 = \langle (\partial\Psi/\partial X)^2 \rangle$.

As follows from Eq. (7.17), in the case $v(j) > \sigma_F$ the mean free path l_+ grows exponentially because the probability of switching-wave localization rapidly diminishes. It is then possible to determine the mean wave velocity $\langle v \rangle$ over one free path. If $v^2 \gg \sigma_F^2$, then

$$\langle v \rangle = v(j) - \frac{\sigma_F^2}{v(j)} . \quad (7.18)$$

The interaction with random inhomogeneities lowers the velocity $\langle v \rangle$, in qualitative agreement with the experiments in which localized switching waves were observed (see Fig. 16).

The range of parameters for which $v(j) < \sigma_F$ corresponds to the strong localization regime. Two cases are possible here, depending on the relative values of thermal length L and correlation radius r_c of random variables $\delta k_i(x)$. Thus, if $r_c \lesssim L$, then free path $l_+ \sim L$, and if $r_c \gg L$, then $l_+ \sim \sqrt{r_c L} \gg L$.

We conclude that if $\sigma_F^2 \gtrsim v^2$, the propagation of switching waves is impossible despite the homogeneity of the specimen on the average ($\langle \Psi \rangle = 0$). The result is the existence of stochastic metastable dissipative structures, namely, of alternating regions of $T = T_1$ and $T = T_3$ phases. The characteristic lengths of these regions are l_- and l_+, respectively.

C. Self-sustained oscillations of the normal zone in superconductors

Now we shall analyze the normal-zone dynamics in superconductors connected to an electric circuit. We shall be interested in the details of self-sustained normal-zone oscillations caused by shunting the superconductor with a resistor of resistance r and inductance $\mathscr{L}$. Such self-sustained oscillations were often observed in experimental studies of composite superconductors (Altov *et al.*, 1977; Baev *et al.*, 1982a, 1982b), thin superconducting films (Eru, Peskovatsky, and Poladich, 1973a; Skocpol, Beasley, and Tinkham, 1974a; Heubener, 1975), whiskers (Meyer, 1975), and ultrathin superconducting filaments in zeolites (Bogomolov *et al.*, 1981).

The factor causing normal-zone self-sustained oscillations is the descending I-V characteristic of the superconductor (Figs. 25 and 28), which in this case plays the role of an active element of the circuit. As an illustration, Fig. 61 shows a typical oscillogram of voltage across the superconductor and shunt. The self-sustained oscillations are obviously of a relaxational type: the normal zone appears in the superconductor periodically, for a short time, after which a relatively slow relaxation of current is observed in the circuit. Similar self-sustained oscillations take place in short specimens, by a homogeneous transition of the whole specimen to the normal state (Rosenberger, 1959; Newhouse, 1964; Berkovich, 1965).

The absolute instability of resistive domains at sufficiently high inductance $\mathscr{L} > \mathscr{L}_k$ of the circuit has already been discussed in Sec. IV. Equations (4.40) and (4.41) for the critical inductance $\mathscr{L}_k$ and frequency ω_k characterizing instability now take the form (Baev *et al.*, 1982a)

$$\mathscr{L}_k = \left[\frac{I_0 r t_h}{4 I_p} - 2\mathscr{L}_h \right] \exp\left[\frac{D(j)}{L} \right] , \quad (7.19)$$

$$\omega_k^2 = \frac{8 I_p r_h}{\mathscr{L} t_h} \left| \frac{\partial \xi}{\partial I} \right|_{I_p} , \quad (7.20)$$

where $r_h = \rho L/A$ and $\mathscr{L}_h = r_h t_h$ are the thermal units of resistance and inductance, respectively. Equations (7.19) and (7.20) are valid for $\omega t_h \ll 1$, i.e., for $\mathscr{L} \gg \mathscr{L}_h$. In composite superconductors $\rho \simeq 10^{-7}$ Ω cm, $A \simeq 10^{-2}$ cm^2, $L \simeq 6$ cm, $t_h \simeq 8 \times 10^{-3}$ s (the regime of film boiling of liquid helium), so that the inductance is $\mathscr{L}_h = 0.5$ μH, and $r_h = 6 \times 10^{-5}$ Ω. As for the thin films, there $\rho \simeq 10^{-7}$ Ω cm, $d \sim 100$ Å, 1 μm in width, $L \sim 1$ μm, $t_h \sim 10^{-8}$–10^{-9} s, so that $r_h \sim 0.1$ Ω, and $\mathscr{L}_h \sim 10^{-9}$–$10^{-10}$ H.

Let us do a qualitative analysis of domain instability. Let the domain length be incremented by δD. If $\mathscr{L} = 0$, current will decrease and thereby damp out the fluctuation δD. If, however, $\mathscr{L} > 0$, the fluctuation $\delta I(t)$ is delayed with respect to $\delta D(t)$ by $t_L \sim \mathscr{L}/(r+R)$, where R is the resistance of the superconductor containing a normal zone. If t_L becomes greater than the time of domain

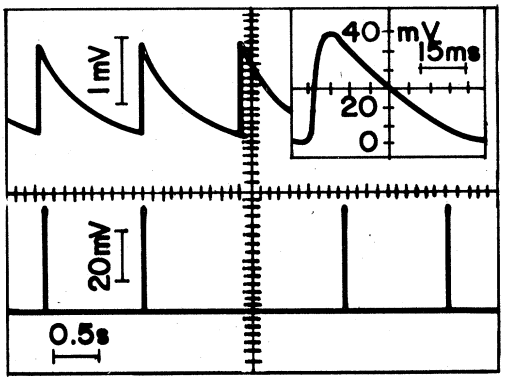

FIG. 61. Typical oscillograms of voltage across the composite superconductor (upper curve) and across the shunt (lower curve) in the regime of self-sustained normal-zone oscillations. The inset shows a scan of one voltage pulse across the superconducting specimen (Baev *et al.*, 1982a).

instability evolution, γ_0^{-1}, in the fixed-current regime, the stabilization by shunting becomes inefficient, and oscillations $\delta D(t)$ and $\delta I(t)$ build up. The critical inductance $\mathscr{L}_k$ is found from the condition $t_L\gamma_0 \sim 1$, so that together with Eq. (4.33) for γ_0 we obtain Eq. (7.19).

Consequently, at $I_0 > I_c$ and $\mathscr{L} > \mathscr{L}_k$, any stationary state of the superconductor is unstable. The result is the buildup of self-sustained oscillations of the normal zone, which can be described as follows. A normal zone, initiated at a "weak" point while $I(t)$ increases, begins to expand and the current $I(t)$ begins to decrease at a delay of $\sim t_L$ with respect to the similar dependence $I(t)$ for $\mathscr{L}=0$. As a result, having reached its equilibrium length $D(I_0)$, the normal zone continues to expand because I remains greater than I_p. Having decreased down to I_p, the current $I(t)$ will further diminish for a time $\sim t_L$, since at this instant $D(t) > D(I_0)$. At $I(t) < I_p$, however, the normal zone begins to collapse. If the time of collapse $t_d < t_L$, the normal zone vanishes before $I(t)$ grows up to I_p, i.e., there is not enough time for the equilibrium state $D = D(I_0)$ to build up.

After the normal zone vanishes, $I(t)$ grows exponentially with time constant $\mathscr{L}/r$ until it reaches $I = I_c$, when a normal zone is reinitiated in the specimen and the process repeats itself at a frequency (Baev *et al.*, 1982a)

$$\omega = \frac{2\pi r}{\mathscr{L}} \ln^{-1} \frac{I_0}{I_0 - I_c}, \quad I_p \ll I_c \ . \tag{7.21}$$

Typical $\omega = \omega(I_0)$ curves are plotted in Fig. 62.

If the inductance is sufficiently high, self-sustained oscillations of the normal zone are of the relaxation type: fast and slow phases of current variation alternate within each period. The fast phase is connected with the growth of the normal zone, which diminishes the current $I(t)$ from I_c to $I \sim I_p$ over a time $\sim t_L + t_d$. The slow phase is caused by current relaxation in the circuit when no normal zone remains.

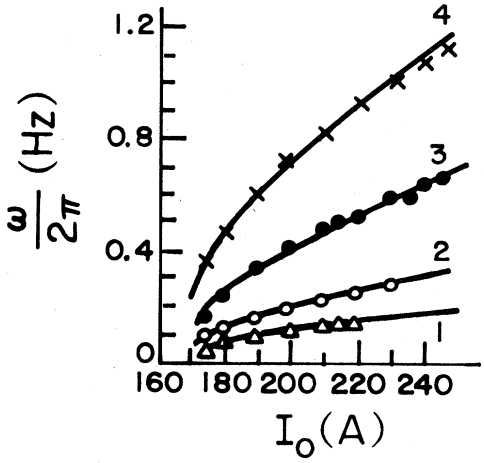

FIG. 62. Frequency of self-sustained oscillations as a function of current I_0, for different circuit parameters: (1) $r=5.9$ $\mu\Omega$, $\mathscr{L}=28.5$ μH; (2) $r=10$ $\mu\Omega$, $\mathscr{L}=28.5$ μH; (3) $r=5.9$ $\mu\Omega$, $\mathscr{L}=82$ μH; (4) $r=10$ $\mu\Omega$, $\mathscr{L}=82$ μH (Baev *et al.*, 1982a). Solid curves plot Eq. (7.21).

Let us estimate the inductance $\mathscr{L}_c$ above which relaxation oscillations become possible. The time of normal-zone collapse is $t_d \sim D_m/\bar{v}$, where D_m is the maximum normal-zone length in the course of oscillations and $\bar{v}$ is some average velocity of the N-S interface in the interval $I_m < I < I_c$ ($\bar{v} \sim v_h$ for $\alpha \sim 1$ and $\bar{v} \sim v_0 = v_h\sqrt{\alpha}$ for $\alpha \gg 1$). The current delay time is $t_L \sim A\mathscr{L}/\rho D_m$. The condition $t_L \sim t_d$ yields

$$D_m \sim \left[\frac{A\bar{v}\mathscr{L}}{\rho}\right]^{1/2} . \tag{7.22}$$

As follows from Eq. (7.22), the maximum normal-zone length D_m may be substantially greater than the equilibrium length of resistive domains, provided the circuit inductance is sufficiently high. Thus, if $\mathscr{L} \sim 10$ μH, $A \sim 10^{-2}$ cm^2, $\bar{v} \sim 10^4$ cm/s, $\rho \sim 10^{-7}$ Ω cm, then $D_m \sim 10^2$ cm.

The threshold for self-sustained oscillations corresponds to $D_m \sim D(I_0)$; taken together with Eqs. (7.22) and (4.42), this yields

$$\mathscr{L}_c \sim \frac{Ar^2}{\rho\bar{v}} \left[\frac{I_0}{I_p} - 1\right]^2 . \tag{7.23}$$

The inductance thus obtained, $\mathscr{L}_c \propto D^2(I_0)$ at $D(I_0) \gg L$, is substantially lower than the inductance $\mathscr{L}_k \propto \exp[D(I_0)/L]$ above which resistive domains are absolutely unstable. This means that in the interval $\mathscr{L}_c < \mathscr{L} < \mathscr{L}_k$ a sufficiently strong perturbation can force a resistive domain, stable with respect to small perturbations, into a self-sustained oscillation regime.

The critical inductance $\mathscr{L}_c(I_0)$ increases with increasing current I_0. Consequently, in the range $I_0 > I_k$, where $\mathscr{L}_c(I_k) = \mathscr{L}$, self-sustained oscillations cease and a static resistive domain is formed in the superconductor. Self-sustained oscillations thus take place in the interval $I_c < I_0 < I_k$. The current I_k corresponding to the breakdown of oscillations can be estimated using Eq. (7.23):

$$I_k \sim \frac{I_p}{r} \left[\frac{\mathscr{L}\rho\bar{v}}{A}\right]^{1/2} , \quad I_k \gg I_p \ . \tag{7.24}$$

The breakdown of self-sustained oscillations at high currents has been observed in composite superconductors (Baev *et al.*, 1982a, 1982b), in thin films (Eru *et al.*, 1973a) and filaments (Bogomolov *et al.*, 1981), and in whiskers (Meyer, 1975).

If the rate of change of current in the course of self-sustained oscillations is sufficiently small ($\dot{I}t_h \ll I$), the normal-zone dynamics is described by the following quasistationary equations:

$$\frac{dD}{dt} = 2v(I) - 4L \exp\left[-\frac{D}{L}\right] , \tag{7.25}$$

$$\mathscr{L}\frac{dI}{dt} + (R + r)I = rI_0 \ , \tag{7.26}$$

where $R = \rho D/A$, $D \gg L$, and $v(I)$ is the steady-state

velocity of the N-S interface. The qualitative peculiarities of self-sustained normal-zone oscillations are clearly seen in the phase plane of Eqs. (7.25) and (7.26) (Fig. 63). For example, in the case $\mathscr{L} < \mathscr{L}_c$ in which self-sustained oscillations are impossible, all phase trajectories terminate at a singular point 0, which is a stable focus [Fig. 63(a)].

In the interval $\mathscr{L}_c < \mathscr{L} < \mathscr{L}_k$ [Fig. 63(b)] there are two limiting cycles, the small-amplitude cycle being unstable. This means that a static resistive domain is stable with respect to any perturbations that do not take the representing point out of the small-amplitude cycle. Stronger perturbations shift it to the outer (stable) limiting cycle, resulting in self-sustained normal-zone oscillations. The unstable limiting cycle vanishes at $\mathscr{L} > \mathscr{L}_k$ [Fig. 63(c)], and the point 0 becomes an unstable focus. In this case the normal zone can only exist in the self-sustained oscillation regime.

As follows from the above arguments, in the $\mathscr{L}_c < \mathscr{L} < \mathscr{L}_k$ interval the self-sustained oscillations are generated through hard excitation and thus result in hysteresis.

The description of the stable limiting cycle is substantially simplified if $\mathscr{L} \gg \mathscr{L}_c$, so that $D_m \gg D(I_0)$ and the last term in the right-hand side of Eq. (7.25) can be dropped, and we can also set $r=0$ in Eq. (7.26). In this case of self-sustained normal-zone oscillations the function $D(I)$ becomes

$$D^2(I)=\frac{4\mathscr{L}A}{\rho}\int_I^{I_c}\frac{v(I)}{I}dI\ . \tag{7.27}$$

As an example, we shall take the stepwise heat production model with $\alpha \gg 1$, when $i_p \sim \alpha^{-1/2} \to 0$ and $v(I)$ is determined by Eqs. (3.39) and (3.40). Equation (7.27) then gives

$$D(I)=\left[\frac{8\mathscr{L}Av_0}{\rho}\right]^{1/2}\left[1-\frac{I}{I_c}\right]^{1/4}. \tag{7.28}$$

This relation describes the stable limiting cycle in Figs. 63(b) and 63(c) in the range $I_p \ll I < I_c$. The normal-zone length is maximal at $I = I_p \ll I_c$, whence

$$D_m=\left[\frac{\kappa}{(T_c-T_0)\rho}\right]^{1/4}\left[\frac{8\mathscr{L}I_c}{\nu}\right]^{1/2}. \tag{7.29}$$

Equation (7.29) coincides with the estimate (7.22) if $\bar{v} \sim v_0$. This occurs because in the case $\alpha \gg 1$ it is the quantity $v_0 = v_h\sqrt{\alpha}$ that gives the characteristic velocity of the N-S interface. The maximum voltage across the superconductor, U_m, is achieved at $I = \frac{4}{5}I_c$. Substituting this value into Eq. (7.28), we find

$$\begin{aligned} U_m &= \tfrac{4}{5}\rho j_c D(\tfrac{4}{5}j_c) \\ &= \frac{8\sqrt{2}}{5^{5/4}}\frac{j_c^{3/2}\rho^{3/4}\kappa^{1/4}A^{1/2}\mathscr{L}^{1/2}}{\nu^{1/2}(T_c-T_0)^{1/4}}\ . \end{aligned} \tag{7.30}$$

If $\mathscr{L} \gg \mathscr{L}_c$, the quantity U_m is independent of the current I_0 in the external circuit, to an accuracy of $rI_0A/\rho D_m I_p \sim (\mathscr{L}_c/\mathscr{L})^{1/2} \ll 1$ (Baev *et al.*, 1982b; Fig. 64).

The substitution of Eq. (7.28) into (7.26) yields, after integration, the following relation for $I = I(t)$ in a superconductor with a normal zone:

$$\ln\frac{1+(1-i)^{1/4}}{1-(1-i)^{1/4}}-2\arctan(1-i)^{1/4}=t\left[\frac{8\rho v_0}{A\mathscr{L}}\right]^{1/2}. \tag{7.31}$$

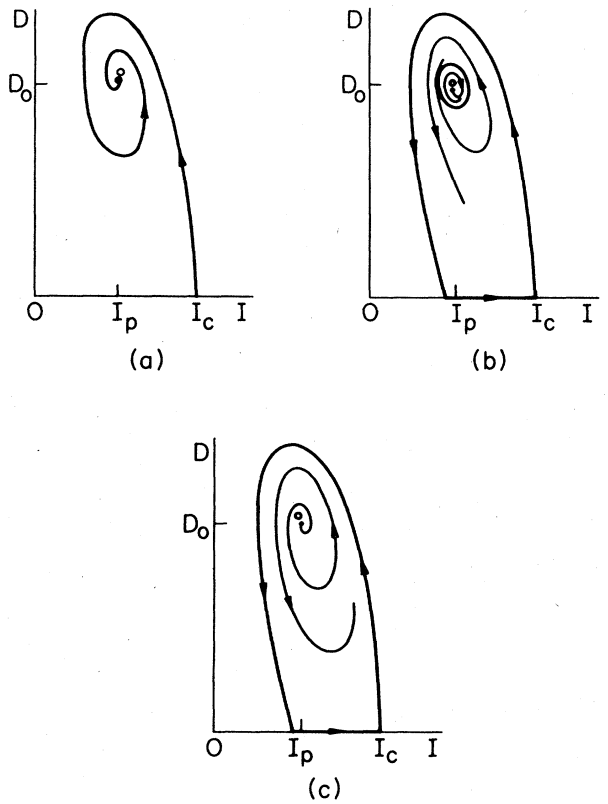

FIG. 63. Phase plane of Eqs. (7.25) and (7.26): (a) $\mathscr{L} < \mathscr{L}_c$; (b) $\mathscr{L}_c < \mathscr{L} < \mathscr{L}_k$; (c) $\mathscr{L} > \mathscr{L}_k$.

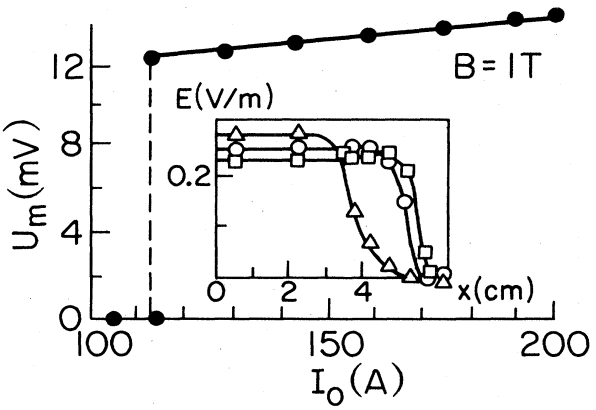

FIG. 64. $U_m = U_m(I_0)$ on a composite superconductor. The inset shows electric field distribution at different instants of time: △, t=3.5 ms; ○, t=5.6 ms; □, t=7 ms (Baev *et al*, 1982b).

Assuming in this expression $i=i_p=(2/\alpha)^{1/2}$, we find the time of normal-zone existence:

$$t_d=\frac{1}{8}\left[\frac{2A\mathscr{L}}{\rho v_0}\right]^{1/2}[\ln(32\alpha)-\pi]\ . \tag{7.32}$$

This quantity is a weak (logarithmic) function of the heat-transfer coefficient, and for $\mathscr{L}\gg r^2A/v_0\rho$ is much less than the period of self-sustained oscillations [see Eq. (7.21)].

VIII. THERMAL DESTRUCTION OF SUPERCONDUCTIVITY IN CURRENT-CARRYING COMPOSITIES WITH HIGH CONTACT RESISTANCES

A. Stable resistive domains

When Eq. (3.1) is used to describe composite superconductors, temperature and electric field are assumed to be uniform over the composite cross section. Owing to high thermal and electrical conductivities of the normal matrix, this situation is more or less typical for most composite superconductors. Hence we can ignore the details of the relatively complex inner structure of modern superconducting composites and operate only with their characteristics averaged over the cable cross section. However, this approach cannot be universally employed because in some composite superconductors the temperature and electric field distributions are essentially nonuniform owing to the presence between the superconductor and the normal matrix of transition layers with high thermal and electrical contact resistance. In these materials superconductivity breakdown in current-carrying conductors manifests certain specific features (Keilin and Ozhogina, 1977; Kremlev, 1980; Akhmetov and Mints, 1982, 1983a, 1983b, 1985; Keilin and Kruglov, 1984), which are discussed in this section.

The transition layer in composite superconductors plays the role of a thermal and resistive "barrier" for the redistribution of current and heat in the conductor cross section. In some cases the creation of such "barriers" is intentional because they reduce matrix losses (Altov *et al.*, 1977; Carr, 1983). A similar barrier is sometimes technologically unavoidable, e.g., in fabricating niobium-stannide-based composites by the "bronze route" process, in utilizing the aluminum matrix, etc. (Hillman, 1981; Roberge, 1981; Suenaga, 1981).

Let us consider now the thermal breakdown of superconductivity in current-carrying superconductors in the case of high contact resistances. We take up the simplest situation, in which a composite is an *n-i-s* sandwich composed of a normal metal (n), a transition layer (i), and a superconductor (s), of thicknesses d_n, d_i, and d_s, respectively (Fig. 65). A model of this type, but ignoring contact resistances, was often discussed in the literature as an example of an active transmitting line or "neuristor" (the relevant publications are cited in Barker, 1973).

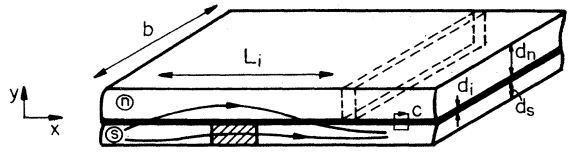

FIG. 65. Model of composite superconductor with contact resistance. Resistive domain region is hatched.

If $d_nh_n\ll\kappa_n$, $d_sh_s\ll\kappa_s$, the equations describing the temperature distributions $T_n(x,t)$ and $T_s(x,t)$ along the normal metal and the superconductor in a composite with contact resistances take the form (Keilin and Ozhogina, 1977; Kremlev, 1980; Akhmetov and Mints, 1982)

$$\nu_n\frac{\partial T_n}{\partial t}=\frac{\partial}{\partial x}\kappa_n\frac{\partial T_n}{\partial x}-(T_n-T_0)\frac{h_n}{d_n}+\rho_nj_n^2 - \frac{(T_n-T_s)\kappa_i}{d_id_n}+\frac{\rho_ij_\perp^2d_i}{2d_n}\ , \tag{8.1}$$

$$\nu_s\frac{\partial T_s}{\partial t}=\frac{\partial}{\partial x}\kappa_s\frac{\partial T_s}{\partial x}-(T_s-T_0)\frac{h_s}{d_s}+E_sj_s - \frac{(T_s-T_n)\kappa_i}{d_id_s}+\frac{\rho_ij_\perp^2d_i}{2d_s}\ , \tag{8.2}$$

where j_n and j_s are the current densities in the normal metal and the superconductor, respectively, $E_s=(j_s-j_c)\rho_s\eta(j_s-j_c)$ is the longitudinal electric field in the superconductor $\eta(x)=0$ if $x<0$, $\eta(x)=1$ if $x\geq0$, and $j_\perp$ is the density of the current crossing the transition layer. If the electrical resistance of the composite is dominated by the contact resistance ($\rho_id_i\gg d_s\rho_s+d_n\rho_n$), then $j_n(x)$ and $j_s(x)$ vary slowly on the scale d_n or d_s, and $j_\perp\ll j_{n,s}$. In this case the equations for j_n, j_s, and $j_\perp$ can be written as (Keilin and Ozhogina, 1977; Kremlev, 1980; Akhmetov and Mints, 1982)

$$\frac{d_n}{d_s}j_n+j_s=j\ , \tag{8.3}$$

$$d_n\frac{\partial j_n}{\partial x}=j_\perp\ , \tag{8.4}$$

$$\rho_id_nd_s\frac{\partial^2j_n}{\partial x^2}-\rho_nj_n+E_s(T_s,j_s)=0\ , \tag{8.5}$$

where j is the current density referred to unit cross-sectional area of superconductor. Equations (8.1)—(8.5) are also valid in the geometry of a superconductor flanked on both sides with normal metal (*n-i-s-i-n*-type sandwich). Then one sets $d_s=d_s/2$, $h_s=0$ in Eqs. (8.1) and (8.2) and $d_n=2d_n$ in Eqs. (8.3)—(8.5).

The system of equations is conveniently rewritten by introducing dimensionless temperatures $\theta_n=(T_n-T_0)/(T_c-T_0)$, $\theta_s=(T_s-T_0)/(T_c-T_0)$. For the sake of simplification, we let $h_n=h_s=h$, assume all parameters except $E_s(T_s,j_s)$ to be independent of T_s, and $E_s(T_s)=\rho_sj_s\eta[j_s-j_c(T_s)]$ to be a step function of T_s. We further assume that $j_c(\theta)=(1-\theta)j_c$ and obtain

$$t_n\frac{\partial\theta_n}{\partial t}=L_n^2\frac{\partial^2\theta_n}{\partial x^2}-\theta_n+2\alpha_i i_n^2+\alpha_i L_i^2\left[\frac{\partial i_n}{\partial x}\right]^2+\psi\theta_s\ , \tag{8.6}$$

$$t_s\frac{\partial\theta_s}{\partial t}=L_s^2\frac{\partial^2\theta_s}{\partial x^2}-\theta_s+2\alpha_i\zeta(i-i_n)^2\eta(i-1+\theta_s-i_n)+\alpha_i L_i^2\left[\frac{\partial i_n}{\partial x}\right]^2+\psi\theta_n\ , \tag{8.7}$$

$$L_i^2\frac{\partial^2 i_n}{\partial x^2}-i_n+\zeta(i-i_n)\eta(i-1+\theta_s-i_n)=0\ , \tag{8.8}$$

where $t_n=d_n\nu_n/h_0$ and $t_s=d_s\nu_s/h_0$ are the corresponding thermal times, $h_0=h+\kappa_i/d_i$ is the effective heat-transfer coefficient, and L_i, L_n, and L_s are characteristic lengths defined as follows:

$$L_i^2=\frac{\rho_i}{\rho_n}d_i d_n,\quad L_n^2=\frac{d_n\kappa_n}{h_0},\quad L_s^2=\frac{d_s\kappa_s}{h_0}\ . \tag{8.9}$$

The dimensionless parameters in Eqs. (8.6)—(8.8) are

$$\alpha_i=\frac{\rho_n j_c^2 d_s^2}{2(T_c-T_0)h_0 d_n},\quad \psi=\frac{\kappa_i}{\kappa_i+d_i h},\quad \zeta=\frac{d_n\rho_s}{d_s\rho_n}\ , \tag{8.10}$$

$$i_n=\frac{j_n d_n}{j_c d_s},\quad i_s=\frac{j_s}{j_c},\quad i=\frac{j}{j_c},\quad i=i_n+i_s\ . \tag{8.11}$$

The Stekly parameter α_i depends in this case on the effective heat-transfer coefficient h_0, which takes into account heat transfer both to the coolant and across the transition layer, L_n and L_s are the respective thermal lengths in the normal metal and in the superconductor ($L_n\gg L_s$), and L_i is the characteristic length over which the current bypasses the normal zone (Fig. 65). Equation (8.8) includes another spatial scale L_b which determines the length over which current flows from the superconductor, transformed to the normal state, into the normal metal. The formula for L_b follows from Eq. (8.8) if we set $\eta=1$:

$$L_b=\frac{L_i}{\sqrt{1+\zeta}}\ . \tag{8.12}$$

If $d_n\sim d_s$, the parameter $\zeta\gg 1$, so that $L_b^2\simeq\rho_i d_i d_s/\rho_s\ll L_i^2$. The case of high contact resistance of transition layers, the only one to be discussed below, corresponds to the inequality $L_i\gg L_b\gg L_n\gg L_s$.

Let us consider now the minimum current of normal phase existence, i_m, taking into account contact resistances. Assuming all derivatives in (8.6)—(8.8) to be zero, we arrive at a quadratic equation for i_m:

$$\frac{2\alpha_i\zeta(1+\psi\zeta)i_m^2}{(1-\psi^2)(1+\zeta)^2}+\frac{i_m}{1+\zeta}-1=0\ . \tag{8.13}$$

If the contact resistance is low ($d_i\to 0,\psi\to 1$), Eq. (8.13) yields the relation $i_m=\alpha^{-1/2}$ given in Sec. II. In the reverse case of high resistances ($\psi\ll 1$) the formula for i_m is

$$i_m=(2\alpha_i)^{-1/2}\left[\frac{\zeta}{1+\psi\zeta}\right]^{1/2}\ . \tag{8.14}$$

It shows that increasing contact resistances substantially increase i_m [by a factor of order $\min(\zeta^{1/2},\psi^{-1/2})$; Keilin and Ozhogina, 1977]. Indeed, the current i_m corresponds, by definition, to homogeneous heating of the superconducting component of the composite to the critical temperature θ_r. When the superconductor transforms to the resistive state, the current is mostly squeezed out into the normal matrix, in which practically the whole Joule heat is deposited. However, high contact resistances thermally insulate the superconductor, so that it heats up to a much lower degree than the normal matrix.

The increase in i_m with increasing contact resistances is not, however, an indication that the thermal destruction of superconductivity takes place at greater currents than at lower contact resistances. In this case the very nature of normal-zone propagation changes: superconductivity destruction occurs by nucleation followed by periodic splitting of resistive domains (Akhmetov, Baev, and Mints, 1983; Akhmetov and Mints, 1983a, 1983b, 1985; Akhmetov and Baev, 1984).

Let us look into detailed properties of such domains and first consider the static resistive domain in two limiting cases, $D\ll L_s$ and $D\gg L_s$. In the first of them the distributions of temperature, $\theta_s(x)$, and current, $i_n(x)$, in the composite are

$$\theta_s(x)=\theta_m\exp\left[-\frac{|x|}{L_s}\right]\ , \tag{8.15}$$

$$i_n(x)=U_0\exp\left[-\frac{|x|}{L_i}\right]\ , \tag{8.16}$$

where the maximum temperature θ_m in the domain and the dimensionless voltage across the domain, $U_0=d_n U/2d_s L_i\rho_n$, depend on the current i as follows:

$$U_0^{\pm}=\tfrac{1}{2}[i\pm(i^2-i_r^2)^{1/2}]\ , \tag{8.17}$$

$$i_r^2=\frac{2L_s}{\alpha_i L_i}\ , \tag{8.18}$$

$$\theta_m=2\alpha_i L_i U_0/(L_s+2\alpha_i L_i U_0)\ . \tag{8.19}$$

The dimensionless I-V characteristic $U_0=U_0(i)$ is shown in Fig. 66. The characteristic is two-valued, indicating that two types of resistive domains can exist in composites with high transition resistances. One of these (stable domain) corresponds to the upper branch U_0^+ and the other (unstable domain) to the lower branch U_0^- of the current-voltage characteristic.

Two types of domains arise because the growth of a resistive domain results in leaking a part of the transport current, bypassing the domain over the length $\sim L_i\gg D$, into the normal metal (Fig. 65). In these conditions the normal metal works as a shunt of the superconductor, with effective resistance $R_i=2\rho_n L_i/d_n b$ which is independent of D, up to the order of $D/L_i\ll 1$. Such "internal" shunt in composites with high contact resis-

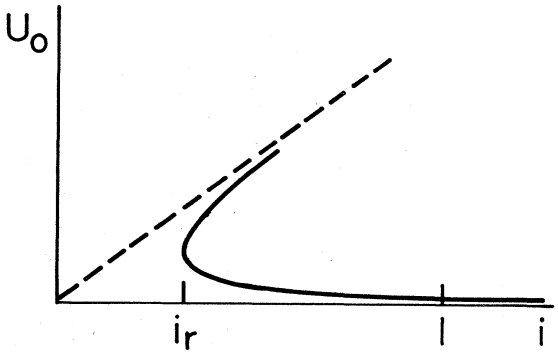

FIG. 66. Qualitative curve $U_0=U_0(i)$.

tances produces a stable branch $U_0=U_0^+(i)$ of the I-V characteristic. The situation is analogous to the case, analyzed in Sec. IV, of a resistive domain in a shunted superconductor, but here R_i is not a parameter of the external circuit but is determined by the values of contact resistances (cf. Figs. 35 and 66).

The current i_r in Eq. (8.17) is the current of complete recovery of superconductivity. As follows from Eq. (8.18), i_r is substantially less than the minimum current of normal phase existence i_m if transition resistances are high. Consequently, the breakdown of superconductivity in current-carrying conductors can start in this case at $j>j_r \ll j_m$, as a result of formation of stable resistive domains in specimens (Akhmetov and Mints, 1982).

Let us consider the reverse case, $D \gg L_s$, in which the current $i_s(x)$ slowly varies over a distance $\sim L_s$, and the resistive domain length is large compared with the thermal width of domain boundaries, also $\sim L_s$. The boundaries can thus be treated independently of each other, and we can derive an expression for the I-V characteristic as follows. At high contact resistances the thermal and electrical coupling of the normal metal to the superconductor is weak. The N-S interfaces are then in equilibrium if the current passing through them equals the minimum current of normal-zone propagation for the superconducting layer, i.e., $i_s(\pm D/2)=i_{ps}$ where $i_{ps}=[2(1-\alpha_i i^2)/\alpha_s]^{1/2}$ and $\alpha_s=2\zeta d_i=d_s\rho_s j_c^2/(T_c-T_0)h$ is the Stekly parameter of this layer. Using this condition, we can find the distribution $i_s(x)$ from Eq. (8.8):

$$i_s(x)=\frac{i}{1+\zeta}+\left[i_{ps}-\frac{i}{1+\zeta}\right]\frac{\cosh(x/L_b)}{\cosh(D/2L_b)}\ , \qquad 2|x|<D\ , \tag{8.20}$$

$$i_s(x)=i+(i_{ps}-i)\exp[(D-2x)/2L_i],\quad 2x>D\ , \tag{8.21}$$

$$D(i)=2L_b\,\mathrm{arctanh}\left[\frac{i-i_{ps}}{i_{ps}\sqrt{1+\zeta}-i/\sqrt{1+\zeta}}\right]\ . \tag{8.22}$$

Substituting the distribution $i_s(x)$ into the expression

$$U_0=\frac{2}{\zeta}\int_0^{D/2} i_s(x)\frac{dx}{L_i}$$

we arrive at the I-V characteristic of the superconductor containing a resistive domain,

$$U_0^+(i)=\frac{iD(i)}{2L_i}+i-i_{ps}\ , \tag{8.23}$$

where $D(i)$ is given by Eq. (8.22). As follows from (8.22), the domain length $D(i)$ monotonically increases with increasing i, tending to a finite limit $2L_b$. For this reason the first term in Eq. (8.23) is small to order $L_b/L_i \ll 1$, and $U_0^+(i)$ is a linear function of i. If $D \ll L_b$, it has the form

$$U^+(j)=2L_i\rho_n\frac{d_s}{d_n}(j-j_{ps})\ . \tag{8.24}$$

The I-V characteristics $U_0(i)$ for the above model are shown in Fig. 67. A significant feature is the threshold current $i=i_f$, above which the stable branch $U_0=U_0^+(i)$ vanishes. This behavior is caused by a characteristic drop in the distributions of temperature, $\theta_s(x)$, and current, $i_s(x)$, at $x=0$ [see Eqs. (8.20)–(8.22) and Fig. 68, which plots the results of numerical simulation]. At $i=i_f$ the temperature at the point $x=0$ drops to below $\theta_r(i_s)$, resulting in the formation of a superconducting "interlayer," i.e., the resistive domain splits in two. The current at the domain center then diminishes below the minimum current of normal phase existence for the superconducting layer, $i_{ms}=\alpha_s^{-1/2}=(2\alpha_i\zeta)^{-1/2}$. Substituting this value of i_{ms} into Eqs. (8.20) and (8.22), we find

$$i_f=\tfrac{1}{2}(\alpha_i)^{-1/2}\ , \tag{8.25}$$

$$D(i_f)=L_b\ln\left[\frac{\sqrt{3}+1}{\sqrt{3}-1}\right]\simeq 1.32L_b\ . \tag{8.26}$$

Consequently, a static resistive domain begins to divide at a current i_f of the order of the minimum current of

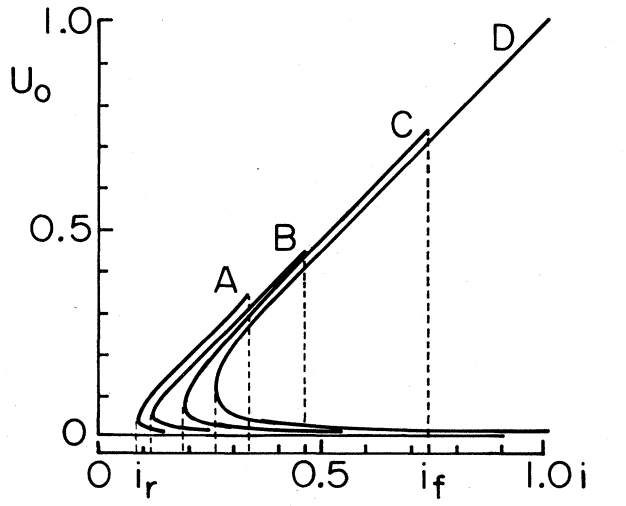

FIG. 67. Numerically calculated I-V characteristic for $L_i/L_s=50$, $\psi=0.1$, $\xi=9\times10^3$, and different values of α: (A) $\alpha=1$; (B) $\alpha=2$; (C) $\alpha=5$; (D) $\alpha=10$ (Akhemtov and Mints, 1983b).

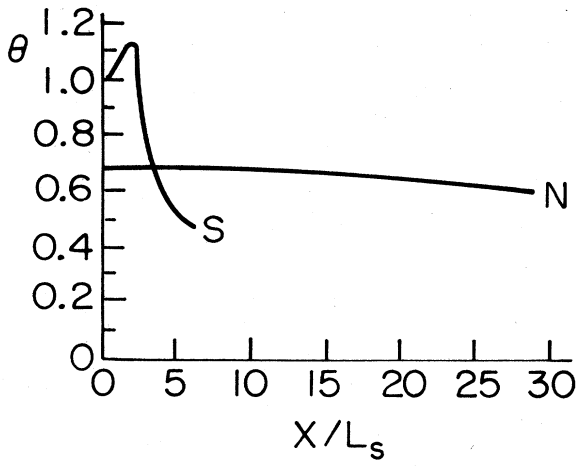

FIG. 68. Temperature distribution in normal metal and superconductor $i=i_f$ (Akhmetov and Mints, 1983b).

normal-zone existence, calculated for negligibly small transition resistances.

B. Periodic splitting of resistive domains. Self-replication of dissipative structures in superconductors

We shall consider now how a normal zone propagates in a composite superconductor with high contact resistances in response to a heat pulse of energy $Q_p > Q_c$. This problem was treated by Akhemtov and Mints (1983b, 1985), who carried out the necessary numerical solution of Eqs. (8.6)—(8.8).

At $i_r < i < i_f$ the heat pulse results in the formation of a stable resistive domain. At $i > i_f$, the perturbation initiates the normal phase propagation in the following manner (Fig. 69). First a normal phase region appears in the superconductor. After a time $t \sim t_s$ a superconducting "interlayer" appears at the center of the normal region.

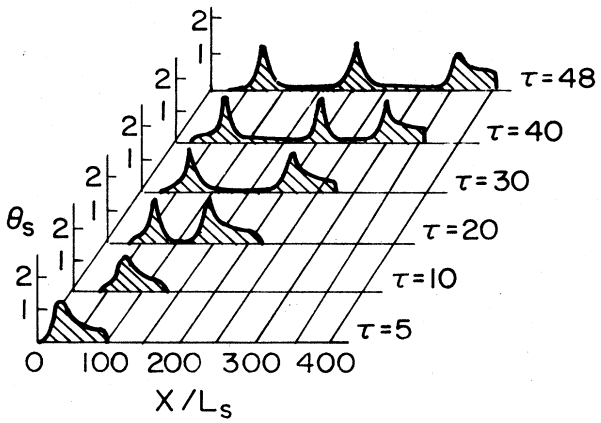

FIG. 69. Dynamic of resistive domain splitting for $i > i_f$. Time τ is given in units of t_s (Akhmetov and Mints, 1983a).

This pair of resistive domains recedes in opposite directions, at the same time increasing in size, and at a distance $\sim L_i$ between domains each of them again splits in two. The two outermost daughter domains (leading domains) continue to move away from the point at which the normal phase nucleated. Their lengths grow in time, and at a distance $\sim L_i$ from the point of the preceding splitting each leading domain splits into a leading and a dropout domain. This process of growth and subsequent splitting of the leading domain is periodically repeated, as shown in Fig. 69 illustrating the dynamics of temperature distribution in the superconductor.

As a result, a "self-replicating" periodic chain of resistive domains is formed in the composite superconductor. The chain length grows at twice the velocity v of the leading domain. Figure 70 plots numerically calculated $v=v(j)$ and the period $l_f(j)$ of the structure as functions of current. The length $l_f(j)$ is of order L_i, and $v(j)$ is of the order of thermal velocity L_s/t_s. The processes of normal phase propagation are, therefore, quite different in composites with high and low contact resistances. The propagation of a switching wave, which transforms the specimen into a uniform normal or superconducting state, is replaced with the growth of a periodic resistive structure. This process is a typical example of self-replication of dissipative structures in nonequilibrium systems (see, for example, Nicolis and Prigogine, 1977; Haken, 1978).

The current I_f, above which the self-replication sets in, is here of the same order of magnitude as the minimum current I_m of normal phase existence, calculated without taking into account the contact resistances. For this reason, the growth of contact resistances does not of itself increase the minimum current I_r of superconductivity recovery. Moreover, high contact resistances diminish I_r, because now individual resistive domains can exist in the specimen even at $I > I_r \sim I_m(L_s/L_i)^{1/2} \ll I_m$.

The effects discussed above were observed in experimental studies of superconductivity breakdown in com-

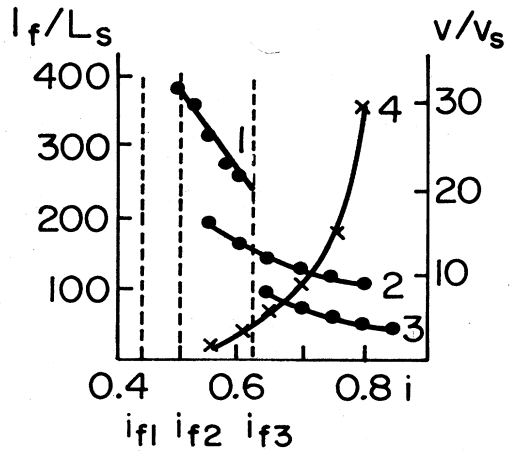

FIG. 70. The period of resistive structure, L_f, as a function of current i: (1) $L_i/L_s=200$; (2) $L_i/L_s=100$; (3) $L_i/L_s=50$. Curve 4 plots current i as a function of the mean velocity of the leading domain for $L_i/L_s=100$ (Akhmetov and Mints, 1983a).

posite superconductors with high contact resistances (Akhemtov, Baev, and Mints, 1983; Akhemtov and Baev, 1984; Keilin and Kruglov, 1984). Thus a stable resistive domain was observed to nucleate in a specimen in response to the application of a single heat pulse.

Figure 71 plots typical I-V characteristics of a composite superconductor containing a resistive domain. The curves in this figure manifest all the qualitative features outlined above, namely, a nearly linear stable branch, an excess current I_v, and threshold currents I_r and I_f at which a single-domain state breaks down. Figure 72 plots these currents as functions of induction B of external magnetic field.

The following pattern was observed in the range of $I > I_f$. At $0.1 < B < 2$ T an external perturbation initiates the nucleation and subsequent multiple splitting of resistive domains, until a predominant part of the specimen fills up with a periodic resistive structure. The formation of each new domain causes a stepwise increase in voltage across the superconductor (Fig. 73).

In stronger fields, $2 < B < 7$ T, such domains usually split once or twice and then are localized on specimen inhomogeneities. Further current increase splits one of the localized domains, producing a step on the I-V characteristic (Fig. 74). When I is reversed, hysteresis is observed, i.e., $I_r \neq I_f$. Note that quite similar characteristics were reported by Baker and Mitchell (1974), who investigated superconductivity breakdown in current-carrying thin films on metal substrates.

The current-voltage characteristics of composite superconductors with high contact resistances thus manifest steps similar to those described in Sec. V. These steps are caused in these two cases by both longitudinal (along the current direction) and transversal (due to contact resistances) inhomogeneities in specimen properties.

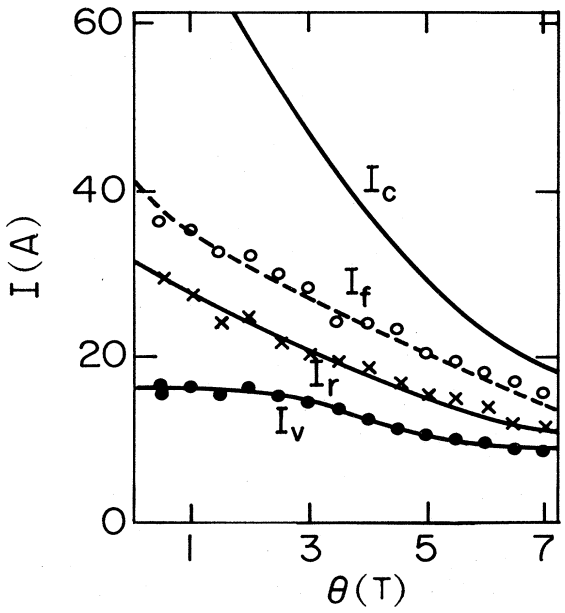

FIG. 72. Currents I_c, I_f, I_v, and I_r as functions of B (Akhmetov and Baev, 1984).

IX. CONCLUSION

The present review is restricted to treating thermal bistability in normal metals and superconductors. Such phenomena can arise in other media with thermal bistability as well, e.g., in combustion wave propagation

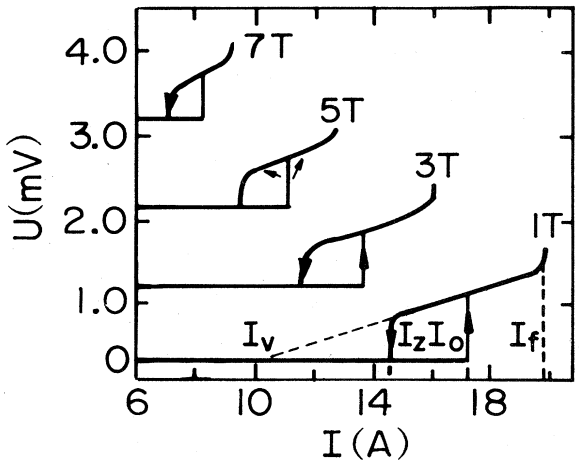

FIG. 71. I-V characteristics of a composite with high contact resistance and different values of B (Akhmetov and Baev, 1984).

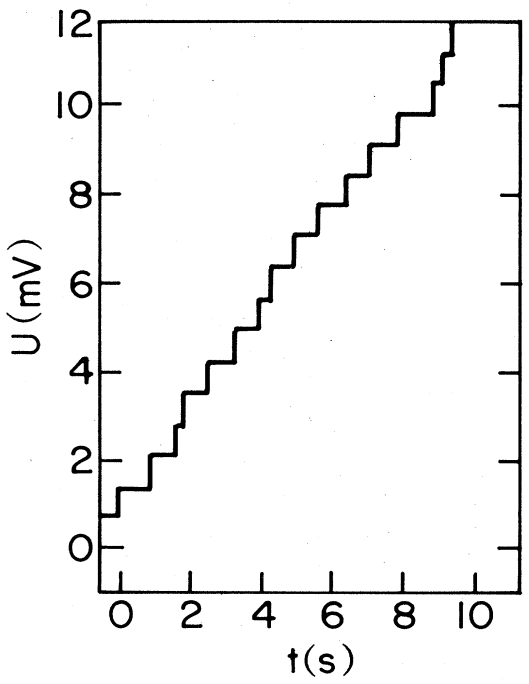

FIG. 73. Oscillogram of voltage across the superconductor in the course of resistive domain splitting ($B < 2$ T) (Akhmetov and Baev, 1984).

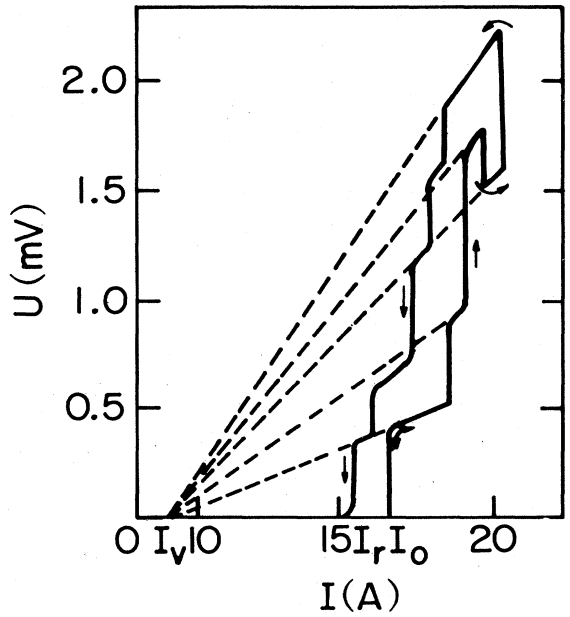

FIG. 74. I-V characteristic of a composite with high contact resistances, in the case of localization of several resistive domains ($B>2$ T) (Akhmetov and Baev, 1984).

(Frank-Kamenetsky, 1967; Zeldovich *et al.*, 1980), in optical gas discharge (Bunkin *et al.*, 1969; Raizer, 1980), in heterogeneous catalysis (Volodin, Barelko, and Merzhanov, 1982; Gurevich and Mints, 1984b), in the heating of gas or semiconductor plasma by electromagnetic field (Bass and Gurevich, 1975; Nedospasov and Khait, 1979; Raizer, 1980), in optical thermal breakdown of dielectrics (Young, 1971; Epshtein, 1978; Rozanov, 1981; Golik *et al.*, 1983), in the flow of helium II through a thin channel (Rumanov, 1978, 1982), in the quantum Hall effect (Cage *et al.*, 1983; Ebert *et al.*, 1983; Gurevich and Mints, 1984c; Komiyama *et al.*, 1985), etc. A mathematical description of these systems can be carried out by analogy to that outlined above, although in some cases a mere change in notation is sufficient.

Note also that a substitution of order parameter $\Delta(x,t)$ or concentration $n(x,t)$ for temperature T in the heat conduction equation (3.1) converts it, for an appropriate choice of ν, κ, Q, and W, into a Ginzburg-Landau-type equation or a nonlinear diffusion equation describing first-order phase transitions, bistability in chemical kinetics, etc. It is thus possible to treat in a uniform framework a wide class of physical, chemical, and biological systems (see, for example, the review of Gurevich and Mints, 1984a).

APPENDIX A: IMPEDANCE OF A CONDUCTOR CONTAINING AN ELECTROTHERMAL DOMAIN

In deriving the expression for $Z(\omega)$ we follow the procedure employed in the physics of semiconductors (Knight and Peterson, 1967). We begin with the current-carrying superconductor. Expressing the quantity $\delta E(x,\omega)$ in Eq. (4.34) through $\delta T(x,\omega)$ and $\delta I(\omega)$, we find

$$Z(\omega)=\frac{\partial}{\partial I}\int_0^{L_c}(j-j_c)\rho\,dx + \int_0^{L_c}\frac{\partial}{\partial T}[(j-j_c)\rho]\frac{\delta T(x,\omega)}{\delta I(\omega)}dx\ , \tag{A1}$$

where L_c is the total length of the superconductor. Linearizing Eq. (3.1) with respect to small perturbations δT and δI, we arrive at an equation for the function $\varphi=\kappa\,\delta T/\delta I$ in Eq. (A1),

$$\frac{d^2\varphi}{dx^2}-\frac{1}{\kappa}\left[i\omega\nu+\frac{\partial f}{\partial T}\right]\varphi=-\frac{\partial Q}{\partial I}\ , \tag{A2}$$

where we have set $G=0$ for the sake of simplification. Now we expand $\varphi(x)$ in the complete set of eigenfunctions $\psi_n(x)$ of the equation,

$$\frac{d^2\psi_n}{dx^2}-\frac{1}{\kappa}\left[\gamma_n\nu+\frac{\partial f}{\partial T}\right]\psi_n=0\ , \tag{A3}$$

$$\varphi(x)=\sum_n c_n\psi_n(x),\quad \int_0^{L_c}\frac{\nu}{\kappa}\psi_m\psi_n dx=\delta_{mn}\ . \tag{A4}$$

The coefficients c_n will be found by multiplying Eq. (A2) by $\psi_n(x)$, and (A3) by $\varphi(x)$, integrating the two equations, and subtracting one from the other. Substituting the thus found function $\varphi(x,\omega)$ into (A1), we obtain for $Z(\omega)$

$$Z(\omega)=R_\infty+\sum_{n=0}^{\infty}\frac{C_n}{\gamma_n-i\omega}\ , \tag{A5}$$

$$C_n=-\int_0^{L_c}\frac{\partial}{\partial T}[(j-j_c)\rho]\psi_n(x)\frac{dx}{\kappa} \times\int_0^{L_c}\frac{\partial Q}{\partial I}\psi_n(x')dx'\ , \tag{A6}$$

where R_∞ is the differential resistance of the specimen at a fixed T_m [the first term in Eq. (A1)]. The quantity R_∞ describes the high-frequency ($\omega t_n\gg1$) impedance of the superconductor. The expression for R_∞ becomes especially illustrative in the case $D\gg L$, in which, to an accuracy of order $L/D\ll1$,

$$R_\infty(j)=\frac{\rho(T_3)D(j)}{A}\ . \tag{A7}$$

The poles in $Z(\omega)$ correspond to different domain modes that change the specimen resistance. For instance, the mode with $n=0$ corresponds to uniform expansion or contraction of the domain. The coefficients C_n vanish for antisymmetrical perturbations [$\psi_n(x)=-\psi_n(-x)$, $n=1,3,5,\ldots$] owing to the domain symmetry [$T(x)=T(-x)$]. These perturbations do not alter the resistance of the specimen and thus make no contribution to $Z(\omega)$ (e.g., the $n=1$ mode corresponds to a small displacement of the domain as a whole).

The general expression (A5) for $Z(\omega)$ gets substantially simpler if $D\gg L$, when the increment of the most "dangerous" perturbation γ_0 is exponentially small com-

pared with other increments $\gamma_n<0$ ($n=2,4,6,\ldots$, $|\gamma_n|\sim t_n^{-1}$). Then we can assume $\omega=0$ for frequencies $\omega t_n \ll 1$ in all terms of Eq. (A5) with $n\geq 2$; this yields

$$Z(\omega)=R_m+\frac{C_0}{\gamma_0-i\omega}\ , \tag{A8}$$

$$R_m=R_\infty+\sum_{n=2}^{\infty}\frac{C_n}{\gamma_n}\ . \tag{A9}$$

The first term in Eq. (A8) describes the resistance of the normal or resistive region of length D, heated to a temperature $T=T_3$. The second term in (A8) represents the motion of domain boundaries. In order to find R_m, we differentiate the expression for voltage across a resistive domain, $U=I\rho(T_3)D/A$, with respect to I, for $D=$const and $D\gg L$:

$$R_m=\frac{\partial U}{\partial I}=\left[\rho(T_3)+\frac{\partial\rho}{\partial T}\frac{\partial T_3}{\partial I}I\right]\frac{D}{A}\ .$$

The derivative $\partial T_3/\partial I$ in this expression will be found by differentiating the heat balance equation $\rho(T_3)j^2=W(T_3)$ with respect to I, whence

$$2j\rho(T_3)=\left[\frac{\partial W}{\partial T}-j^2\frac{\partial\rho}{\partial T}\right]_{T_3}\frac{\partial T_3}{\partial j}\ .$$

Finally, we find from the last two equations

$$R_m(j)=\left[1+\frac{2j_p^2\frac{\partial\rho}{\partial T}}{\frac{\partial W}{\partial T}-j_p^2\frac{\partial\rho}{\partial T}}\right]_{T_3}R_\infty(j)\ . \tag{A10}$$

This expression takes into account that if $D\gg L$, then $I\approx I_p$.

The coefficient C_0 in Eq. (A8) will be found by using the identity $Z(0)=R(I)$, where $R(I)=dU/dI$ is the static differential resistance of the domain-containing specimen and $U(I)$ is given by Eq. (4.5). Assuming $Z=R$ and $\omega=0$ in (A8), we find $C_0=(R-R_m)\gamma_0$. As a result, the low-frequency ($\omega t_n\ll 1$) impedance $Z(\omega)$ takes the form

$$Z(\omega)=R_m(j)+\frac{R(j)-R_m(j)}{1-i\omega/\gamma_0}\ . \tag{A11}$$

For example, if a superconductor is shunted by a resistor r, and the whole circuit is supplied with a current I_0 from a dc unit, then $I_pR_\infty=(I_0-I)r$, whence

$$R_m=r\left[\frac{I_0}{I_p}-1\right]\left[1+\frac{2j_p^2\frac{\partial\rho}{\partial T}}{\frac{\partial W}{\partial T}-j_p^2\frac{\partial\rho}{\partial T}}\right]_{T_3}\ . \tag{A12}$$

The low-frequency impedance of a normal conductor with an electrothermal domain is also given by Eq. (A11), but then R_m is

$$R_m=(L_c-D)\frac{\rho(T_1)}{A}\left[1+\frac{2\frac{\partial Q}{\partial T}}{\frac{\partial W}{\partial T}-\frac{\partial Q}{\partial T}}\right]_{T_1}+\frac{D\rho(T_3)}{A}\left[1+\frac{2\frac{\partial Q}{\partial T}}{\frac{\partial W}{\partial T}-\frac{\partial Q}{\partial T}}\right]_{T_3} \tag{A13}$$

and $D(U)$ is given by Eq. (4.22).

As an example, consider the stepwise heat production model. The equation for small temperature perturbations, $\delta\theta(x/L)\exp(\lambda t/t_h)$, is

$$\delta\theta''-\left[1+\lambda-\frac{\alpha i^2L}{\theta_r}\delta\left[|x|-\frac{D}{2}\right]\right]\delta\theta=0\ , \tag{A14}$$

where $\lambda=\gamma t_h$ is a dimensionless increment. The solution of Eq. (A14), with a boundary condition $\delta\theta(\pm\infty)=0$, yields a dispersion relation for λ_0:

$$\left[1+\tanh\left[\frac{D\sqrt{1+\lambda_0}}{2L}\right]\right]\theta_r\sqrt{1+\lambda_0}=\alpha i^2\ . \tag{A15}$$

In the limit $i\to i_p$, ($\alpha i^2\to 2\theta_r$) Eq. (A15) yields

$$\lambda_0=4\exp\left[-\frac{D}{L}\right]=\frac{4}{\alpha i_p^2}(\alpha i^2-2\theta_r)\ , \tag{A16}$$

which is in agreement with the qualitative estimate of Eq. (4.33). Equation (A15) was derived for an infinite specimen. The stability of a resistive domain in a finite-size specimen has been studied by Bedeaux and Mazur (1981).

Let us derive an expression for $Z(\omega)$ of a superconductor containing a resistive domain. In the stepwise heat production model an electric field fluctuation δE is related to current fluctuation δI and temperature fluctuation $\delta\theta$ as follows:

$$\delta E=\{\eta[\theta(x)-\theta_r]\delta i+\delta[\theta(x)-\theta_r][\delta\theta-\theta_r'\delta i]i\}\rho j_c\ , \tag{A17}$$

where $\delta(x)$ is the delta function, $\theta_r'=\partial\theta_r/\partial i$ and $\theta(x)$ is the temperature distribution in a steady-state domain. Substituting Eq. (A17) into Eq. (4.34), we find

$$Z(\omega)=\left\{D(i)+\frac{2iL}{\theta_r}\left[\varphi\left[\frac{D}{2},\omega\right]-\theta_r'\right]\right\}\frac{\rho}{A}\ , \tag{A18}$$

where $\varphi=\delta\theta/\delta i$. The equation for φ is

$$\varphi''-\left[1+i\omega_0-\frac{\alpha i^2}{\theta_r}\delta\left[|x|-\frac{D}{2}\right]\right]\varphi=2\alpha i\eta\left[|x|-\frac{D}{2}\right]+\frac{\alpha i^2}{\theta_r}\theta_r'\delta\left[|x|-\frac{D}{2}\right]\ , \tag{A19}$$

where $\omega_0=\omega t_h$ is the dimensionless frequency. Solving Eq. (A19) and substituting $\varphi(x,\omega)$ into Eq. (A18), we finally obtain

$$Z(\omega)=\left[D+\frac{2[2K\alpha i^2-a_0^2 i(1+K)\theta_r']L}{a_0[(1+K)a_0\theta_r-\alpha i^2]}\right]\frac{\rho}{A}\ , \tag{A20}$$

where $K=\tanh(a_0 D/2L)$ and $a_0(\omega)=\sqrt{1+i\omega t_h}$. Equation (A20) gives a complete description of the linear response of a superconductor containing a resistive domain, which is the nonlinear element of the electric circuit. The poles of $Z(\omega)$ determine the spectrum of eigenfrequencies in the fixed-current regime. Assuming $\lambda=i\omega t_h$ and setting the denominator of Eq. (A20) to zero, we again obtain Eq. (A15). The zeros of $Z(\omega)$ give the spectrum of eigenfrequencies of a resistive domain in the fixed-voltage regime.

APPENDIX B: NORMAL-ZONE DYNAMICS IN THE STEPWISE HEAT PRODUCTION MODEL

First we derive equations describing the dynamics of normal-zone boundaries (Lvovsky and Lutset, 1979; Gurevich and Mints, 1982; Bezuglyj and Shkovskij, 1984, 1985). Formally, the solution of the heat conduction equation (3.1) for the stepwise heat production model is

$$\theta(x,t)=\int_{-\infty}^{\infty}\theta_0(x')G(x-x',t)dx'+\int_0^t du\int_{-\infty}^{\infty}dx'G(x-x',t-u)i^2(u)\alpha(x')\eta[\theta(x',u)-\theta_r]\ , \tag{B1}$$

$$G(x,t)=\frac{1}{2\sqrt{\pi t}}\exp\left[-\frac{x^2}{4t}-t\right]\ , \tag{B2}$$

where $G(x)$ is a Green's function and $\theta_0(x)$ is the initial temperature distribution produced by an external perturbation. Let us consider the dynamics of normal-zone boundaries $D_+(t),D_-(t)$ in the neighborhood of a point inhomogeneity if $\alpha(x)=[1+\Gamma\delta(x/L)]\alpha$ (Fig. 59). Using the self-consistency conditions $\theta(\pm D_\pm(t),t)=\theta_r$ and integrating over x' in the second term of Eq. (B1), we obtain a system of nonlinear integral equations for $D_\pm(t)$ (Gurevich and Mints, 1982):

$$2\theta_r(i)=\frac{e^{-\tau}}{\sqrt{\pi\tau}}\int_{-\infty}^{\infty}\theta_0(s)\exp\left[-\frac{(\pm z_\pm(\tau)-s)^2}{4\tau}\right]ds$$
$$+\alpha\int_0^\tau e^{-u}i^2(\tau-u)\left[\frac{\Gamma}{\sqrt{\pi u}}\exp\left[-\frac{z_\pm^2(\tau)}{4\tau}\right]+\operatorname{erf}\left[\frac{z_\pm(\tau-u)-z_\pm(\tau)}{2\sqrt{u}}\right]+\operatorname{erf}\left[\frac{z_\mp(\tau-u)+z_\pm(\tau)}{2\sqrt{u}}\right]\right]du\ , \tag{B3}$$

where $z_\pm=D_\pm/L$, $\tau=t/t_h$. This system offers certain advantages for describing normal-zone dynamics, because it requires no "redundant" information on details of temperature distribution $\theta(x,t)$ in the specimen.

As $z_-\to\infty$, Eqs. (B3) describe a nonstationary motion of the N-S boundary $z_+=z_+(\tau)$ which arises, for example, in a superconductor carrying time-dependent transport current. The normal-zone dynamics was treated in this case by Lvovsky and Lutset (1979) and Bezuglyj and Shklovskij (1985).

Equations (B3) describe, among other things, the normal-zone dynamics in a homogeneous specimen after a local heat pulse, for which

$$\theta_0(x)=\frac{Q_p}{Q_0}\delta(s)\delta(\tau)\ ,$$
$$z_+(\tau)=z_-(\tau)=z(\tau)$$

is the dimensionless length of the normal zone, Q_p is the perturbation energy, and $Q_0=\nu AL(T_c-T_0)$. For a fixed current we find

$$\frac{2\theta_r}{\alpha i^2}=\frac{Q_p}{\alpha i^2 Q_0}\exp\left[-\tau-\frac{z^2(\tau)}{4\tau}\right]$$
$$+\int_0^\tau e^{-u}\left[\operatorname{erf}\left[\frac{z(\tau-u)-z(\tau)}{2\sqrt{u}}\right]+\operatorname{erf}\left[\frac{z(\tau-u)+z(\tau)}{2\sqrt{u}}\right]\right]du\ . \tag{B4}$$

This equation implies that the following scaling law holds for the critical energy Q_c: $Q_c=Q_0\alpha i^2\varphi(\xi)$ where $\varphi(\xi)$ is a function of a single dimensionless parameter $\xi=\theta_r/\alpha i^2$ (Gurevich, Kazantsev, and Parizh, 1983).

Now let us derive equations describing normal-zone dynamics when a resistive domain or an N-S interface is localized at a point inhomogeneity. Such localization arises in the current range $|I-I_p|\lesssim\Gamma I_p\ll I_p$, where the velocity of motion of N-S interfaces is low $[v(I)\ll v_h]$. We can, therefore, expand the functions $D_\pm(\tau-u)\approx D_\pm(\tau)-u\dot{D}_\pm(\tau)$ in Eq. (B3), assuming $D_\pm\gg L$. Assuming that the current $I(\tau)$ also varies sufficiently slowly ($\dot{I}\ll I$), we arrive at the following quasistationary differential equations (Gurevich and Mints, 1982):

$$\tfrac{1}{2}\dot{y}_+ +2y_+\frac{\dot{I}}{I}=\Gamma-(2\xi-1)y_+-\frac{1}{y_-}\ , \tag{B5}$$

$$\tfrac{1}{2}\dot{y}_- +2y_-\frac{\dot{I}}{I}=\Gamma-(2\xi-1)y_--\frac{1}{y_+}\ , \tag{B6}$$

where $y_\pm=\exp[D_\pm(\tau)/L]$. The conditions of validity of Eqs. (B5) and (B6), $\dot{D}_\pm\ll L$, hold if $\Gamma\ll 1$, $|2\xi-1|$, $y_+y_-\gg 1$.

Equations (B5) and (B6) for $\dot{I}=0$ have an exact solution. To obtain it, we use more convenient variables u and v:

$$y_+ +y_-=2uv\ , \tag{B7}$$

$$y_+ -y_-=2u(v^2-1)^{1/2}\ . \tag{B8}$$

This gives

$$u'=\frac{1}{v^2-1}(au^2-uv+a)\ , \tag{B9}$$

where the prime denotes differentiation with respect to v, and $a=\sqrt{(2\xi-1)}/\Gamma$ (we specify $\Gamma>0$, which means that localization occurs at $2\xi-1>0$, i.e., at $i<i_p$). A substitution

$$u(v)=-\frac{1}{a}(v^2-1)\frac{\psi'}{\psi}$$

reduces Eq. (B9) to a linear second-order equation for $\psi(v)$,

$$(v^2-1)^2\psi''+3v(v^2-1)\psi'+a\psi=0\ . \tag{B10}$$

The solution of this equation is

$$\psi(v)=C_1(v^2-1)^k[F(k,k+1,\tfrac{1}{2},v^2) +C_2vF(k+\tfrac{1}{2},k+\tfrac{3}{2},\tfrac{3}{2},v^2)]\ , \tag{B11}$$

$$k=-\tfrac{1}{4}\pm\left[\frac{1}{16}-\frac{a^2}{4}\right]^{1/2}\ , \tag{B12}$$

where $F(b_1,b_2,b_3,x)$ is a hypergeometric function and C_1 and C_2 are arbitrary constants. Equations (B11) and (B12) completely define the phase trajectories of the system of Eqs. (B5) and (B6) (see Fig. 60). The constant C_2 is determined by the initial conditions, i.e., by $y_+(0)$ and $y_-(0)$.

REFERENCES

Abramov, G. I., A. Vl. Gurevich, V. M. Dzugutov, R. G. Mints, and L. M. Fisher, 1983, Pis'ma Zh. Eksp. Teor. Fiz. **37**, 453 [JETP Lett. **37**, 535 (1983)].

Abramov, G. I., A. Vl. Gurevich, S. I. Zakharchenko, R. G. Mints, and L. M. Fisher, 1985, Fiz. Tverd. Tela (Leningrad) **27**, 2250 [Sov. Phys. Solid State **27**, 1350 (1985)].

Akhmetov, A. A., and V. P. Baev, 1984, Cryogenics **24**, 67.

Akhmetov, A. A., V. P. Baev, and R. G. Mints, 1983, Zh. Tekh. Fiz., Pis'ma Red. **9**, 1188.

Akhmetov, A. A., and R. G. Mints, 1982, Zh. Tekh. Fiz. Pis'ma Red. **8**, 1093.

Akhmetov, A. A., and R. G. Mints, 1983a, Zh. Tekh. Fiz. Pis'ma Red. **9**, 1306.

Akhmetov, A. A., and R. G. Mints, 1983b, J. Phys. D **16**, 2505.

Akhmetov, A. A., and R. G. Mints, 1985, J. Phys. D **18**, 925.

Akopov, S. G. and G. G. Svalov, 1985, Cryogenics **25**, 251.

Altov, V. A., M. G. Kremlev, V. V. Sytchev, and V. B. Zenkevitch, 1973, Cryogenics **13**, 420.

Altov, V. A., V. B. Zenkevitch, M. G. Kremlev, and V. V. Sytchev, 1977, *Stabilization of Superconducting Magnetic Systems* (Plenum, New York).

Anashkin, O. P., V. E. Keilin, and V. V. Lyikov, 1979, Cryogenics **19**, 77.

Anashkin, O. P. V. E. Keilin, and V. V. Lyikov, 1981, Cryogenics **21**, 169.

Anderson, A. C., 1981, in *Nonequilibrium Superconductivity, Phonons, and Kapitza Boundaries,* edited by K. E. Gray (Plenum, New York/London), p. 1.

Ando, T., Y. Takahashi, M. Nichi, E. Tada, K. Okuno, and S. Shimamoto, 1985, IEEE Trans. Magn. **21**, 165.

Aomine, T., and K. Miyake, 1979, J. Low Temp. Phys. **37**, 85.

Aronov, A. G., Yu. M. Gal'perin, V. L. Gurevich, and V. I. Kozub, 1981, Adv. Phys. **30**, 539.

Aronson, D. C., and H. F. Weinberger, 1978, Adv. Math. **30**, 33.

Atrazhev, V. M., and I. T. Yakubov, 1980, Teplofiz. Vys. Temp. **18**, 16.

Ausloos, M., 1981, Physica B **108**, 969.

Baev, V. P., A. Vl. Gurevich, R. G. Mints, and M. S. Ushomirsky, 1982a, Fiz. Tverd. Tela (Leningrad) **24**, 1544 [Sov. Phys. Solid State **24**, 886 (1982)].

Baev, V. P., A. Vl. Gurevich, R. G. Mints, and M. S. Ushomirsky, 1982b, IEEE Trans. Magn. **19**, 236.

Baker, I. W., and E. N. Mitchell, 1974, Phys. Rev. B **10**, 4593.

Barelko, V. V., V. M. Beibutyan, Yu. E. Volodin, and Ya. B. Zeldovich, 1981, Dok. Akad. Nauk SSSR **257**, 339 [Sov. Phys. Dokl. **26**, 335 (1981)].

Barker, D. C., 1973, J. Comput. Phys. **11**, 333.

Bartlett, R. J., R. V. Carlson, and W. C. Overton, 1979, IEEE Trans. Magn. **15**, 343.

Bass, F. G., and Yu. G. Gurevich, 1975, *Hot Electrons and Strong Electric Waves in Semiconductor and Gas Phase Plasma* (Nauka, Moscow).

Bedeaux, D., and P. Mazur, 1981, Physica A **105**, 1.

Bedeaux, D., P. Mazur, and R. A. Pasmanter, 1977, Physica A **86**, 355.

Berkovich, S. Ya., 1965, Radiotekhn. Elektron. **10**, 736.

Bezuglyj, A. I., and V. A. Shklovskij, 1984, J. Low Temp. Phys. **57**, 227.

Bezuglyj, A. I., and V. A. Shklovskij, 1985, Fiz. Tverd. Tela (Leningrad) **27**, 2980 [Sov. Phys. Solid State **27**, 1790 (1985)].

Bindari, A. E., and R. E. Bernert, 1968, J. Appl. Phys. **39**, 2529.

Bogomolov, V. N., B. E. Kvyatkovsky, E. B. Kolla, S. A. Ktitorov, Yu. A. Kumzerov, and N. M. Okuneva, 1981, Fiz. Tverd. Tela (Leningrad) **23**, 2173 [Sov. Phys. Solid State **23**, 1271 (1981)].

Boiko, V. V., Yu. F. Podrezov, and N. P. Klimova, 1982a, Zh. Eksp. Teor. Fiz. **82**, 1704 [Sov. Phys. JETP **55**, 985 (1982)].

Boiko, V. V., Yu. F. Podrezov, and N. P. Klimova, 1982b, Pis'ma Zh. Eksp. Teor. Fiz. **35**, 524 [JETP Lett. **35**, 649 (1982)].

Boiko, V. V., Yu. F. Podrezov, and N. P. Klimova, 1984, Fiz. Nizk. Temp. **10**, 921.

Bonch-Bruevich, V. L., I. P. Zvyagin, and A. G. Mironov, 1972, *Domain Electric Instability in Semiconductors* (Nauka, Moscow).

Brechna, H., 1973, *Superconducting Magnetic Systems* (Springer, Berlin/Heidelberg/New York).

Breemer, I. W., and V. L. Newhouse, 1958, Phys. Rev. Lett. **1**, 282.

Breemer, I. W., and V. L. Newhouse, 1959, Phys. Rev. **116**, 309.

Broom, R. F., and E. H. Rhoderick, 1960, Brit. J. Appl. Phys. **11**, 292.

Bunkin, F. V., V. I. Konov, A. M. Prokhorov, and V. B. Fyodorov, 1969, Pis'ma Zh. Eksp. Teor. Fiz. **9**, 609 [JETP Lett **9**, 371 (1969)].

Bush, H., 1921, Ann. Phys. (Leipzig) **64**, 401.

Büttiker, M., and R. Landauer, 1982, in *Nonlinear Phenomena at Phase Transitions and Instabilities,* edited by T. Ristle (Plenum, New York/London), p. 111.

Cage, M. E., R. F. Dziuba, B. F. Field, E. R. Williams, S. M. Girvin, A. C. Gossard, D. C. Tsui, and R. I. Wagner, 1983,

Phys. Rev. Lett. **51**, 1374.
Campbell, A. M. and I. E. Evetts, 1972, *Critical Currents in Superconductors* (Taylor and Francis, London).
Carr, W. J., 1983, *AC loss and macroscopic theory of superconductors* (Gordon and Breach, New York).
Cesnak, L., 1983, Cryogenics **23**, 662.
Cesnak, L., and I. Kokavec, 1969, Cryogenics **9**, 376.
Chechetkin, V. R., E. B. Levchenko, A. I. Sigov, 1985, J. Phys. D **18**, 461.
Chen, W. Y., and I. R. Purcell, 1978, J. Appl. Phys. **49**, 3546.
Cherry, W. H., and J. I. Gittleman, 1960, Solid State Electron. **1**, 287.
Christianson, O., and R. W. Boom, 1984, Adv. Cryog. Eng. **29**, 207.
Clem, J. R., and R. J. Bartlett, 1983 IEEE Trans. Magn. **19**, 424.
Cornelissen, M. C. M., and C. J. Hoogendoorn, 1985, Cryogenics **25**, 3.
Decker, S. K., and D. W. Palmer, 1977, J. Appl. Phys. **48**, 2043.
Dharmadurai, G., 1980a, Phys. Status Solid A **62**, 9.
Dharmadurai, G., 1980b, J. Low Temp. Phys. **40**, 51.
Dharmadurai, G., 1981, Nuovo Cimento B **64**, 503.
Dharmadurai, G., and V. Chopra, 1982, Phys. Status Solidi A **67**, 677.
Dharmadurai, G., and B. A. Ratnam, 1979, Solid State Commun. **29**, 205.
Dresner, L., 1976, Cryogenics **16**, 675.
Dresner, L., 1979, IEEE Trans. Magn. **15**, 328.
Dresner, L., 1980, Adv. Cryog. Eng. **26**, 647.
Dresner, L., 1985, IEEE Trans. Magn. **21**, 392.
Ebert, G., K. von Klitzing, K. Ploog, and G. Weimann, 1983, J. Phys. C **16**, 5441.
Eckern, V., A. Schmid, M. Smutz, and G. Schön, 1979, J. Low Temp. Phys. **36**, 643.
Efferson, K. P., 1969, J. Appl. Phys. **40**, 1995.
Elesin, V. F., and Yu. V. Kopaev, 1981, Usp. Fiz. Nauk **133**, 259 [Sov. Phys. Usp. **24**, 116 (1981)].
Elrod, S. A., J. W. Lue, J. R. Miller, and L. Dresner, 1981, IEEE Trans. Magn. **17**, 1083.
Epshtein, E. M., 1978, Zh. Tekh. Fiz. **48**, 1733.
Eru, I. I., V. A. Kaschei, S. A. Peskovatsky and V. S. Sulima, 1974, Fiz. Tverd. Tela (Leningrad) **16**, 3133 [Sov. Phys. Solid State **16**, 2028 (1974)].
Eru, I. I., V. A. Kotashko, A. P. Krut'ko, S. A. Peskovatsky, and A. V. Poladich, 1975, Fiz. Tverd. Tela (Leningrad) **17**, 3119 [Sov. Phys. Solid State **17**, 2068 (1975)].
Eru, I. I., S. A. Peskovatsky, and A. V. Poladich, 1973a, Fiz. Tverd. Tela (Leningrad) **15**, 1599 [Sov. Phys. Solid State **15**, 1069 (1973)].
Eru, I. I., S. A. Peskovatsky, and A. V. Poladich, 1973b, Fiz. Tverd. Tela (Leningrad) **15**, 2228 [Sov. Phys. Solid State **15**, 1488 (1973)].
Eru, I. I., S. A. Peskovatsky, and A. V. Poladich, 1979, Fiz. Tverd. Tela (Leningrad) **21**, 2004 [Sov. Phys. Solid State **21**, 1149 (1979)].
Feuer, M. D., and D. E. Prober, 1981, IEEE Trans. Magn. **17**, 81.
Fife, P. C., 1979, *Mathematical Aspects of Reacting and Diffusion Systems* (Springer, Berlin).
Frank-Kamenetsky, D. A., 1967, *Diffusion and Heat Transfer in Chemical Kinetics* (Nauka, Moscow).
Fulton, T. A., and L. N. Dunkleberger, 1974, J. Appl. Phys. **45**, 2283.
Funaki, K., F. Irie, M. Takeo, V. Ruppert, K. Lüders, and G. Klipping, 1985, Cryogenics **25**, 139.
Gall, W., and P. Turowski, 1978, Cryogenics **18**, 103.
Genevey, P., J. Le Bars, A. Sagnier, and B. Turck, 1983, IEEE Trans. Magn. **19**, 737.
Giarratano, P. J., and N. V. Frederick, 1980, Adv. Cryog. Eng. **25**, 455.
Ginzburg, V. L., 1958, Dok. Akad. Nauk SSSR **118**, 464 [Sov. Phys. Dokl. **3**, 102 (1958)].
Golik, L. L., A. V. Grigor'ants, M. I. Elinson, and Yu. I. Balkarei, 1983, Opt. Commun. **46**, 51.
Golovashkin, A. I., A. N. Lykov, L. M. Lyn'kova, and S. L. Prishepa, 1984, Fiz. Tverd. Tela (Leningrad) **26**, 2985 [Sov. Phys. Solid State **26**, 1801 (1984)].
Goncharov, I. N., G. L. Dorofeev, V. V. Pasyuk, and I. S. Khukhareva, 1980, Fiz. Nizk. Temp. **6**, 698.
Gray, K. E., 1976, J. Low Temp. Phys. **23**, 679.
Gray, K. E., R. T. Kampwirth, J. F. Zasadzinski, and S. F. Ducharme, 1983 J. Phys. F **13**, 405.
Grigor'iev, V. A., Yu. M. Pavlov, and E. V. Ametistov, 1977, *Boiling in Cryogenic Liquids* (Energy, Moscow).
Gubankov, V. N., K. K. Likharev, and N. N. Margolin, 1972, Fiz. Tverd. Tela (Leningrad) **14**, 953 [Sov. Phys. Solid State **14**, 819 (1972)].
Gurevich, A. Vl., 1982, Fiz. Tverd. Tela (Leningrad) **24**, 1776 [Sov. Phys. Solid State **24**, 1010 (1982)].
Gurevich, A. Vl., N. A. Kazantsev, and M. B. Parizh, 1983, Zh. Tekh. Fiz. **53**, 1678.
Gurevich, A. Vl., S. L. Leikin, and R. G. Mints, 1984, Phys. Lett. A **105**, 31.
Gurevich, A. Vl., and R. G. Mints, 1980, Pis'ma Zh. Eksp. Teor. Fiz. **31**, 52 [JETP Lett. **31**, 48 (1980)].
Gurevich, A. Vl., and R. G. Mints, 1981a, Fiz. Tverd. Tela (Leningrad) **23**, 103 [Sov. Phys. Solid State **23**, 57 (1981)].
Gurevich, A. Vl., and R. G. Mints, 1981b, Cryogenics **21**, 102.
Gurevich, A. Vl., and R. G. Mints, 1982, Dok. Akad. Nauk SSSR **267**, 1103 [Sov. Phys. Dokl. **27**, 1037 (1982)].
Gurevich, A. Vl., and R. G. Mints, 1984a, Usp. Fiz. Nauk. **124**, 61 [Sov. Phys. Usp. **27**, 19 (1984)].
Gurevich, A. Vl., and R. G. Mints, 1984b, Khim. Fiz. **3**, 871.
Gurevich, A. Vl., and R. G. Mints, 1984c, Pis'ma Zh. Eksp. Teor. Fiz. **39**, 318 [JETP Lett. **39**, 381 (1984)].
Gurevich, A. Vl., and R. G. Mints, 1985, Phys. Lett. A **109**, 405.
Haken, H., 1978, *Synergetics. An Introduction* (Springer, Berlin/Heidelberg/New York).
Hartlin, E. M., R. M. Wertheimer, and G. M. Graham, 1964, Can. J. Phys. **42**, 1282.
Hillman, H., 1981, in *Superconductor Materials Science,* edited by S. Foner and B. Schwartz (Plenum, New York/London), p. 275.
Hoenig, M. O., 1980, Cryogenics **20**, 375.
Hoffer, J. K., E. C. Kerr, and W. C. Overton, 1977, IEEE Trans. Magn. **13**, 408.
Huebener, R. P., 1975, J. Appl. Phys. **46**, 4982.
Huebener, R. P., 1979, *Magnetic Flux Structures in Superconductors* (Springer, Berlin/Heidelberg/New York).
Huebener, R. P., 1984, Rep. Prog. Phys. **47**, 175.
Hulm, J. K., and B. T. Matthias, 1981, in *Superconductor Materials Science,* edited by S. Foner and B. Schwartz (Plenum, New York/London), p. 1.
Ishibashi, K., M. Wake, M. Kobayashi, and A. Kotase, 1979, Cryogenics **19**, 467.
Ivanchenko, Yu. M., V. F. Khirnyi, and P. N. Mikheenko, 1979, Zh. Eksp. Teor. Fiz. **77**, 952 [Sov. Phys. JETP **50**, 479

(1979)].
Ivanchenko, Yu. M., Yu. V. Medvedev, and A. N. Yarish, 1985, Fiz. Nizk. Temp. **11**, 132.
Ivanchenko, Yu. M., and P. N. Mikheenko, 1982, Zh. Eksp. Teor. Fiz. **82**, 488 [Sov. Phys. JETP **55**, 281 (1982)].
Ivanchenko, Yu. M., and P. N. Mikheenko, 1983a, Pis'ma Zh. Eksp. Teor. Fiz. **37**, 182 [JETP Lett. **37**, 217 (1983)].
Ivanchenko, Yu. M., and P. N. Mikheenko, 1983b, Zh, Eksp. Teor. Fiz. **85**, 2116 [Sov. Phys. JETP **58**, 1228 (1983)].
Ivanchenko, Yu. M., P. N. Mikheenko, and V. F. Khirnyi, 1981, Zh. Eksp. Teor. Fiz. **80**, 171 [Sov. Phys. JETP **53**, 86 (1981)].
Ivanchenko, Yu. M., P. N. Mikheenko, and Ya. M. Yuzhelevsky, 1983, Zh. Tekh. Fiz. **53**, 1608.
Ivlev, B. I., N. B. Kopnin, and A. I. Larkin, 1983, J. Low Temp. Phys. **53**, 731.
Iwanyshin, O., and H. J. T. Smith, 1972, Phys. Rev. B **6**, 120.
Iwasa, Y. and B. A. Apgar, 1978, Cryogenics **18**, 267.
Jahn, M. T. and Y. H. Kao, 1976, J. Phys. Soc. Jpn. **40**, 377.
Jones, R. G., E. H. Rhoderick, and A. C. Rose-Innes, 1967, Phys. Lett. A **24**, 318.
Jüngst, K. P., and L. Yan, 1985, IEEE Trans. Magn. **21**, 253.
Kadigrobov, A. M., and A. A. Slutskin, 1978, Pis'ma Zh. Eksp. Teor. Fiz. **28**, 219 [JETP Lett. **26**, 335 (1978)].
Kadigrobov, A. M., A. A. Slutskin, and I. V. Krivoshei, 1984, Zh. Eksp. Teor. Fiz. **87**, 1314 [Sov. Phys. JETP **60**, 754 (1984)].
Kadin, A. M., W. J. Skocpol, and M. Tinkham, 1977, J. Low Temp. Phys. **33**, 481.
Kalafati, Yu. D., I. A. Serbinov, and L. A. Ryabova, 1979, Pis'ma Zh. Eksp. Teor. Fiz. **29**, 637 [JETP Lett. **29**, 583 (1979)].
Kametaka, Y., 1976, Osaka J. Math. **13**, 11.
Kashani, A., and S. W. Van Sciver, 1985, Cryogenics **25**, 238.
Kaschei, V. A., 1977, Fiz. Tverd. Tela (Leningrad) **19**, 1600 [Sov. Phys. Solid State **19**, 934 (1977)].
Kaschei, V. A., 1978, Fiz. Tverd. Tela (Leningrad) **20**, 1454 [Sov. Phys. Solid State **20**, 837 (1978)].
Kaschei, V. A., and V. A. Shklovsky, 1976 Fiz. Tverd. Tela (Leningrad) **18**, 2090 [Sov. Phys. Solid State **18**, 1216 (1976)].
Keilin, V. E., E. Yu. Klimenko, M. G. Kremlev, and N. B. Samoilov, 1967, *Les Champs Magnetique Intenses* (SNRS, Paris), p. 231.
Keilin, V. E., and S. L. Kruglov, 1984, Cryogenics **24**, 525.
Keilin, V. E., and V. K. Ozhogina, 1977, *Sverkhprovodimost'* (Superconductivity) **4**, 170.
Keilin, V. E., and V. R. Romanovsky, 1982, Cryogenics **22**, 313.
Kerzberg, M., 1983, Phys. Rev. B **27**, 6798.
Kirichenko, Yu. A., and K. B. Rusanov, 1983, *Teploobmen v gelii v usloviyakh svobodnogo dvizheniya* (Heat Transfer under Free Motion Conditions) (Naukova Dumka, Kiev).
Knight, B. W., and G. A. Peterson, 1967, Phys. Rev. **155**, 393.
Kolmogorov, A. N., I. G. Petrovsky, and N. S. Piskunov, 1937, Vestn. Mosk. Univ. Ser. Mat. Mekh. **1**, 6.
Kolchin, A. M., A. G. Mikhailov, N. I. Rainov, A. V. Rumyantseva, A. P. Smirnov, and V. N. Totubolin, 1961, Zh. Eksp. Teor. Fiz. **40**, 1543 [Sov. Phys. JETP **13**, 1083 (1961)].
Komiyama, S., T. Takamusu, S. Hiyamizu, and S. Sasa, 1985, Solid State Commun. **54**, 479.
Kramer, L., and R. Rangel, 1984, J. Low Temp. Phys. **57**, 391.
Kremlev, M. G., 1980, Izv. Akad. Nauk SSSR, Ser. Energetika i Transport, No. **4**, 10.
Kumakura, H., K. Togano, T. Takeuchi, and K. Tachikava, 1985, IEEE Trans. Magn. **21**, 760.
Kutateladze, S. S., 1979, *Osnovi Teorii Teploobmena* (Fundamentals of Heat Transfer) (Atomizdat, Moscow).
Kutateladze, S. S., M. O. Lutset, and Yu. M. Lvovsky, 1978, Cryogenics **18**, 310.
Landau, L. D., and E. M. Lifshitz, 1974, *Kvantovaya Mekhanika. Nerelyativistskaya Teoriya* (Quantum Mechanics. Nonrelativistic Theory) (Nauka, Moscow).
Landau, L. D., and E. M. Lifshitz, 1982, *Elektrodinamika Sploshnykh Szed* (Electrodynamics of Continuous Media) (Nauka, Moscow).
Landauer, R., 1977, Phys. Rev. A **15**, 2117.
Langer, J. S, 1980, Rev. Mod. Phys. **52**, 1.
Latyshev, Yu. I., and F. Ya. Nad', 1976, Zh. Eksp. Teor. Fiz. **71**, 2158 [Sov. Phys. JETP **44**, 1136 (1976)].
Likharev, K. K., 1979, Rev. Mod. Phys. **51**, 101.
Lvovsky, Yu. M., 1984, Zh. Tekh. Fiz. **54**, 1663.
Lvovsky, Yu. M., and M. O. Lutset, 1979, Cryogenics **19**, 483.
Lvovsky, Yu. M., and M. O. Lutset, 1982, Cryogenics **22**, 581.
Maddock, B. I., G. B. James, and W. T. Norris, 1969, Cryogenics **9**, 261.
Martinelli, A. P., and S. L. Wipf, 1973, in Proc. Appl. Supercond. Conf. Annapolis IEEE 72 CH0682-5-TABS, p. 331.
Mazur, P., and D. Bedeaux, 1981, J. Stat. Phys. **24**, 215.
McFadden, G. B., and S. R. Coriel, 1984, Physica D **12**, 253.
Meuris, C., 1984, J. Phys. (Paris) **45**, No. 1, Suppl.
Meyer, J. D., 1975, J. Appl. Phys. **7**, 127.
Mikhailov, A. S., L. Schimanksy-Geier, and W. Ebeling, 1983, Phys. Lett. A **96**, 453.
Mints, R. G, 1979, Dok. Akad. Nauk SSSR **248**, 352 [Sov. Phys. Dokl. **24**, 757 (1979)].
Mints, R. G., and A. L. Rakhmanov, 1981, Rev. Mod. Phys. **53**, 551.
Mints, R. G., and A. L. Rakhmanov, 1984, *Neustoichivost' v sverkhprovodnikakh* (Instabilities in Superconductors) (Nauka, Moscow).
Mizuno, K., and T. Aomine, 1980, J. Phys. Soc. Jpn. **48**, 1908.
Morse, F. M., and G. Feschbach, 1953, *Methods of Theoretical Physics* (McGraw-Hill, New York/Toronto/London).
Mullins, W. W., and R. F. Sekerka, 1963, J. Appl. Phys. **34**, 323.
Mullins, W. W., and R. F. Sekerka, 1964, J. Appl. Phys. **35**, 444.
Nad' F. Ya., and O. Yu. Polyansky, 1973, Radiotekh. Elektron. **18**, 2445 [Sov. Radio Eng. Electron. **18**, 1784 (1973)].
Nedospasov, A. V., and V. D. Khait, 1979, *Kolebaniya i Neustoichivost v Nizkotemperaturnoi Plazme* (Oscillations and Instabilities in Low-Temperature Plasma) (Nauka, Moscow).
Newhouse, V. L., 1964, *Applied Superconductivity* (Wiley, New York).
Nick, W., M. Krauth, and G. Ries, 1979, IEEE Trans. Magn. **15**, 359.
Nicolis, G., and I. Prigogine, 1977, *Self-Organization in Nonequilibrium Systems* (Wiley Interscience, New York).
Overton, W. C., 1971, J. Low Temp. Phys. **5**, 397.
Pals, J. A., and J. Doben, 1979, Phys. Rev. B **20**, 935.
Pasmanter, R. A., D. Bedeaux, and P. Mazur, 1978, Physica A **90**, 151.
Pasztor, G., and C. Schmidt, 1978, J. Appl. Phys. **49**, 886.
Petukhov, B. S., and S. A. Kovalev, 1963, Izv. Vuzov. Ser. Energetika, No. 4, p. 81.
Posada, E., and L. Rinderer, 1975a, J. Low. Temp. Phys. **21**, 27.
Posada, E., and L. Rinderer, 1975b, J. Low. Temp. Phys. **21**, 223.
Purcell, J. R., and J. M. Brooks, 1968, J. Appl. Phys. **39**, 2529.

Raizer, Yu. P., 1980, Usp. Fiz. Nauk **132**, 549 [Sov. Phys. Usp. **23**, 789 (1980)].
Rakhmanov, A. L., 1983, Cryogenics **23**, 487.
Roberge, R., 1981, in *Superconductor Materials Science,* edited by S. Foner and B. Schwartz (Plenum, New York/London), p. 389.
Romanovsky, V. R., 1984a, Izv. Akad. Nauk SSR, Ser. Energetika i Transport, No. 4, 115.
Romanovsky, V. R., 1984b, Dok. Akad. Nauk SSSR **279**, 884 [Sov. Phys. Dokl. **29**, 1053 (1984)].
Rosenberger, G. B., 1959, IBM J. Res. Dev. **3**, 189.
Ross, B., and J. D. Lister, 1977, Phys. Rev. A **15**, 1246.
Rozanov, N. N., 1981, Zh. Eksp. Teor. Fiz. **80**, 96 [Sov. Phys. JETP, **53**, 47 (1981)].
Rumanov, E. N., 1978, Zh. Eksp. Teor. Fiz. **74**, 1422 [Sov. Phys. JETP **47**, 744 (1978)].
Rumanov, E. N., 1982, Pis'ma Zh. Eksp. Teor. Fiz. **35**, 286 [JETP Lett **35**, 354 (1982)].
Schmidt, C., 1978, Cryogenics **18**, 605.
Scott, A., 1970, *Active and Nonlinear Wave Propagation in Electronics* (Wiley, New York/London/Sydney/Toronto).
Shimamoto, S., and H. Desportes, 1970, J. Appl. Phys. **41**, 3286.
Schulze, H. J., and K. Keck, 1983, Z. Phys. B **51**, 215.
Schulze, H. J., and K. Keck, 1984, Appl. Phys. A **34**, 243.
Schulze, G. E. R., 1967, *Metallphysik* (Academic-Verlag, Berlin).
Shklovsky, V. A., 1975, Fiz. Tverd. Tela (Leningrad) **17**, 3076 [Sov. Phys. Solid State **17**, 2040 (1975)].
Skocpol, W. J. 1981, in *Nonequilibrium Superconductivity Phonons and Kapitza Boundaries,* edited by K. E. Gray (Plenum, New York/London), p. 559.
Skocpol, W. J., M. R. Beasley, and M. Tinkham, 1974a, J. Appl. Phys. **45**, 4054.
Skocpol, W. J., M. R. Beasley, and M. Tinkham, 1974b, J. Low. Temp. Phys. **16**, 145.
Smirnov, A. P., and N. F. Fedorov, 1971, Fiz. Tverd. Tela (Leningrad) **13**, 796 [Sov. Phys. Solid State **13**, 657 (1971)].
Smirnov, A. P., I. S. Parshina, T. A. Rusanova, and V. N. Totubolin, 1968, Zh. Tekh. Fiz. **38**, 1588.
Smirnov, A. P., V. N. Totubolin, and I. S. Parshina, 1965, Zh. Eksp. Teor. Fiz. **49**, 117 [Sov. Phys. JETP **22**, 84 (1966)].
Smith, C. W., and J. J. Bohner, 1975, Phys. Lett. A **51**, 453.
Stekly, Z. J. J., 1965, Adv. Cryog. Eng. **8**, 585.
Stekly, Z. J. J., 1966, J. Appl. Phys. **37**, 324.
Stekly, Z. J. J., R. Thome, and B. Strauss, 1969, J. Appl. Phys. **40**, 2238.
Stuivinga, M., T. M. Klapwijk, J. E. Moo-ij, and A. Bezuijen, 1983, J. Low. Temp. Phys. **53**, 473.
Suenaga, M., 1981, in *Superconductor Materials Science,* edited by S. Foner and B. Schwartz (Plenum, New York/London), p. 201.
Superczynski, M. J., 1979, IEEE Trans. Magn. **15**, 325.
Tinkham, M., 1981, in *Nonequilibrium Superconductivity. Phonons and Kapitza Boundaries,* edited by K. E. Gray (Plenum, New York/London), p. 231.
Tinkham, M., M. Octavio, and W. J. Skocpol, 1977, J. Appl. Phys. **48**, 1311.
Tsuchiya, K., and M. Suenaga, 1985, Cryogenics **25**, 457.
Tsukamoto, O., and F. Miyagi, 1979, IEEE Trans. Magn. **15**, 367.
Tsukamoto, O., and M. Nakada, 1985, IEEE Trans. Magn. **21**, 370.
Turck, B., 1980, Cryogenics **20**, 146.
Tzyan, Yu. N., and I. I. Logvinov, 1982, Fiz. Nizk. Temp. **8**, 774.
Vakser, A. I., and Yu. G. Gurevich, 1982, Fiz. Tverd. Tela (Leningrad) **24**, 3000 [Sov. Phys. Solid State **24**, 1698 (1982)].
Vinnikov, L. Ya., V. I. Grigoriev, and O. V. Zharikov, 1976, Zh. Eksp. Teor. Fiz. **71**, 252 [Sov. Phys. JETP **44**, 130 (1976)].
Volkov, A. F., and Sh. M. Kogan, 1968, Usp. Fiz. Nauk **96**, 633 [Sov. Phys. Usp. **11**, 881 (1969)].
Volkov, A. F., and Sh. M. Kogan, 1974, Pis'ma Zh. Eksp. Teor. Fiz. **19**, 9 [JETP Lett. **19**, 4 (1974)].
Volodin, Yu. E., V. V. Barelko, and A. G. Merzhanov, 1982, Khim. Fiz. **1**, 670.
Volotskaya, V. G., N. E. Musienko, I. M. Dmitrienko, and Yu. V. Kalyakin, 1976, Fiz. Nizk. Temp. **2**, 500.
West, A. W., W. H. Warnes, D. L. Moffat, and D. C. Larbalestier, 1983, IEEE Trans. Magn. **19**, 749.
Whetstone, C. N., and C. E. Ross, 1965, J. Appl. Phys. **38**, 783.
Wilson, M. N., 1983, *Superconducting Magnets* (Oxford University Press, Oxford).
Wilson, M. N., and Y. Iwasa, 1978, Cryogenics, **18**, 17.
Wilson, M. N., C. R. Walters, J. D. Lewin, P. F. Smith, and A. H. Spurway, 1970, J. Phys. D **3**, 1517.
Wipf, S. L., 1979, IEEE Trans. Magn. **15**, 379.
Wyatt, A. F. G., 1969, in *Tunneling Phenomena in Solids,* edited by E. Burstein and S. Lundquist (Plenum, New York/London), p. 541.
Wyatt, A. F. G., 1981, in *Nonequilibrium Superconductivity. Phonons and Kapitza Boundaries,* edited by K. E. Gray (Plenum, New York/London), p. 31.
Yamasaki, S., and T. Aomine, 1979, Jpn. J. Appl. Phys. **18**, 667.
Young, P. A., 1971, Appl. Opt. **10**, 638.
Zeldovich, Ya. B., G. I. Barenblatt, V. B. Librovich, and G. Makhviladze, 1980, Matematicheskaya Teoriya Goreniya i Vzryva (Mathematical Theory of Combustion and Explosion) (Nauka, Moscow).
Zhukov, S. A., V. V. Barelko, and A. G. Merzhanov, 1979, Int. J. Heat Mass Transfer **24**, 47.
Zhukov, S. A., L. E. Bokova, and V. V. Barelko, 1983, Int. J. Heat Mass Transfer **26**, 269.
Zinoviev, V. E., 1984, *Kineticheskiye Svoistva Metallov Privysokikh Temperaturakh* (Kinetic Properties of Metals at High Temperatures) (Metallurgiya, Moscow).

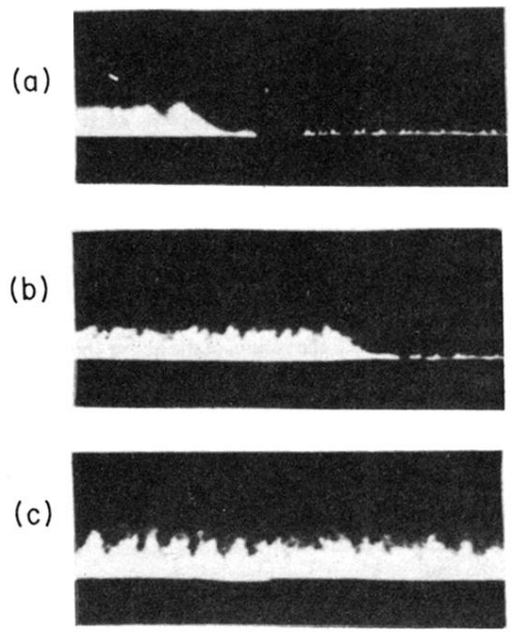

FIG. 14. Propagation of vapor film on the surface of water-cooled platinum wire heated by current. $T_0=371$ K, $I=2.96$ A, $v=1.1$ cm/s (Zhukov, Barelko, and Merzhanov, 1979).